BIOGEOGRAFIA HISTÓRICA

ENFOQUES FUNDAMENTAIS

Dispersialismo – Darwin 1859, Wallace 1876

Biogeografia filogenética – Hennig 1966, Brundin 1966

Áreas ancestrais – Bremer 1992, Ronquist 1994

Panbiogeografia – Croizat 1958, Craw 1988, Page 1987

Biogeografia cladística – Nelson 1974, D. Rosen 1976, Nelson & Platnick 1981

Análise de parcimônia de endemismos (PAE) - B. Rosen 1988, Craw 1988, Morrone 1988

Métodos baseados em eventos – Page 1994, Ronquist 1997

Filogeografia – Avise *et al.* 1987

Biogeografia experimental – Haydon, Tadtkey & Pianka 1994

Biogeografia Integrativa – Donoghue & Moore 2003

Donoghue & Moore 2003

Métodos da Biogeografia Cladística são fundamentalmente baseados em topologia = padrões gerais são delineados com base em comparação ou combinação somente das topologias dos cladogramas de táxons e áreas.

Necessidade de incorporação de datação absoluta (temporalidade) da diversificação das linhagens componentes:

“ Biogeografia Integrativa”

Teste de tempo na Biogeografia Histórica

Donoghue & Moore 2003

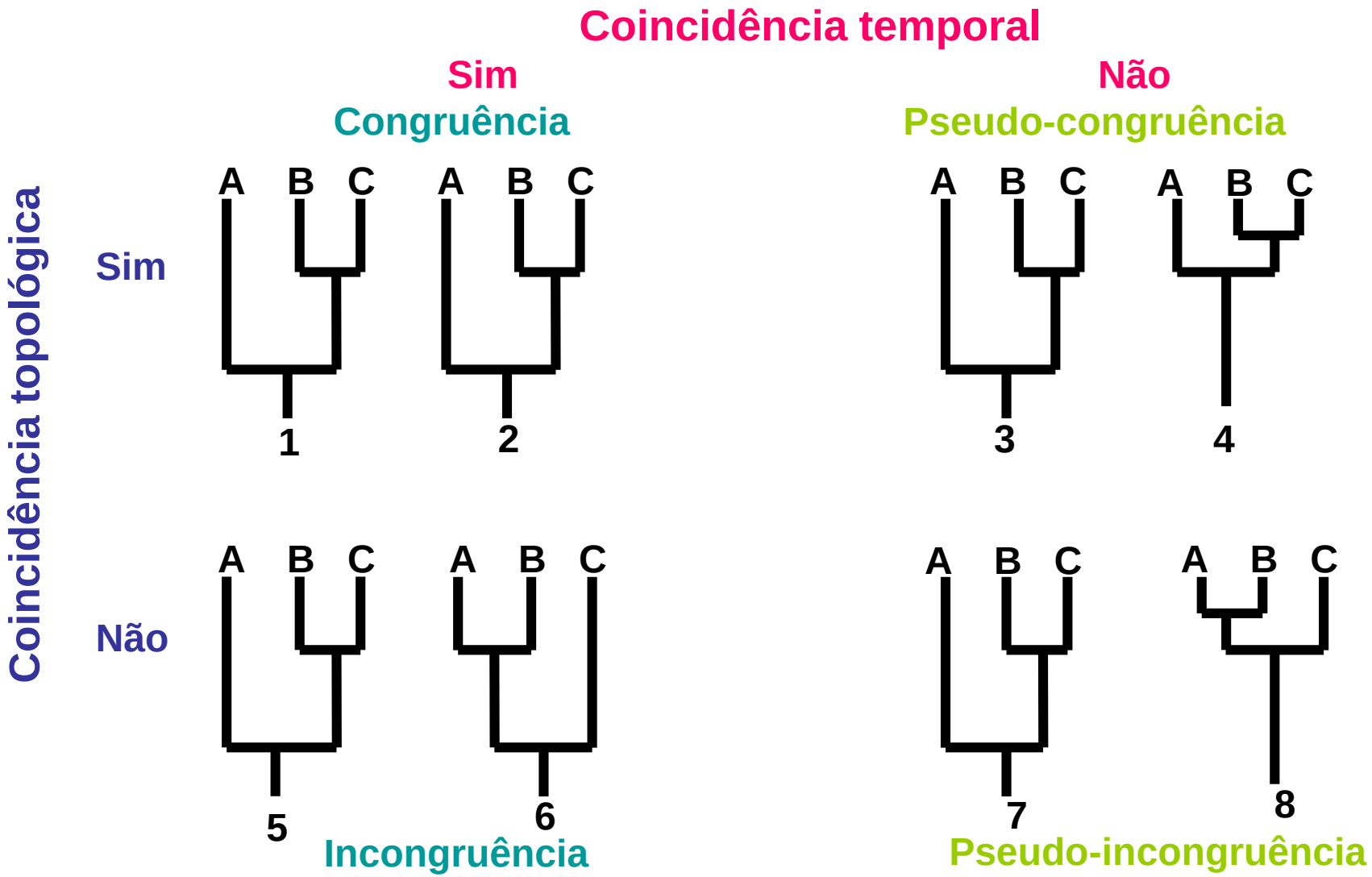

“BIOGEOGRAFIA MOLECULAR”

Caccone *et al.* 1994, Lavin *et al.* 2000

Reconstrução da história biogeográfica de 1 táxon sob 2 perspectivas:

1. **Uso de filogenia molecular como dado bruto de métodos da Biogeografia Histórica**

2. **Aplicação de relógio molecular para incorporar tempo nos métodos da Biogeografia Histórica**

“Paradigma cronobiogeográfico”

Hunn & Upchurch 2000

Elaboração lógica e não uma substituição do paradigma atual.

Requer métodos que permitam atribuir valores de tempo a táxons, i.e., tempo de origem e tempo de cada evento cladogenético numa filogenia.

Os dados de distribuição temporal dos organismos poderão prover reforço ou rejeição de hipóteses sobre a causalidade dos eventos filogenéticos.

“Biogeografia Integrativa”

Donoghue & Moore 2003

Sistemática molecular

sequenciamento de segmentos dos ácidos nucléicos (nuclear e cloroplasto)

- **número elevado de caracteres, menos influenciados por fatores ambientais**

(muitos podem estar em evolução neutra ou quase neutra, sem o forte componente de seleção natural que pode levar a evolução convergente)

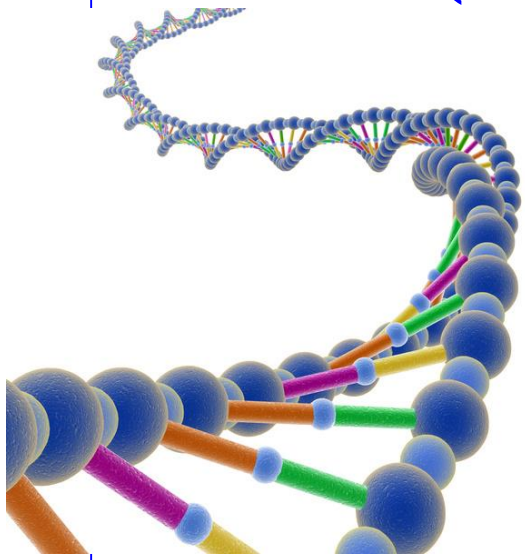

- **seleção objetiva de caracteres**

permite comparação entre quaisquer grupos de organismos (grandes amostras de OTUs: centenas)

3 genomas nas plantas: DNA nuclear
DNA mitocondrial – 80 000 pares de bases
DNA cloroplasto – 120.000 pares de bases

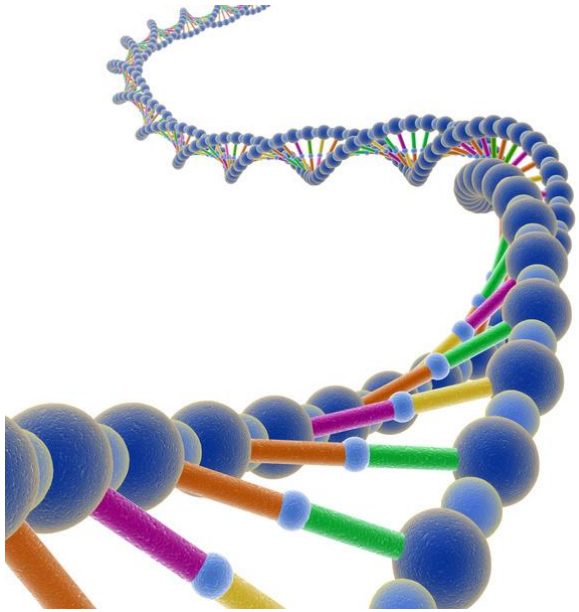

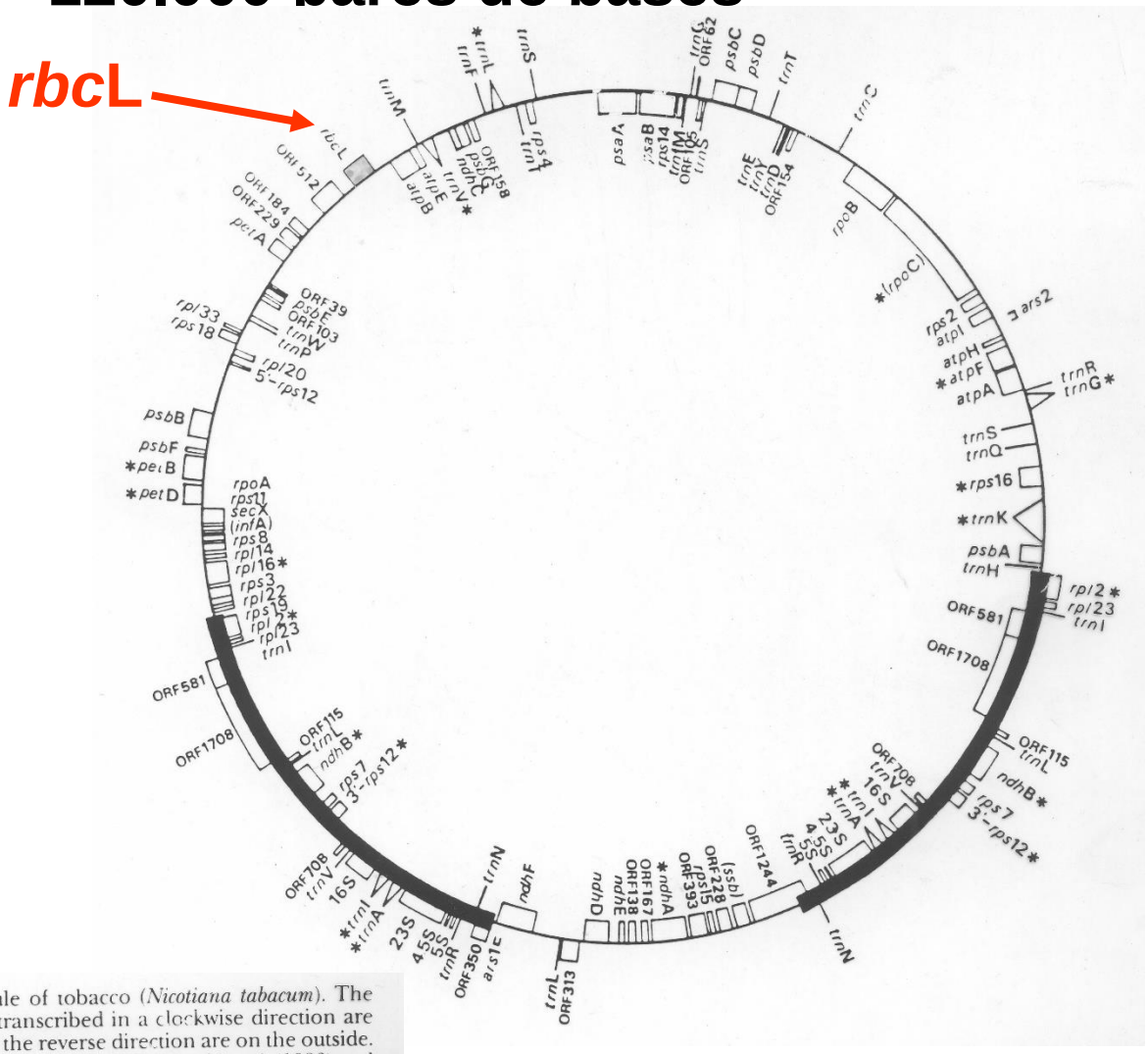

Figure 9.1. Map of the circular chloroplast DNA molecule of tobacco (*Nicotiana tabacum*). The inverted repeat is indicated by the dark bars. Genes transcribed in a clockwise direction are shown on the inside of the circle; those transcribed in the reverse direction are on the outside. Asterisks indicate intron containing genes. The map is from work of Shinozaki et al. (1986) and is reprinted with permission from the EMBO Journal.

OLMSTEAD & PALMER 1991

Obtenção de seqüências

Folhas secas em sílica → Extração DNA → PCR

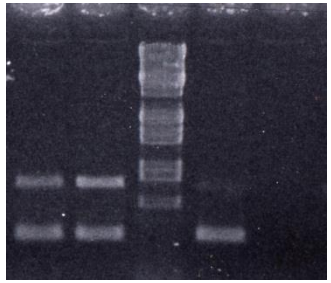

→ Purificação de DNA

Purificação de DNA → nuclear → clonagem

Purificação de DNA → cloroplasto → Seqüência

clonagem → Reamplificação de gene a partir de colônias de bactérias → Seqüência

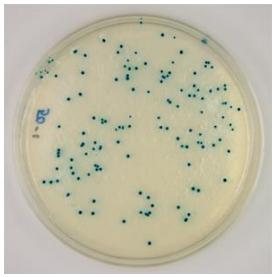

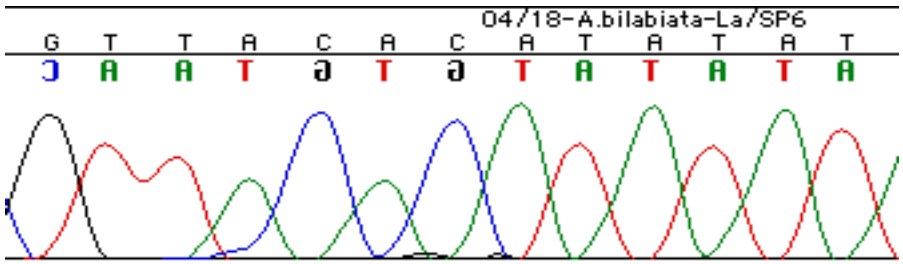

ABI PRISM™

Gel File

Sequencing Analysis 3.0, ©1989-1996 PE Applied Biosystems

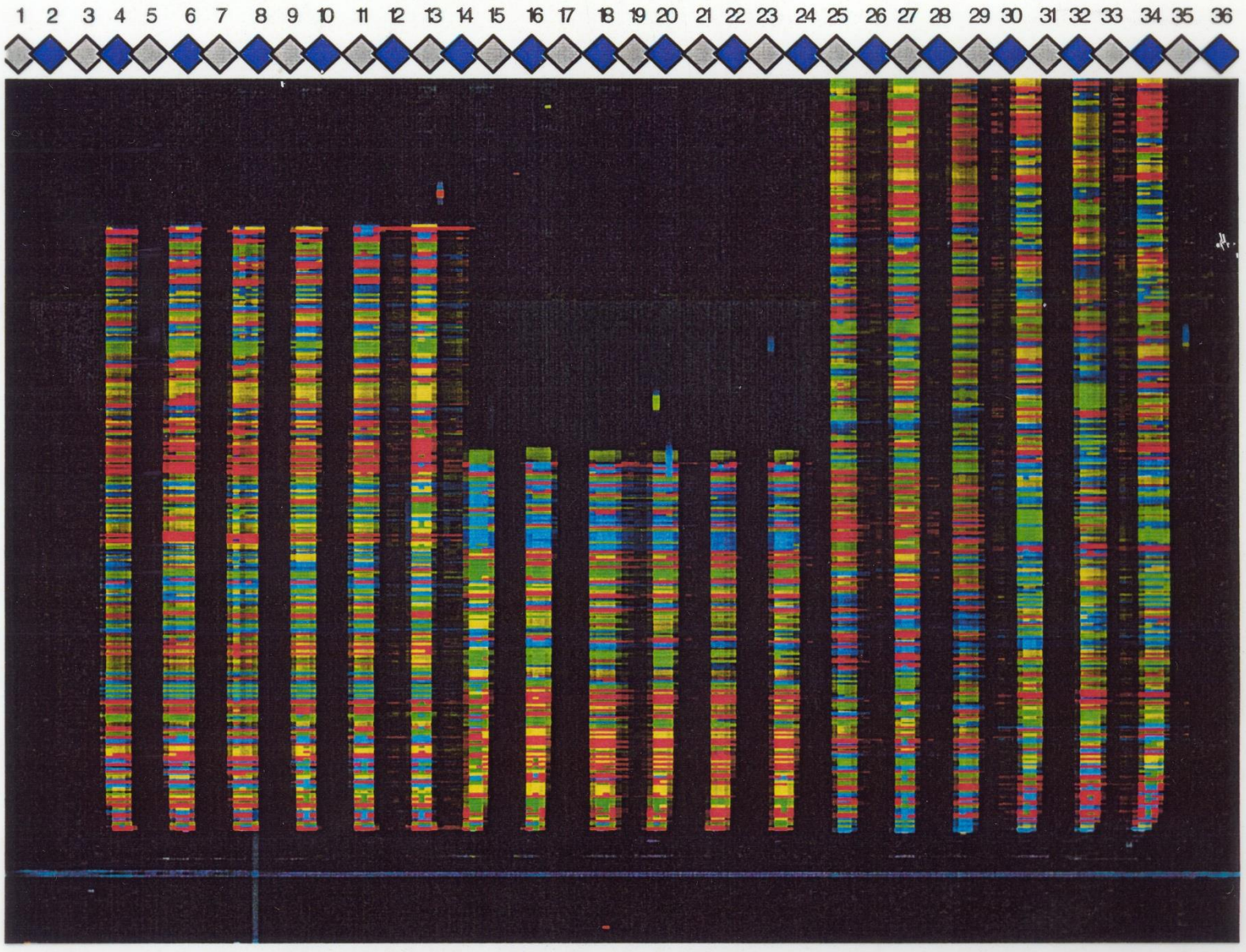


ABI PRISM™
Model 377
Version 3.0
ABI200
Version 3.0
14•B. reflexa - 1448 -tab c
B. reflexa - 1448 -tab c
Lane 14
Signal G:225 A:271 T:183 C:274
DT {BD Set Any-Primer}
dRhodamine Matrix
Points 940 to 8000 Base 1: 940
Page 1 of 2
Mon, May 25, 1998 12:49 PM
Sat, May 23, 1998 2:00 PM
Spacing: 11.72{11.72}
GCTTAATTGAATTGAGCCTTAGTATGGAAACCTGCTAAGTGGTAACTTCCAATTCAGAGAAACCCTGGAATTAAAAAAGGGCAATCCTGAGCCAAATCTTTATTTTTAGAAAACAAGGGTTTAGAAAAC
10 20 30 40 50 60 70 80 90 100 110 120
CTGGAATAAAAAAAGAAAGATAGGTGCAGAGACTCGATGGAAGCTGTTCTAACGAATGGAGTTGACTGTGTTACGTTGGTAGCTGAAATCCCTATACATAAGGGATTACTTCATA
130 140 150 160 170 180 190 200 210 220 230 240
ATACGTAATATAATACGTACGTATACAAACTTACATATCAAATGATTAATCACGACCATAATCCAATCCCGAATTATTGTGAATCGATTTCCATCGAAATCGCGAAGTTC
250 260 270 280 290 300 310 320 330 340 350

Pareamento das sequências de bases:

alinhamento mais provável

CTCAGGATTC....
AGCTCAACGGG...

- - CTCAGGAT...
AGCTCAACGG...

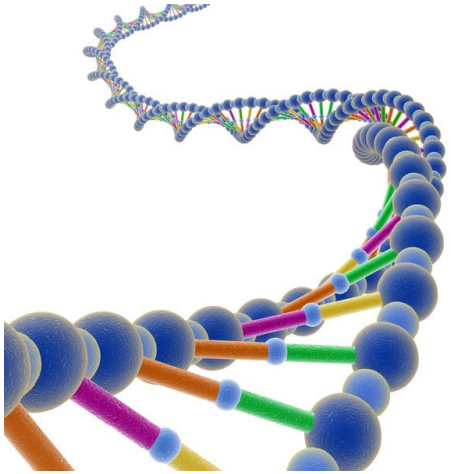

ITS 1 Region (positions 1-234)

```
                          10         20         30         40         50         60         70         80         90        100
                          .          .          .          .          .          .          .          .          .          .
Heteromorpha              TCGAATCCTG CGATAGCAGA A.GACCCGCT AACTCGT--A AACACATTGG GCAAGCGTCA GAGGGCTTC- -GGTCCCCTG TTTGCGAACC CT---TGGTA
Daucus Yoko.              TCGAATCCTG TGATACCAGA ATGACTTGTT AACATGT--A ACAACAACGG GCAAGCAACT GTGGGCCTT- TGGTCCTCTG TCTGTGAACC CA---AGGCA
Daucus                    TCGAATCCTG TGATACCAGA ATGACTTGTT AACATGT--A ACAACAACGG GCAAGCAACT GTGGGCCTT- TGGTCCCCTG TCTGTGAACC CA---AGGCA
Pseudorlaya               TCGAATCCTG CGATACTAGA ATGACCCGTT AACATGT--A AAAACACTGG GCAAGCAACT TCGGACCTG- TGGTCCCCTG TCTGCAAACC CA---AGGCA
Orlaya gran.              TCGAATCCTG CGAGAGCAGA ATGACCCGTA AACATGT--A AAAACATCGG GGAAGTAACA GGGGGCCT-- TGGTCCCTTG TATGCAAACC CA---AGGCA
Orlaya koch.              TCGAATCCTG CGAGAGCAGA GTGACCCGTA AACATGT--A AAAACATCGG GCAAGCAACT GGGGGCCT-- TGGTCCCTTG TTTGCAAACC CA---AGGCA
Laserpitium               TCGAATCCTG CGATAGCAGA ATGACCCGTT AACACGT--A AAAACATCGG GCAAGCGTCG GGGGGCCTT- GTGTCCCCTG TTTGCAAACC CA---AGGTA
Myrrhis                   TCGAATCCTG CTCTAGCGGA ATGACCCGTT AACGCGT--T AAAACACCGG GCAAGCATCA GGAGGCCCA- AGGTCCCCTC TTTGCGACCC CA---GGGCA
Anthriscus                TCGAATCCTG CTCTATTGGA ATGACCCGTT AACTCGT--T AAAACATCGG GCAAGCATTT GGGGGTCCA- AGGCCCCCTC TTTGCAACCC CA---TGGTA
Torilis                   TCGAAACCTG CAATAGCAGA ACGACCCGTT AACACGTCAA AAAACATTGG GCGAGCATCA GGTGGCCCCT AGGGCCCTTG TCTGCAAACC CA---AGGTA
Aegopodium                TCGAATCCTG TGATAGCAGA ACGACCCGCT AACTGGT--A AATATATTGG GCAAGC-TCA TGGGGATTT- -TATCCCCTG TTGGTGAACC CT---TGGTA
Scandix                   TCAAATCCTG CTTTAGCGGA ATGACCCGTT AACTTGT--T AAAATATTGG GGAAGCTTCA GGGTGCCTC- AGGTCCCTTG TTTGCGATCC CA---GGGTA
Crithmum                  TCGAAGCCTG CAACAGCAGT ACAACCCGCT AACTCGT--A AACACATTGG GCAAGC-TAA TGGGGATTT- -GGTTCCTCG TTTGCGAACC CCT--TGGCA
Heracleum lana.           TCGAATCCTG CAATAGCAGA ATGACCTGCT AACATGT--A AGTACATCGG GCAAGCGTAT GGGGGCTTT- -GGTCCCCTG TTAGCGAAAC CC---TGGTA
Heracleum spho.           TCGAATCCTG CAATAGCAGA ATGACCCGCT AACATGT--A ATTACATCGG GCAAGCGTAT GGGGGCTTT- -GGTCCCCTG TTAGCAAAAC CC---TGGTA
Pastinaca                 TCGAATCCTG CAATAGCAGA ATGACCTGCT AACATGT--A AGCACATTGG GCAAGCGTAT GGGGGCTTT- -GGTCCCTTG TTAGCGAAAC CCTGGTAGTA
Heracleum rige.           TCGAATCCTG CAATAGCAGA ATGACCCGCT AACATGT--A AGCACATTGG GCAAGCGTAT GGGGGCTTT- -GCTCCCCTG TCAGCGAAAC CC---TGGTA
Anethum                   TCGAATCCTG CGATAGCAGA ATGACCCGCT AACACGT--A AACACATTGG GCAAGCTTCA GAGGGCTTC- -GGTCCCCTG TTTGCAAACC CT---TGGTA
Apium                     TCGAATCCTG CGATAGCAGA ATGACCCGCT AACACGT--A AACACATTGG GCAAGCGTCG GTGGGCTTT- -GGTCCGCCG TTTGCAAACC TT---TGGTA
Myrrhidendron             TCGAATCCTG CAATAGCAGA ATGACCCGCT AACACGT--C AACAATTTGG GCAAGCGTCG GGGGGCCTC- -GGTCTCCTG TCTGCGAATC CCCC-TGGTA
Arracacia nels.           TCGAATCCTG CAATAGCAGA ATGACCCGCT AACACGT--C AACAATTTGG GCAAGCGTCG GGGGGCCTC- -GGTCTCCTG TATGCGAATC CCCC-TGGTA
Enantiophylla             TCGAATCCTG CAATAGCAGA ACGACCCGCT AACACGT--C AACAATTTCG GCAAGCGTCG GGGGACCTC- -GGTCTCCTG TCTGCGAATC CC---TGGTA
Coulterophytum            TCGAATCCTG CAATAGCAGA ACGACCCGCT AACACGT--C AACAATTTCG GCAAGCGTCG GGGGGCCTC- -GGTCTCCTG TCTGCGAATC CC---TGGTA
Carlesia                  TCGAATCCTG CAACAGCAGA ATGACCCGCT AACACGT--C AACATTTTGG GCAAGCATCG GGGGGCCTC- -GGTCTCCTG TCTGCGAATC CC---TGGTA
Selinum                   TCGAATCCTG CAACAGCAGA ATGACCCGCT AACTCGT--C AACAATTTGG GCAAGCGTCG GGGGGCCTC- -GGTCTCCTG TTTGCGAATC CC---TGGTA
Rhodosciadium             TCGAATCCTG CAATAGCAGA ATGACCCGCT AACACGT--C AACAATTTGG GCAAGCGTCG GGGGGCCTC- -GGTCTCCTG TCTGCCAATC CC---TGGTA
Prionosciadium            TCGAATCCTG CAATAGCAG
Arracacia bran.           TCGAATCCTG CAATAGCAG
Coaxana                   TCGAATCCTG CAATAGCAG
Zizia                     TCGAACCCTG CAATAGCAG
Angelica                  TCGAATCCTG CAATAGCAG
Seseli                    TCGAATCCTG CAATAGCAG
Lomatium                  TCGAATCCTG CAATAGCAG
Aethusa                   TCGAATCCTG CAATAGCAG
Endressia                 TCGAATCCTG CAGTAGCAG
Coriandrum                TCGAAACCTG CAGAAGCAG
Conium                    TCGAATCCTG CGATGGCAG
Pimpinella saxi.          TCGAATCCTG CGATAGCAG
Pimpinella pere.          TCGAATCCTG CGATAGCAG
Smyrnium                  TCGAATCCTG CAATAGCAG
```

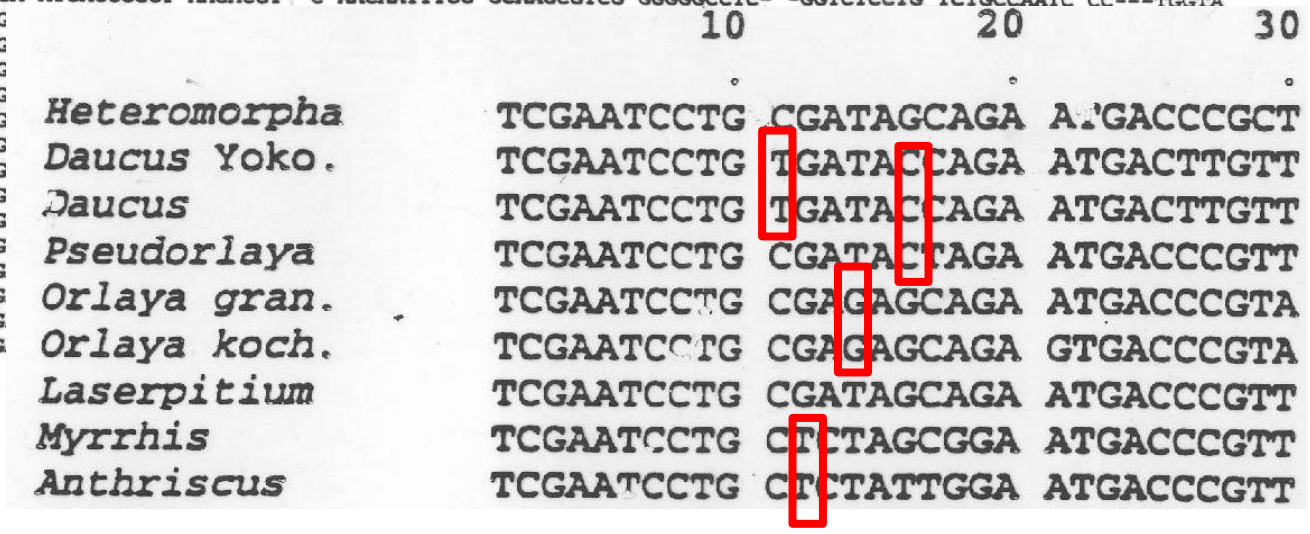

Sistemática molecular

CLADÍSTICA **Bases = caracteres multiestados não-ordenados**

Táxons **sequência de bases**

Columnea	A A T T C G T A C T T G A T C G T
Gloxinia	A A T T C A T A C T T G A T C G T
Saintpaulia	A A C T C T T A C T C G A T C G T
grupo-externo Sauge	A G G T G C C G C T G G A T C G T

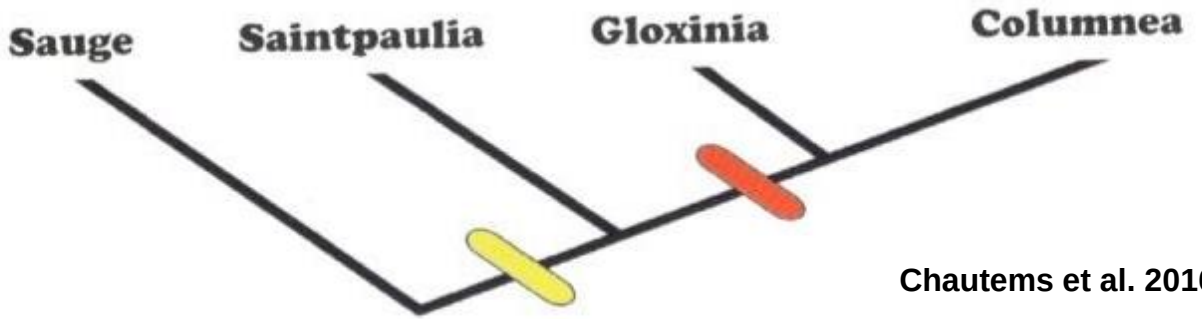

Chautems et al. 2016

- método de comparação com grupo-externo

- critério de parcimônia

-outros critérios: Máxima Verossimilhança, Bayesiano.

GENES

Regiões comumente utilizadas como fonte de informação:

Inferência filogenética entre gêneros e espécies:

***ndh*F (2100 – 2200 pb)**
***mat*K (1100 pb)**
***trn*L-F (1100 – 1400 pb)**
***rps16* (729 pb)**

} cloroplasto

ITS 1 (210 – 270 pb)
ITS 2 (205 – 240 pb)
ETS (100 pb)

} núcleo

entre famílias e ordens:

***rbc*L**
***atp*B**

} cloroplasto

18SnrDNA núcleo

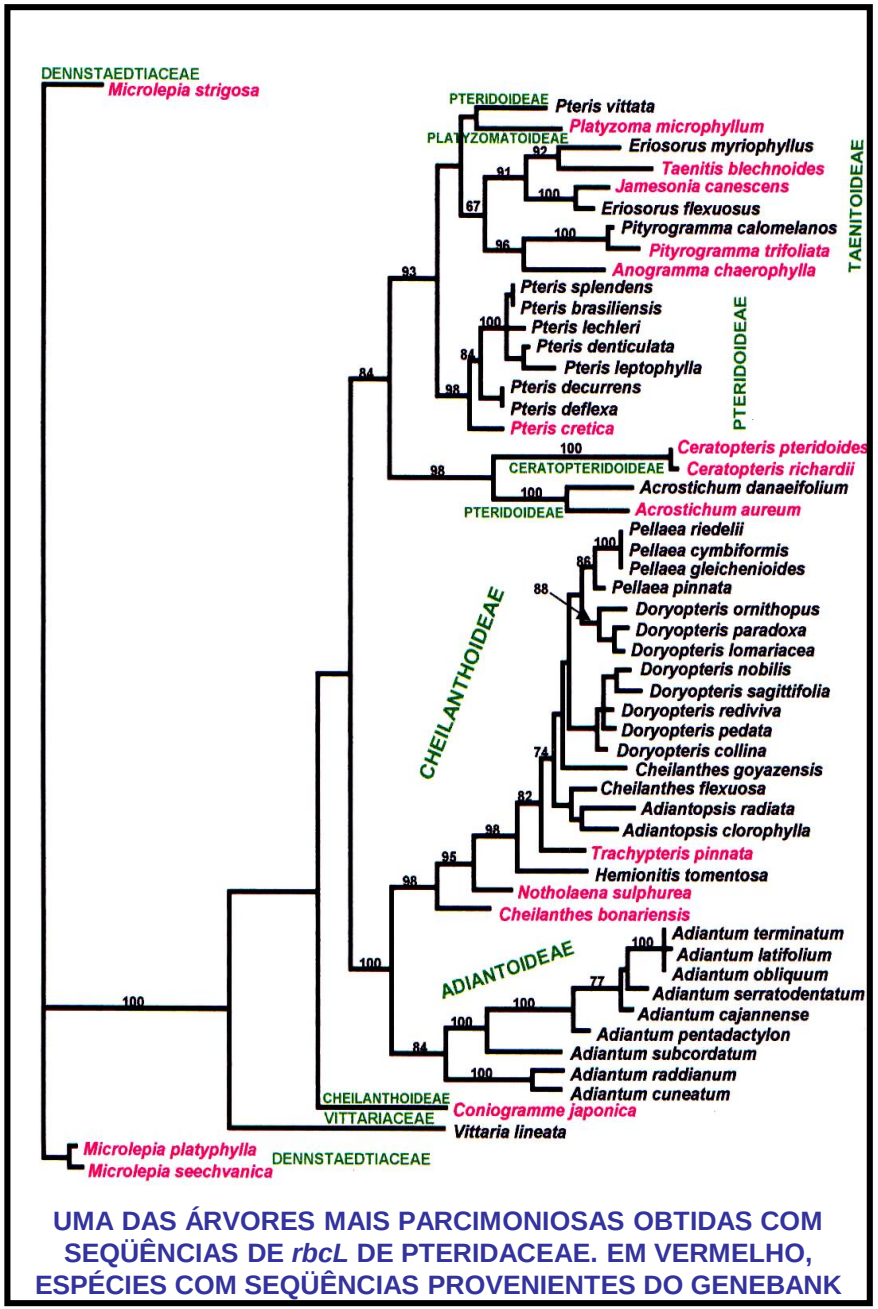

UMA DAS ÁRVORES MAIS PARCIMONIOSAS OBTIDAS COM SEQÜÊNCIAS DE *rbcL* DE PTERIDACEAE. EM VERMELHO, ESPÉCIES COM SEQÜÊNCIAS PROVENIENTES DO GENEBANK

Pteris gleichnioides

FILOGENIA DE PTERIDACEAE BASEADA EM SEQÜÊNCIAS DE *rbcL*

Salatino et al. 2008

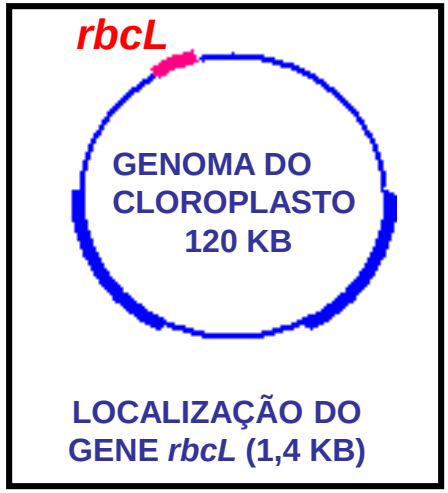

LOCALIZAÇÃO DO GENE *rbcL* (1,4 KB)

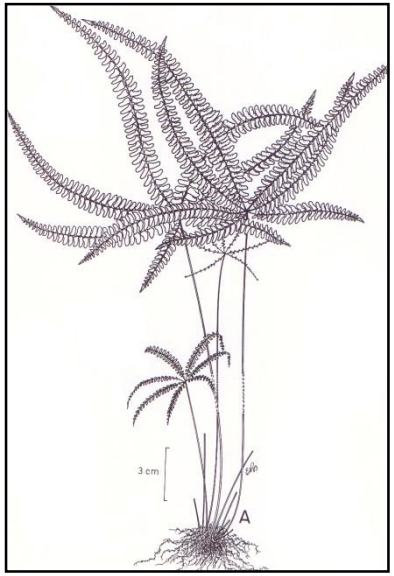

Adiantopsis radiata

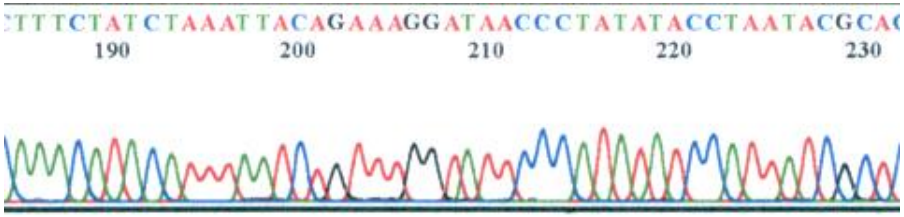

Next generation Sequencing (NGS)

Mapa do genoma cloroplastidial de *Aldama kunthiana* e *A. linearifolia*

Os dois genomas são idênticos em tamanho (151.102 bp), organização e ordem dos genes; diferem somente em 70 nucleotídeos (0,046%); comparando com *Helianthus annuus*:
***A. kunthiana* difere em 627 nucleotídeos (4,1%) e *A. linearifolia em 614* (4%) = taxas muito baixas para reconstrução filogenética.**

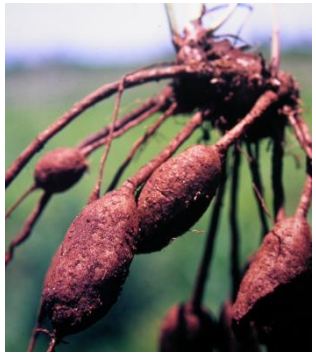

Aldama - ASTERACEAE - HELIANTHEAE

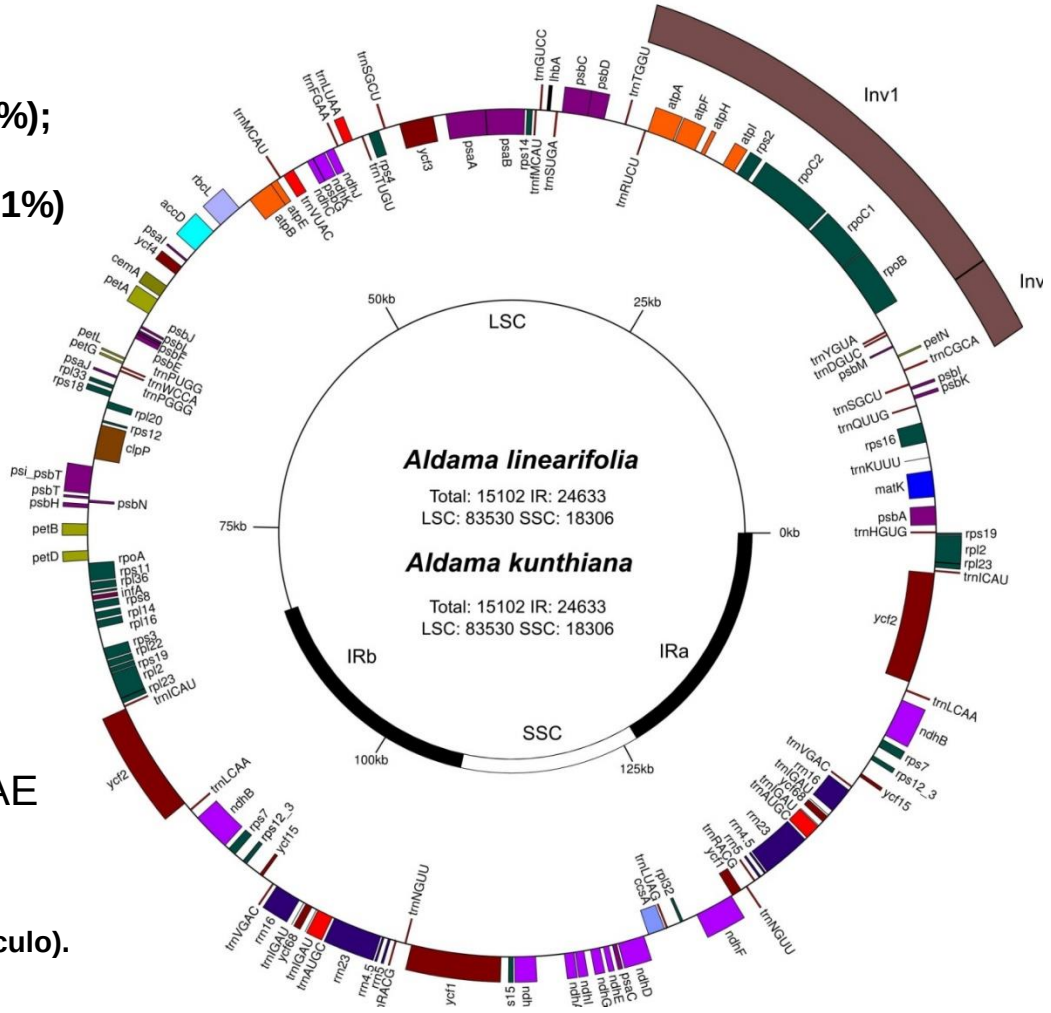

Genes transcritos no sentido horário (fora do circulo), genes transcritos no sentido anti-horário (dentro do círculo). INV: inversão; IRa: repetição invertida A; IRb: repetição invertida B; LSC: região grande de cópia única; SSC: região pequena de cópia única.

Loeuille et al. in prep.

Aplicações das filogenias

aprimorar a classificação

Angiosperm Phylogeny Group APG-II - 2003

***rbc*L, *atp*B**

18S rDNA

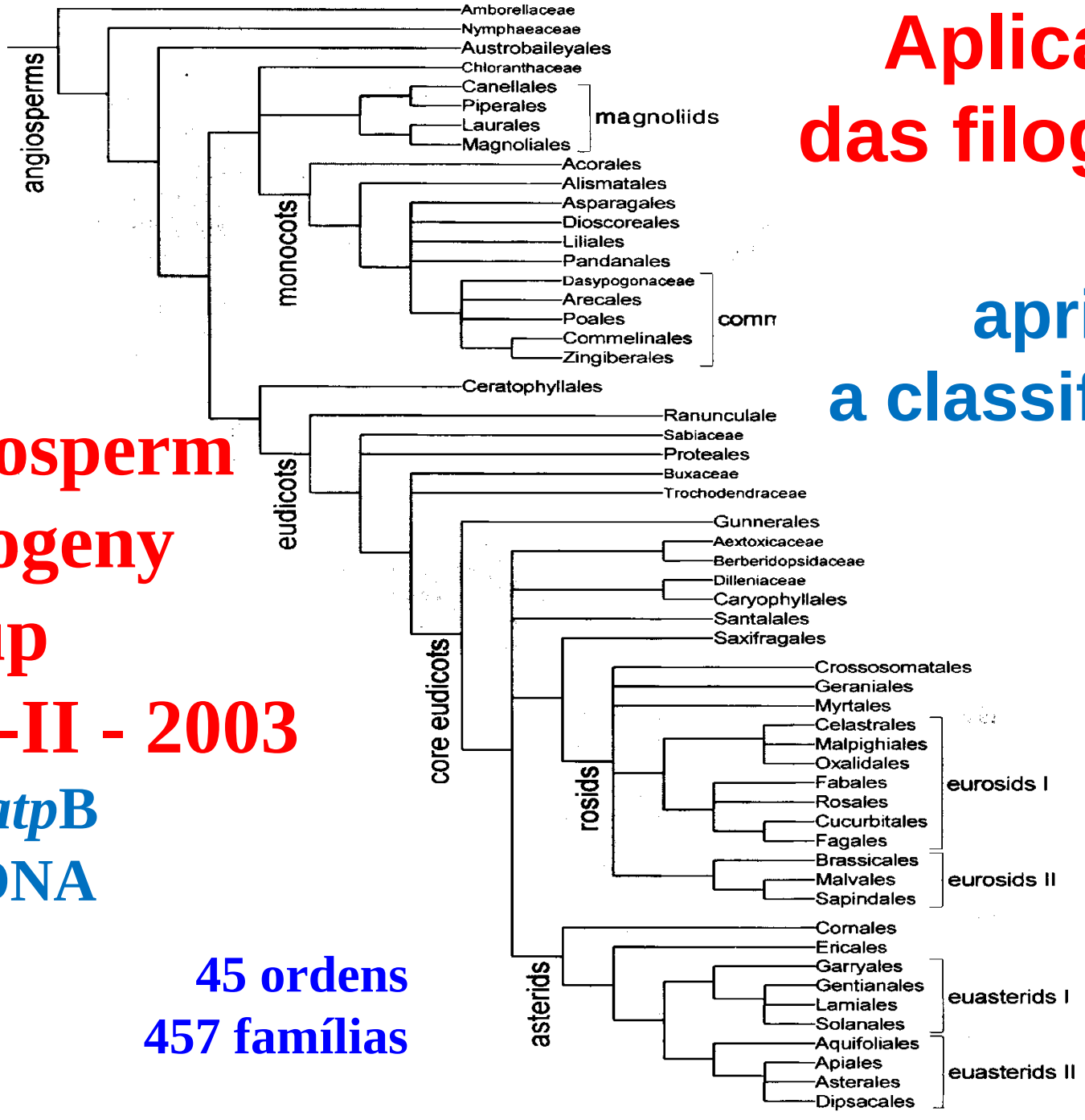

45 ordens

457 famílias

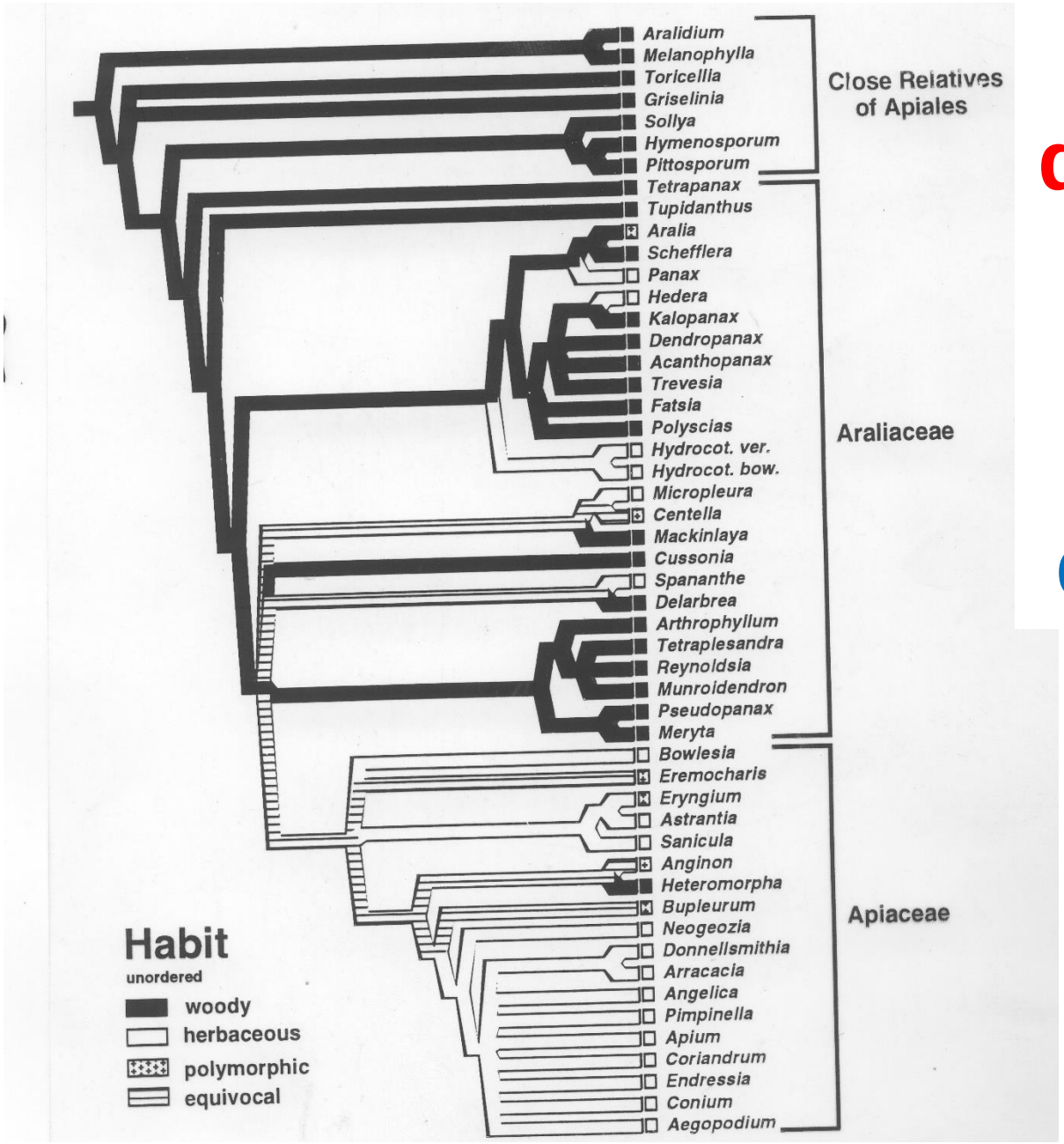

Aplicações das filogenias

hipóteses de evolução de caracteres

Plunkett et al. 1996

Aplicações das filogenias hipóteses de evolução

Evolução da polinização em *Ficus*

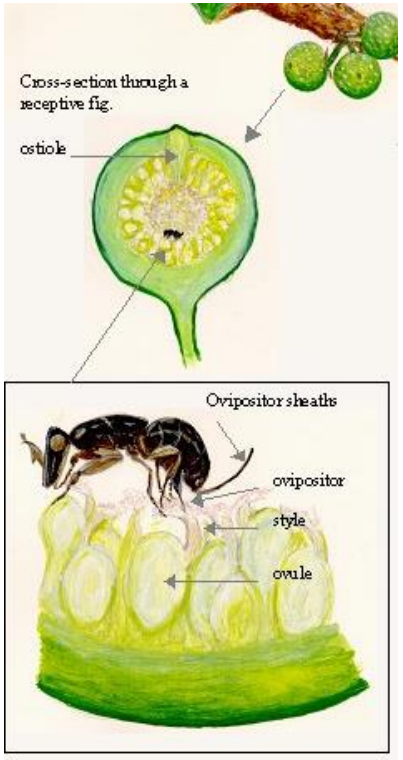

Weiblen 2000

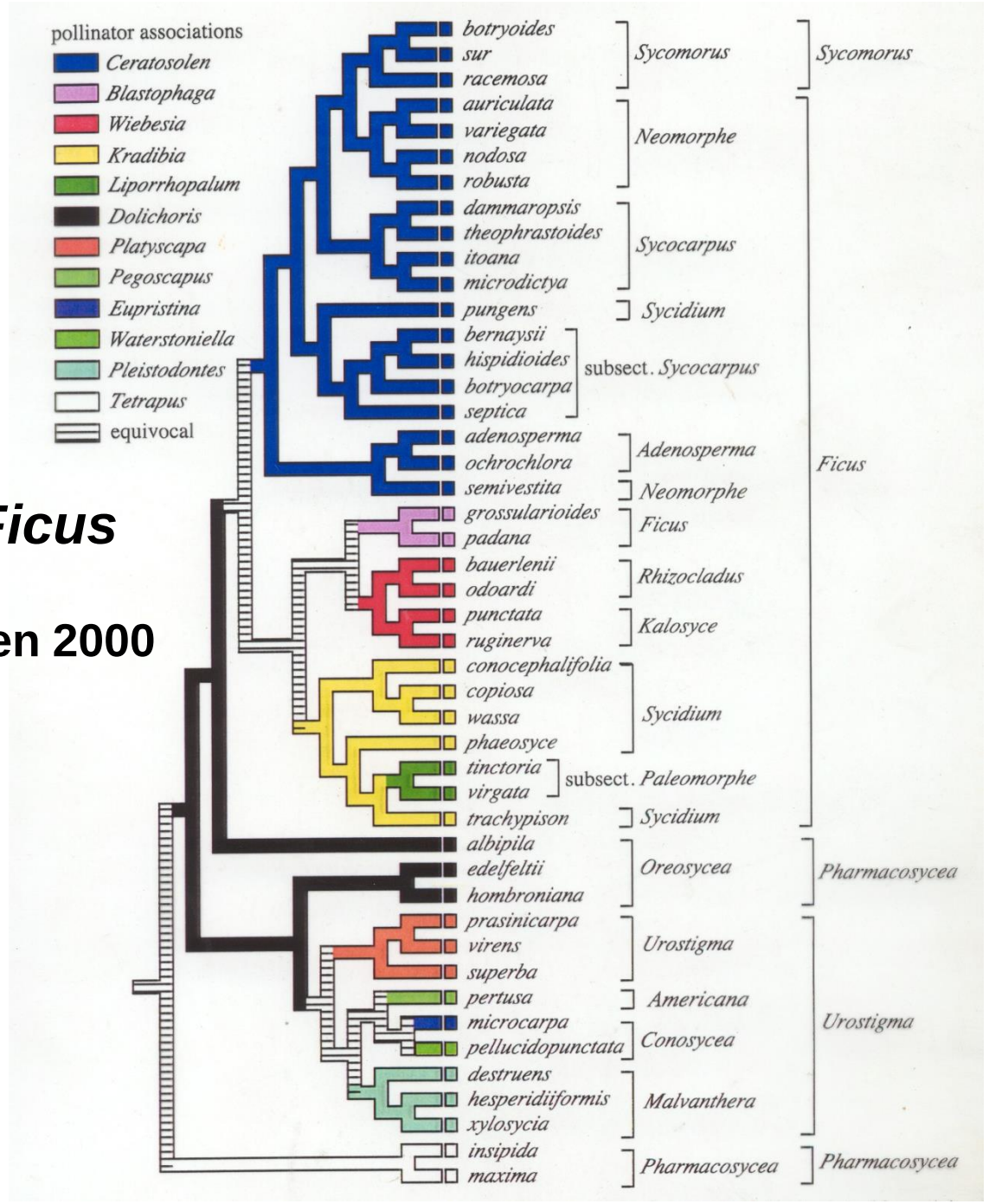

Aplicações das filogenias

hipóteses biogeográficas

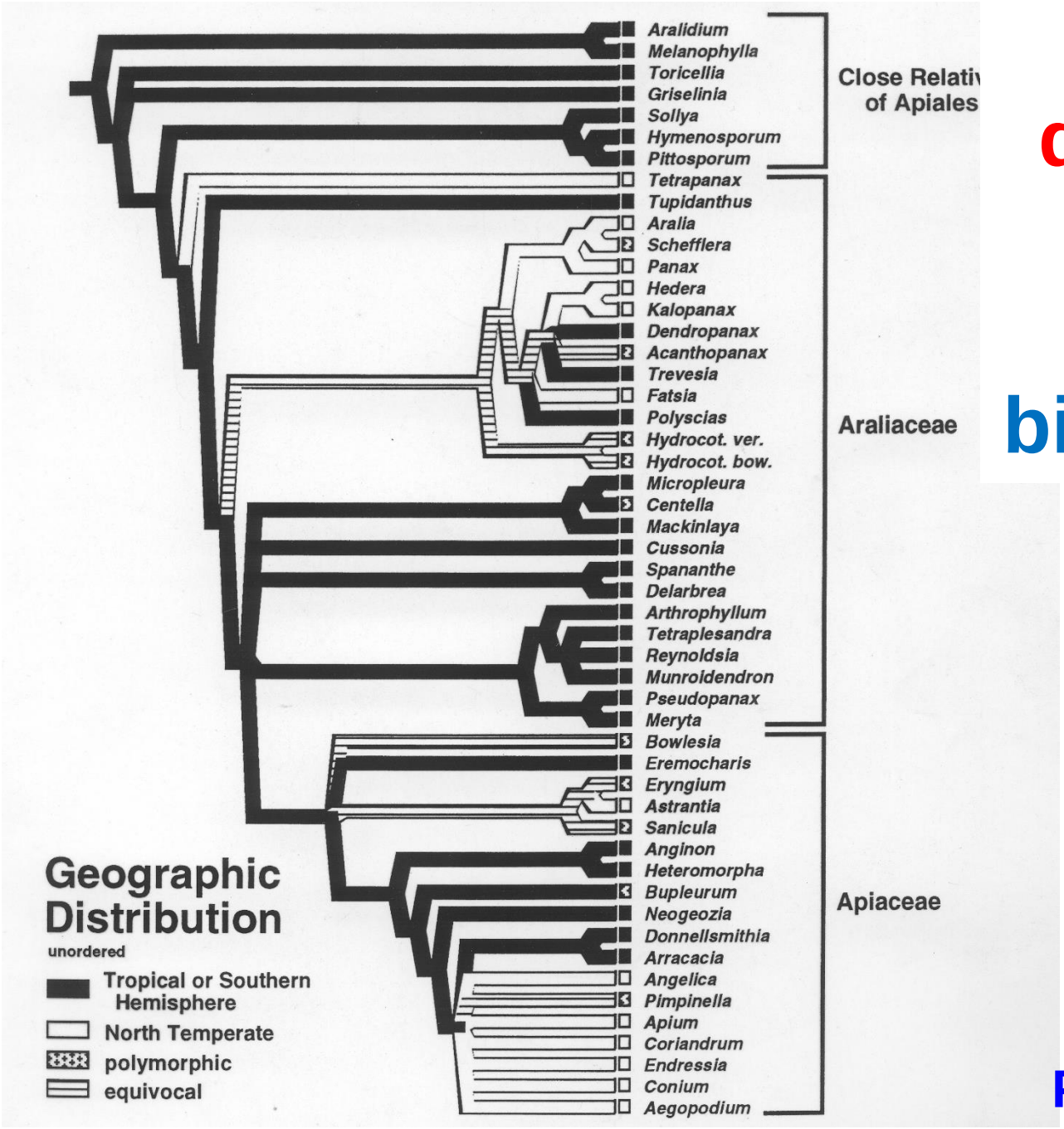

Plunkett et al. 1996

Filogenia de Araucariaceae com mapeamento das áreas geográficas

Givnish 2004

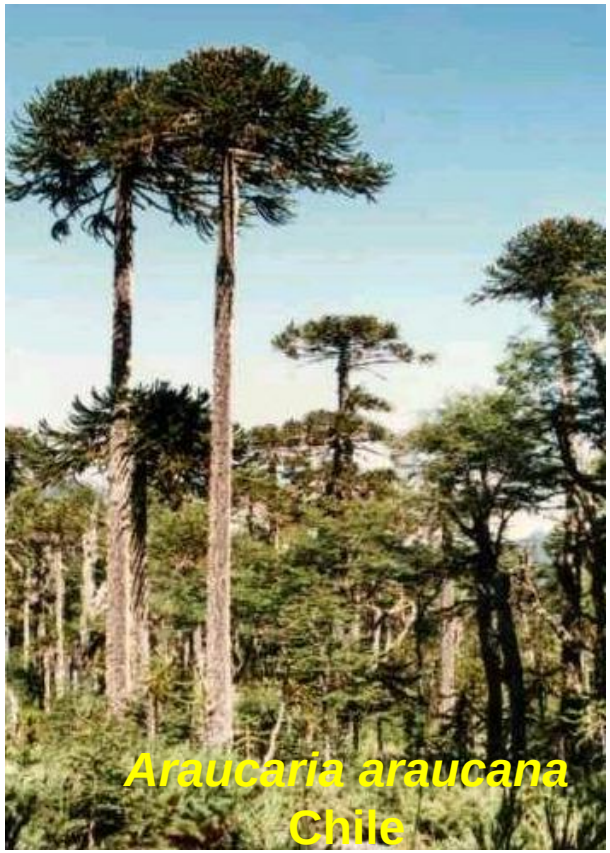

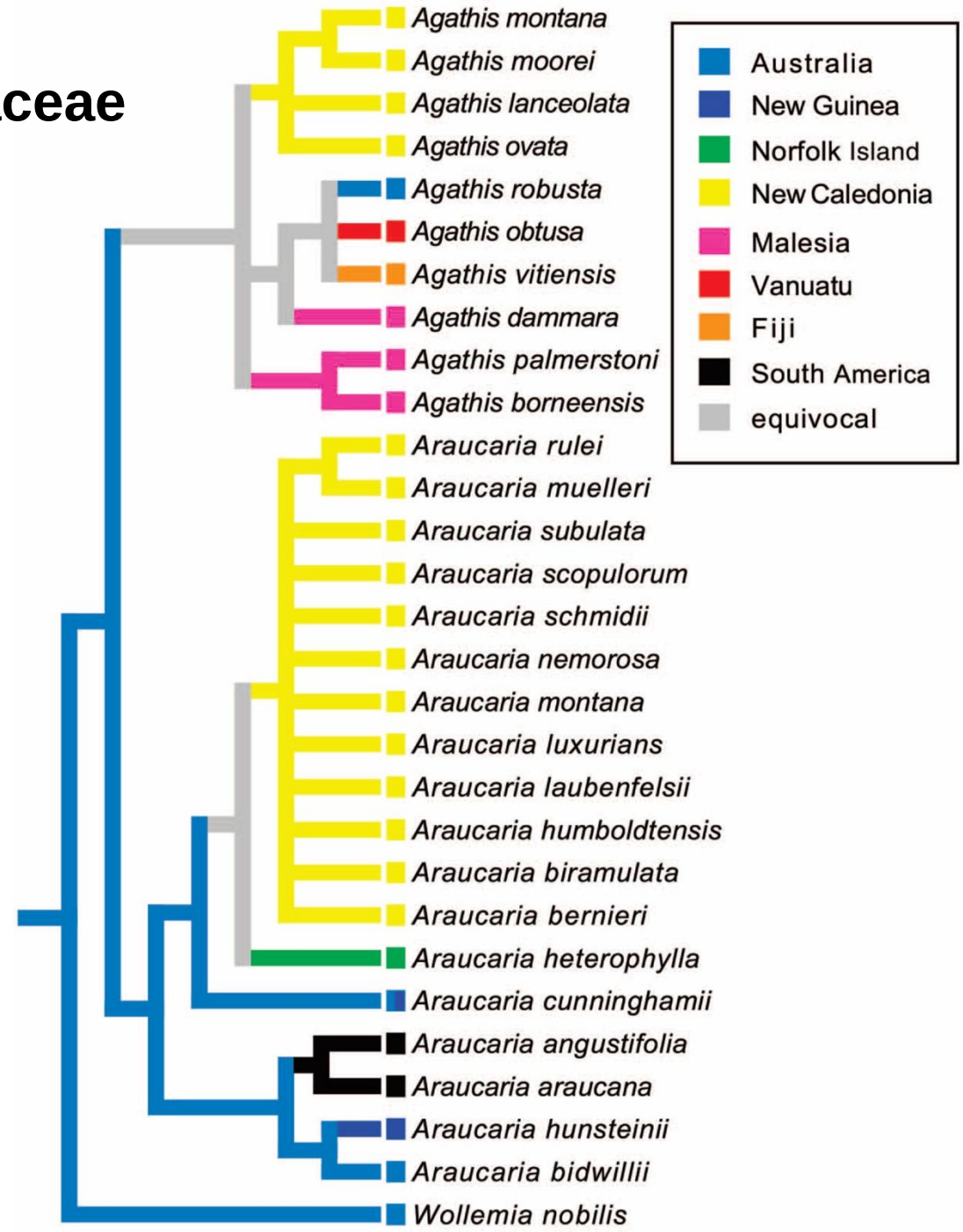

Craspedia ASTERACEAE

Ford *et al.* 2007

Taxon 56(3)

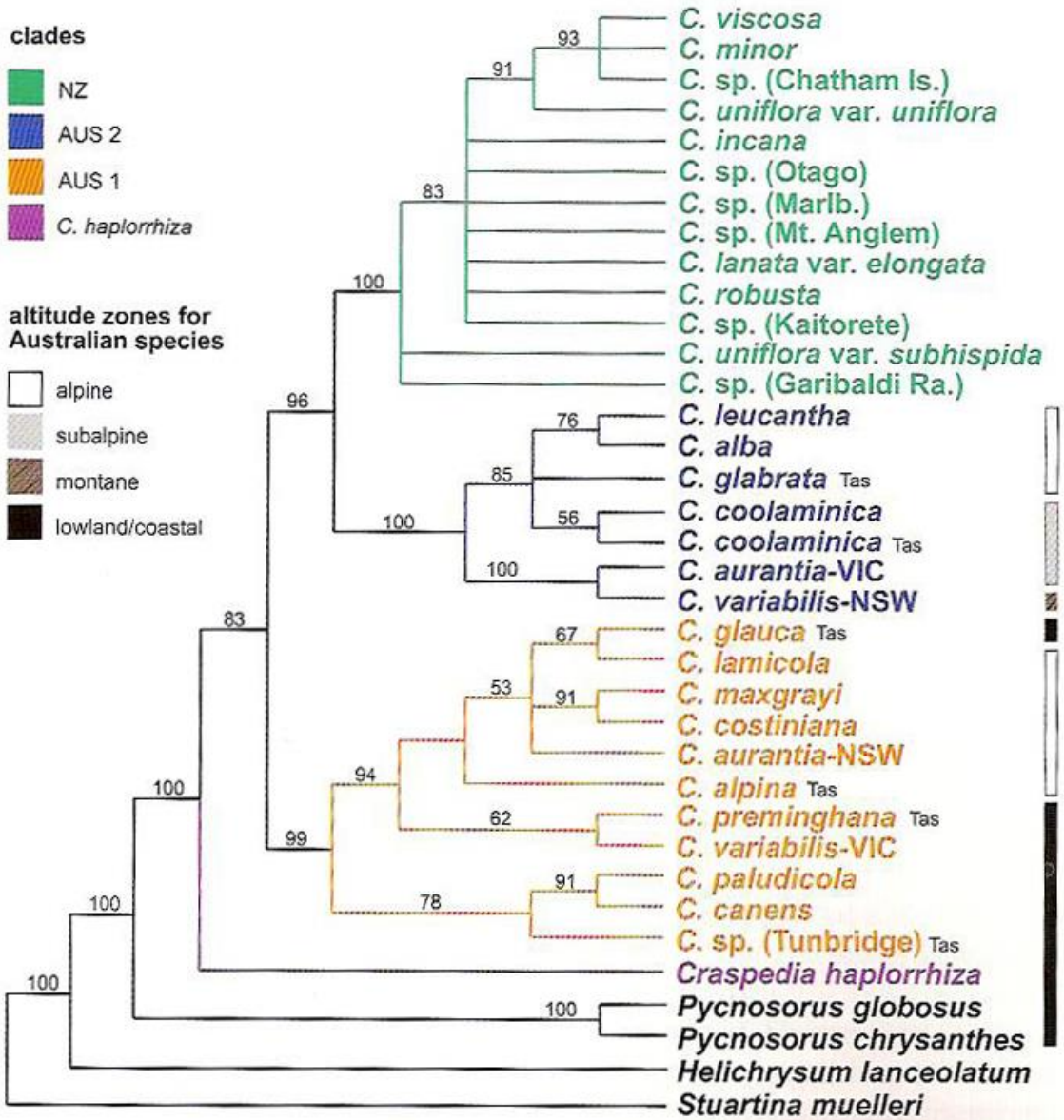

Fig. 3. Strict consensus of shortest parsimony trees for combined ITS and ETS sequences, with bootstrap values. Tas, Tasmania.

Mapping extrinsic traits such as extinction risks or modelled bioclimatic niches on phylogenies: does it make sense at all?

Grandcolas et al. 2010

Three different problems are implied by the trend in using a increasing variety of **extrinsic traits** in comparative studies aimed at testing evolutionary hypotheses.

Some extrinsic traits are only surrogates for phenotypic traits, and should be redefined to better fit the requisites for phylogenetic analysis, such as selective regimes and extinction risks.

Some others are already adequately defined and cannot be made less extrinsic, such as **taxon age, geographical distribution, associates** (parasites, symbionts, etc.), **and bioclimatic modelled niches.** Because **they are not heritable**, **they should not be analysed by optimization onto a tree,** but are **better considered in sister-group comparisons or within a reconciliation procedure, as already done for areas of biogeography.**

The Molecular Clock
Relógio Molecular

T. Michael Dodson

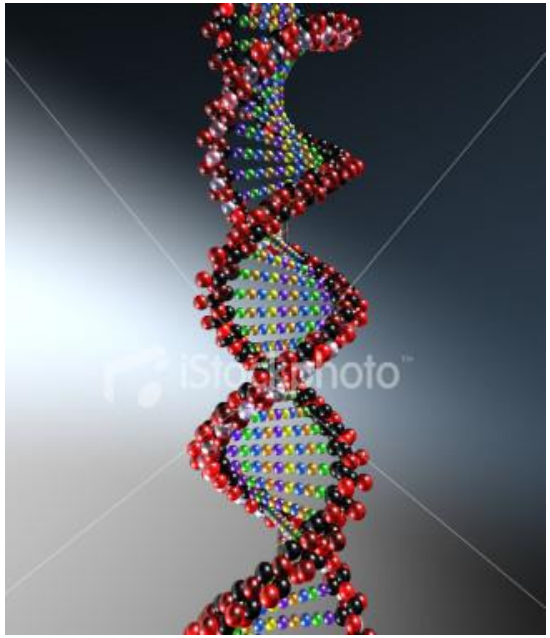

Relógio Molecular

- 1960s- Zuckerkandl & Pauling observaram que um número de diferenças entre aminoácidos e hemoglobinas mostravam uma relação aproximadamente linear com o tempo de divergência a partir do ancestral comum (estimado com registro fóssil).

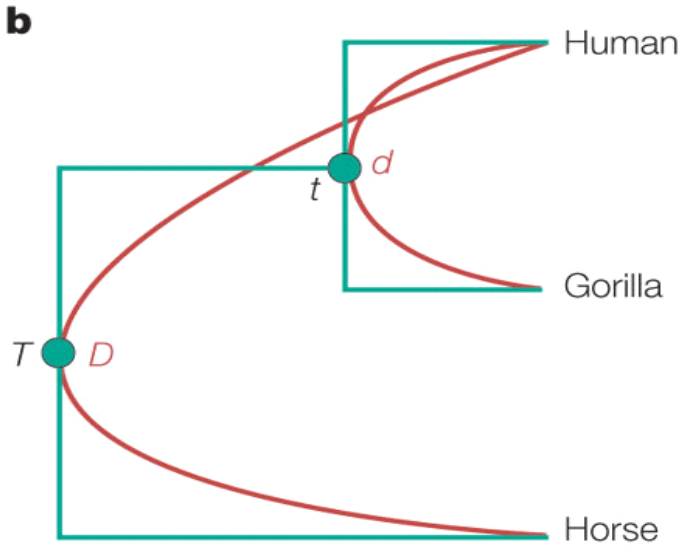

Nature Reviews | Genetics

Relógio Molecular
Hipótese

- “For any given macromolecule (a protein or DNA sequence) the rate of evolution is approximately constant over time in all evolutionary lineages” (Zuckerkandl & Pauling 1965 *in* Wen-Hsiung Li 1997)

Linus Pauling

Emile Zuckerkandl

Teoria do Relógio Molecular

Zuckerland & Pauling 1962:

Taxa de evolução molecular é aproximadamente constante no tempo para todas as proteínas em todas as linhagens.

Tempo de divergência entre proteínas, genes ou linhagens pode ser estimado por meio do n° de mudanças entre seqüências (ou proteínas) uma vez que as alterações moleculares acumulam nas populações em função do tempo.

Tempo de coalescência: a diferença entre seqüências de DNA num gene em 2 espécies seria proporcional ao tempo em que elas divergiram de um ancestral comum (MRCA).

Teoria do Relógio Molecular

"Tics" do relógio correspondem às mutações ou substituições; não ocorrem em intervalos regulares, mas em momentos ao acaso. Esse tempo pode ser estimado em unidades arbitrárias e então calibrado em milhares ou milhões de anos para um dado gene.

Assume-se que o gene tenha evolução neutra e que esta tenha taxa constante no tempo - embora variável entre genes:

- mtDNA tem taxa de mutação 10 x maior que a média dos genes cromossômicos humanos = presta-se para estudos em nível de raças;
- genes que codificam para histonas, citocromo c, ATPase, rRNA – taxa bem baixa = adequados para inferir relações em altos níveis hierárquicos, incluindo Eubacteria e Archaeobacteria!

Hawaii

Bromham & Penny 2003

- Honeycreeper (ave)

- Fruitflies (drosofilídeos)

- Molecular dates form a linear relationship between genetic divergence and time

Havaí

Bromham & Penny 2003

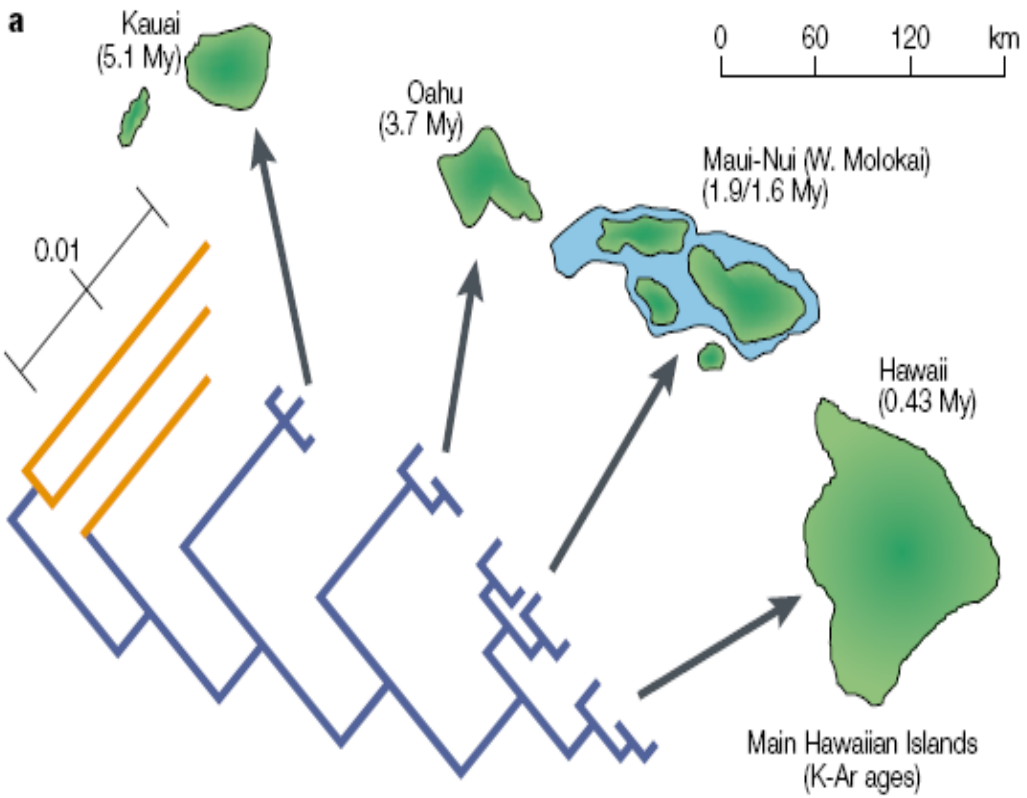

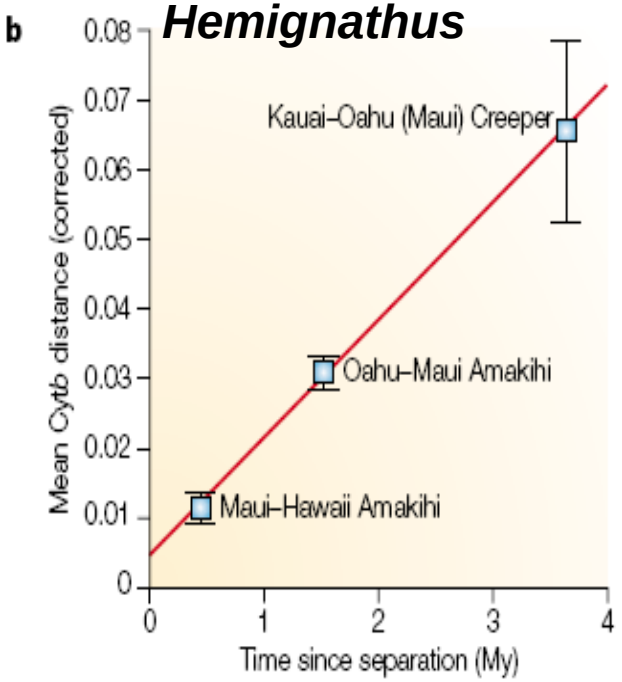

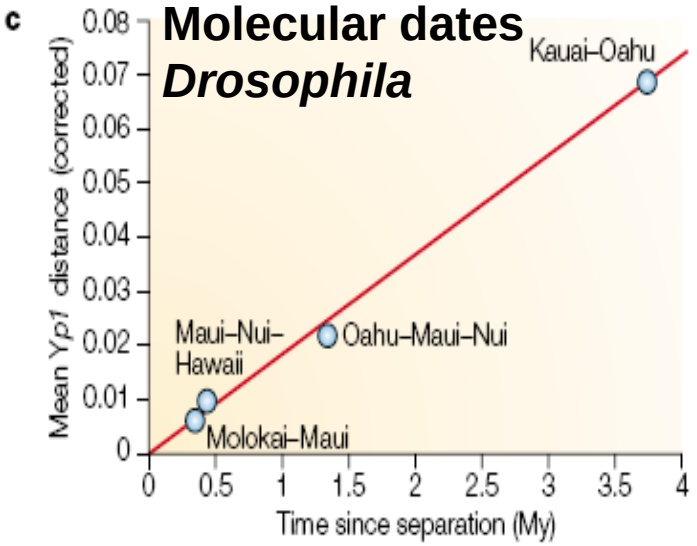

Figure 2 | **A molecular clock for the Hawaiian islands. a** | The volcanic origin of the Hawaiian islands has produced a chain of islands of increasing geological age. The phylogenetic relationships of island endemic birds (for example, the drepananine (honeycreeper) species such as the amakihi, *Hemignathus virens* and the akiapolaau *Hemignathus wilsoni*, shown in the tree) and fruitflies (*Drosophila* spp.) reflect this volcanic 'conveyer belt', with the species of the oldest islands forming the deepest branch of the tree, and the younger islands on the tips of the tree. Orange lines represent the outgroups. **b,c** | Molecular dates for *Hemignathus* (panel **b**) and *Drosophila* (panel **c**) confirm this order of colonization, and produce a remarkably linear relationship between genetic divergence and time when DNA distance is plotted against island age. My, million years. Figures reproduced with permission from REF. 10 © (1998) Blackwell Publishing.

Teoria do Relógio Molecular

Calibração do relógio: 2 modos:

1. Registro fóssil (bem datado e diagnosticado)

Usam-se pelo menos 2 spp atuais cuja época de especiação possa ser estimada pelo registro fóssil, para determinar o tempo transcorrido desde a especiação;
Determina-se a sequência de DNA do mesmo gene para as 2 spp modernas e infere-se ou conta-se diretamente o n° de substituições de nucleotídeos entre seus genes.
Assume-se que todas as subst. inferidas ou observadas tenham aparecido subsequentemente ao evento de especiação.

Taxa de evolução do DNA para o gene em estudo =
n° de diferenças no DNA entre as 2 spp. / tempo desde especiação

Teoria do Relógio Molecular

Calibração do relógio: 2 modos:

1. Registro fóssil

Assumindo-se que a taxa de mutação seja relativamente constante no gene em estudo,
usa-se essa taxa estimada para extrapolar as datas aproximadas de especiação de outras ssp. para as quais não se possa determinar a data de especiação a partir de fóssil.

Maioria dos grupos carece de bons fósseis, então muitas vezes usa-se taxas calibradas para outros grupos!

Numerosas substituições de nucleotídeos entre spp + topologia consistente com origem das ssp a partir do MRCA

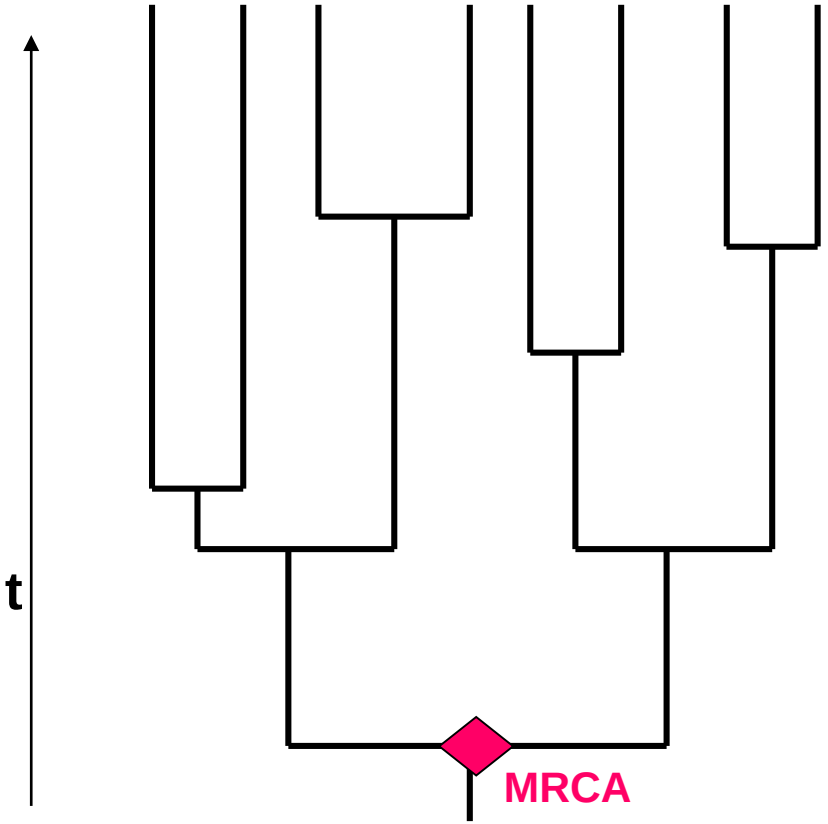

Acumulação gradual de diversidade a partir do MRCA (Ancestral Comum Mais Recente) das spp atuais, resultando em filogenia resolvida

Poucas substituições de nucleotídeos diferenciando spp + topologia com ramos curtos a partir do MRCA onde a diversificação iniciou

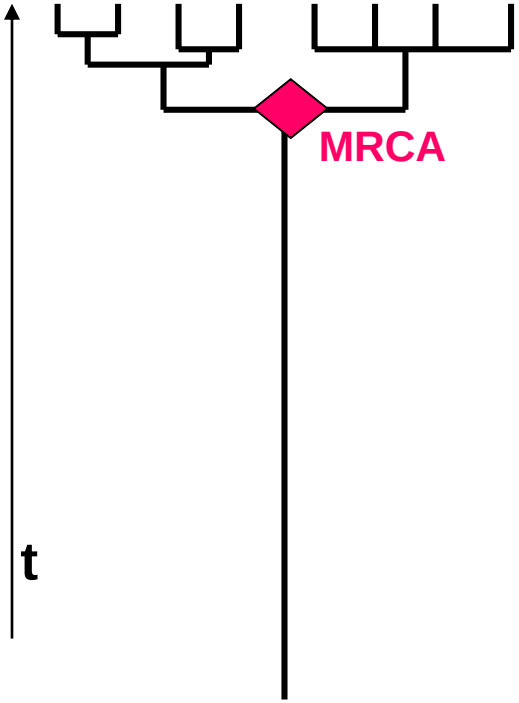

Diversificação rápida e recente a partir do MRCA das spp. atuais, resultando em filogenia com baixa resolução

Modelo de MUSEU (Wallace 1878, Stebbins 1974)

numerosas substituições de nucleotídeos entre spp + topologia consistente com origem das ssp a partir do MRCA

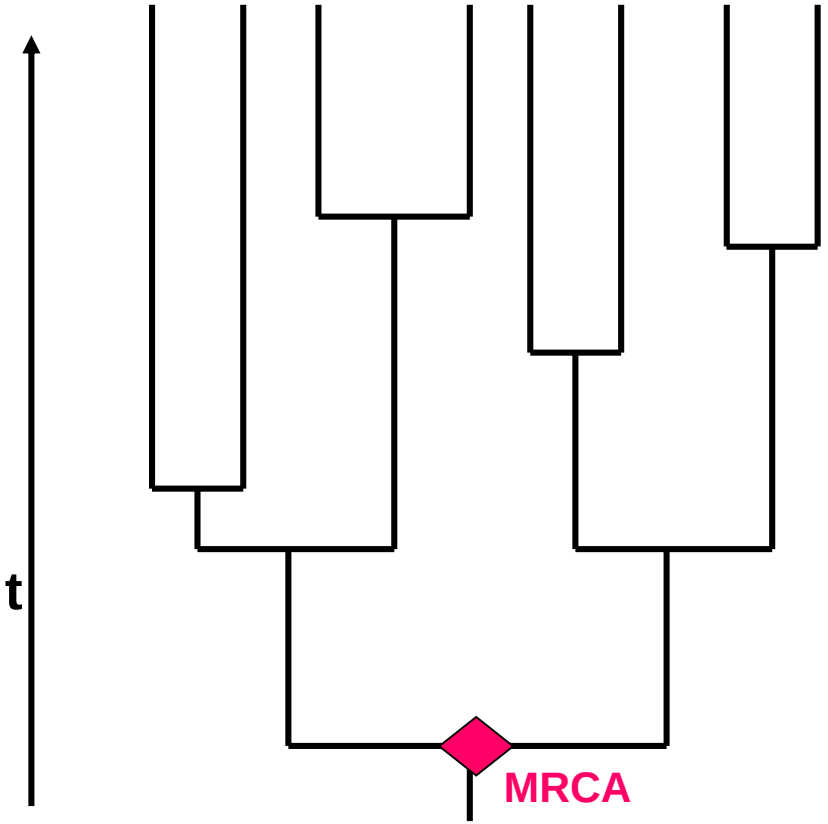

Acumulação gradual de diversidade a partir do MRCA (Ancestral Comum Mais Recente) das spp atuais: filogenia resolvida

Baixa taxa de EXTINÇÃO

Modelo de BERÇÁRIO (*cradle*) (Stebbins 1974)

poucas substituições de nucleotídeos diferenciando spp + topologia com ramos curtos a partir do MRCA onde a diversificação iniciou

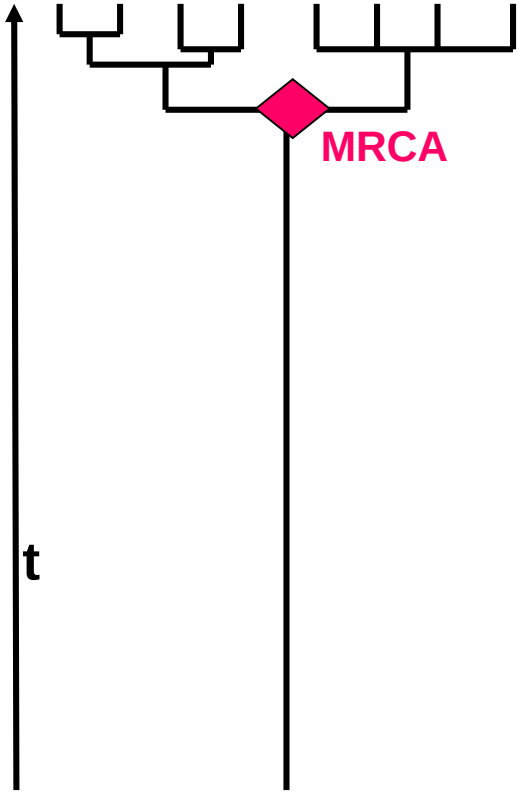

Diversificação rápida e recente a partir do MRCA das spp. atuais: filogenia com baixa resolução

Alta taxa de ESPECIAÇÃO

Cronobiogeografia – permite avaliar os dois modelos

Tempo estimado de divergência a partir do MRCA das spp. de *Inga* com base no n° médio de substituições a partir da diversificação de *Inga* de acordo com relógio molecular calibrado a partir de outros táxons

Fonte da taxa	Habitat /tempo mínimo de geração	Marcador	Taxa calibrada (subst./sítio/ano)	Tempo médio de divergência (m.a.)
Astragalus	ervas anuais/1-2 anos	ITS	$3,5 \times 10^{-9}$	6,6
Gossypium	arbustos perenes/1-3 anos	ITS1	$5,0 \times 10^{-9}$ a $9,0 \times 10^{-9}$	7,3 a 4,0
Gossypium	arbustos perenes/1-3 anos	ITS2	$2,5 \times 10^{-9}$ a $4,5 \times 10^{-9}$	4,6 a 2,6
Inga	árvores e arbustos/2-3 anos	ITS	$2,34 \times 10^{-9}$	9,8
Lupinus	ervas perenes ou anuais /1-2 anos	ITS1/ITS2	$3,6 \times 10^{-9}$/ $3,3 \times 10^{-9}$	10,1/3,5
Inga	árvores e arbustos/2-3 anos	*trnL-F*	$8,24 \times 10^{-9}$	1,6
Phylica	árvores e arbustos/2-3 anos	*trnL-F*	$4,87 \times 10^{-9}$	4,3
Aichryson	ervas perenes ou anuis/1-2 anos	*trnL-F*	$8,24 \times 10^{-9}$	0,3

Richardson et al. 2001

Richardson et al. 2001

ITS:
Em média, espécies de *Inga* têm no ITS 14 substituições a partir do nó do MRCA até o ápice de cada ramo.
10 das outras estimativas de ITS caem entre 1,72 x 10^{-9} e 7,83 x 10^{-9} s/s/ano.

Com base nessas estimativas -
tempo de diversificação de *Inga* fica entre 13,4 e 2,0 m.a. (média de 5,9 m.a.)

trnL-F:
Indica tempo de diversificação entre 4,3 m.a. e 300.000 anos (média 1,8 m.a.)

Congruência entre as estimativas das taxas de divergência molecular de 658 genes nucleares e as estimativas derivadas diretamente do registro fóssil de Synapida e Diapsida (Kumar & Hedges 1998)

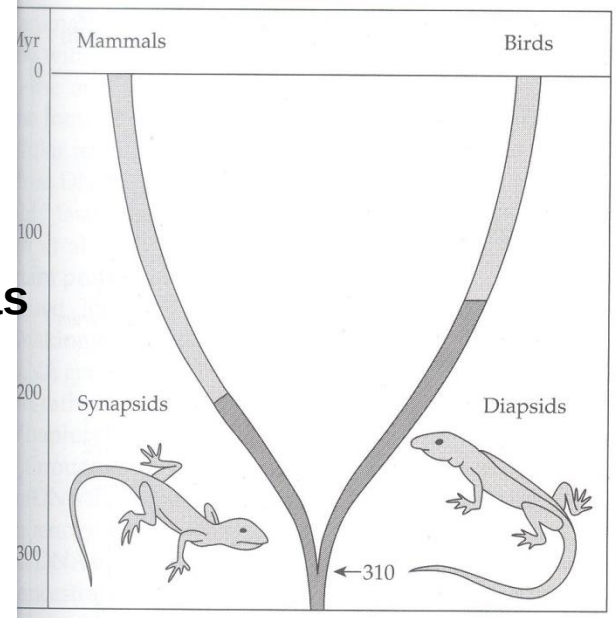

A

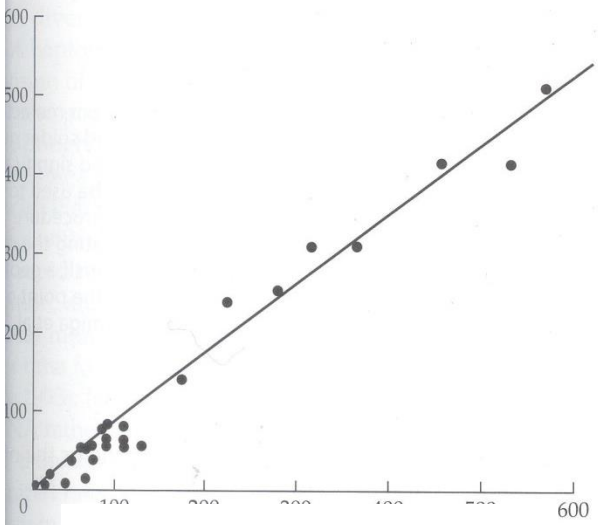

B

Datação com fóssil m.a.

Datação molecular m.a.

FIGURE 11.8 (A) Calibration of molecular divergence times from the fossil record requires one or more well-dated and diagnostic fossils that can be used to "fix" the time of a cladogenetic divergence event. In this case, synapsids—the stem amniote lineage (darker shading) leading to mammals (lighter shading), and diapsids—the stem amniote lineage (darker shading) leading to birds (lighter shading) have diagnostic cranial morphologies that allow paleontologists to infer a "first appearance" of each in the fossil record at 310 million years ago. (B) This point was then used to estimate rates of molecular divergence across 658 different nuclear genes (details of estimation methods provided in original article), and the composite estimates derived from all genes agreed remarkably well with estimates derived directly from the fossil record. (After Kumar and Hedges 1998.)

Lomolino et al. 2006

Datação Molecular

Calibração do relógio mol.: 1. Registro fóssil:

- Usam-se pelo menos 2 spp atuais cuja época de especiação possa ser estimada pelo registro fóssil, para determinar o tempo transcorrido desde a especiação;

- Assume-se que todas as subst. inferidas ou observadas tenham aparecido subsequentemente ao evento de especiação.

*Viés: o fóssil só fornece a **idade mínima** do grupo (Heads 2012):*

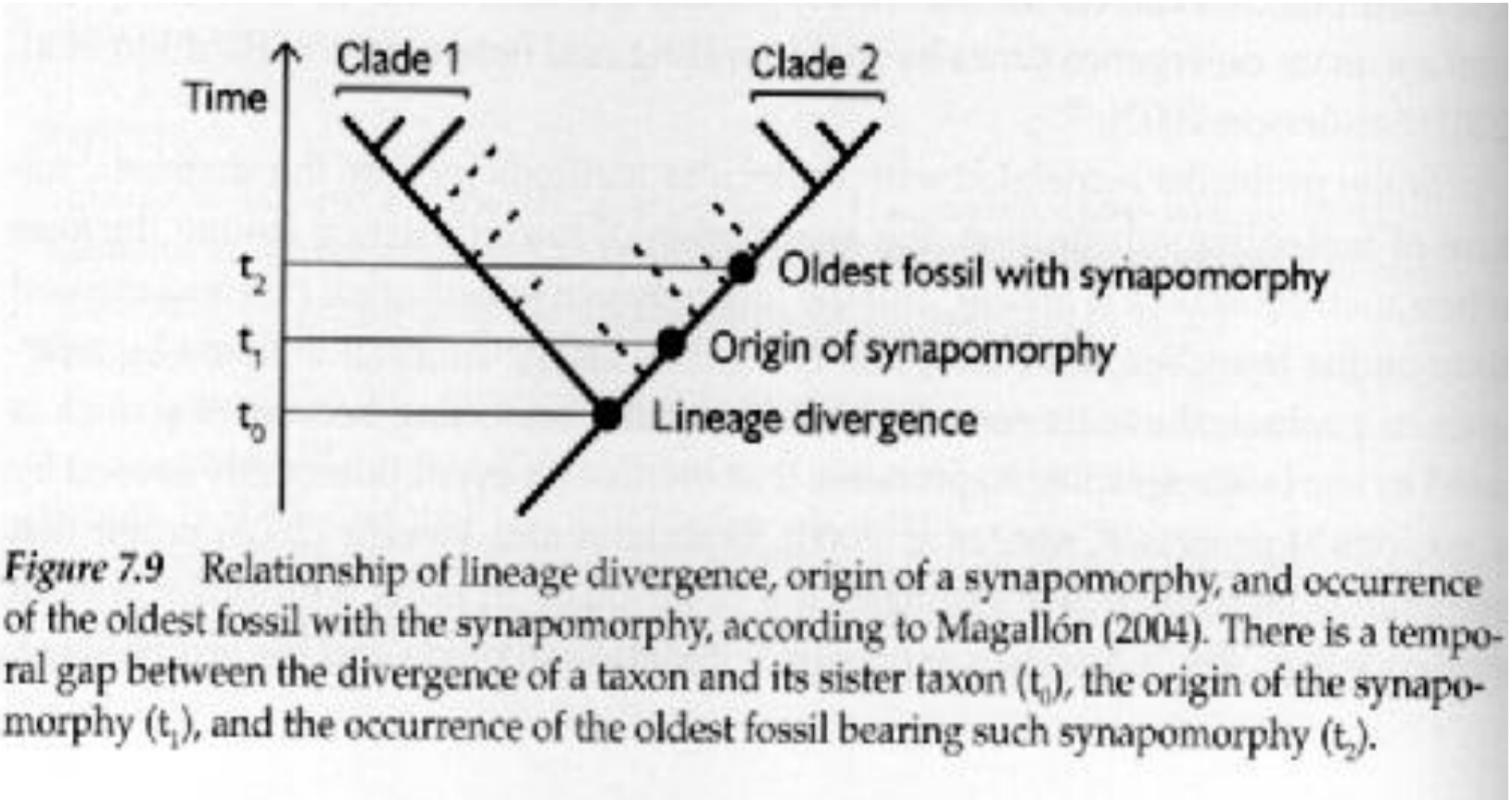

Figure 7.9 Relationship of lineage divergence, origin of a synapomorphy, and occurrence of the oldest fossil with the synapomorphy, according to Magallón (2004). There is a temporal gap between the divergence of a taxon and its sister taxon (t_0), the origin of the synapomorphy (t_1), and the occurrence of the oldest fossil bearing such synapomorphy (t_2).

Morrone 2009

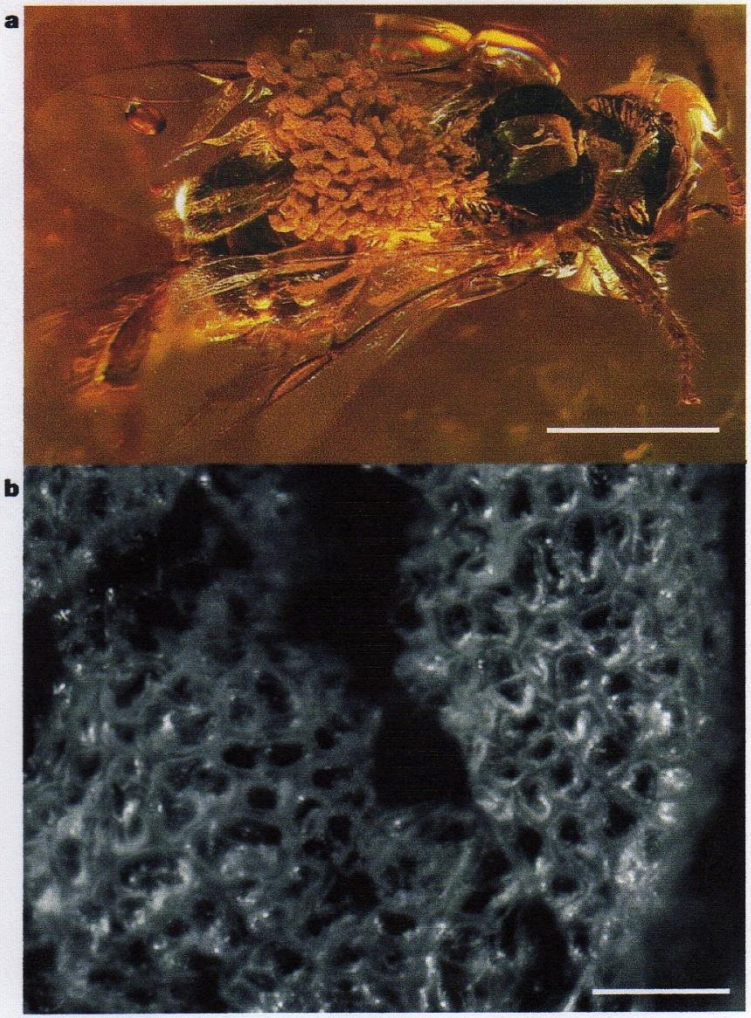

Figure 1 | Holotype of *Meliorchis caribea* gen. et sp. nov. This orchid pollinarium, carried by a worker stingless bee (*Proplebeia dominicana*), is preserved in amber from the Dominican Republic and represents the first definitive fossil record for the family Orchidaceae. **a**, General view of encapsulated specimen (scale bar, 1,000 μm). **b**, Detailed view of the pollinia surface showing pollen units (scale bar, 50 μm).

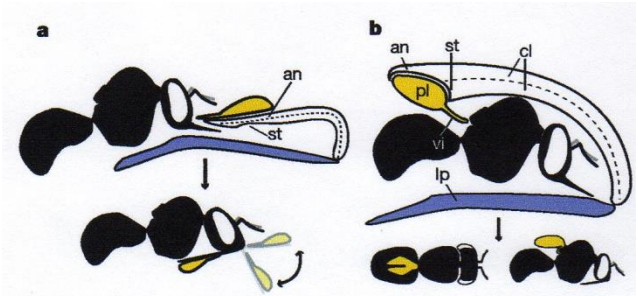

Figure 2 | Morphology and pollinarium placement of modern Goodyerinae and hypothetical reconstruction of floral morphology of *Meliorchis caribea*. **a**, The parallel lip (lp) and column (cl) and the erect anther (an) of extant Goodyerinae typically result in the pollinarium (pl) attachment on the pollinator's mouthparts. **b**, The attachment of the pollinarium to the mesoscutellum (dorsal surface of thorax) of a worker bee is only possible when the lip and column of the flower are parallel but the anther is bent. Under this scenario, the distance between the lip and the column must be ~2.5 mm to enable a *P. dominicana* worker to crawl into the flower and remove the pollinarium with its mesoscutellum as it retreats; st, stigma; vi,viscidium.

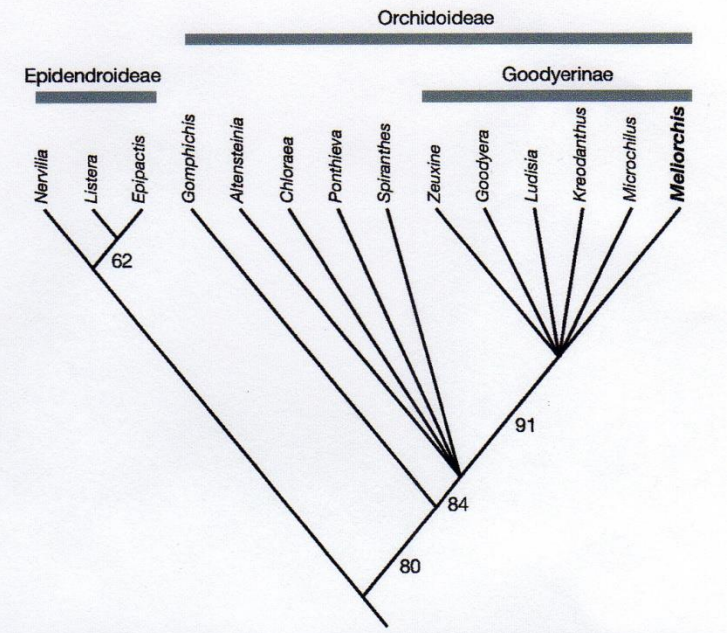

Figure 3 | Cladogram showing the estimated position of *Meliorchis* among modern clades in the orchid subfamily Orchidoideae. A strict consensus of the 129 shortest trees (tree length = 42, consistency index = 0.619, retention index = 0.660) obtained using 25 morphological characters for 15 taxa; values beside nodes correspond to bootstrap percentages (1,000 replicates). None of the shortest trees recovered *Meliorchis* as sister to all the other Goodyerinae included.

Ramirez et al. 2007 Nature 448

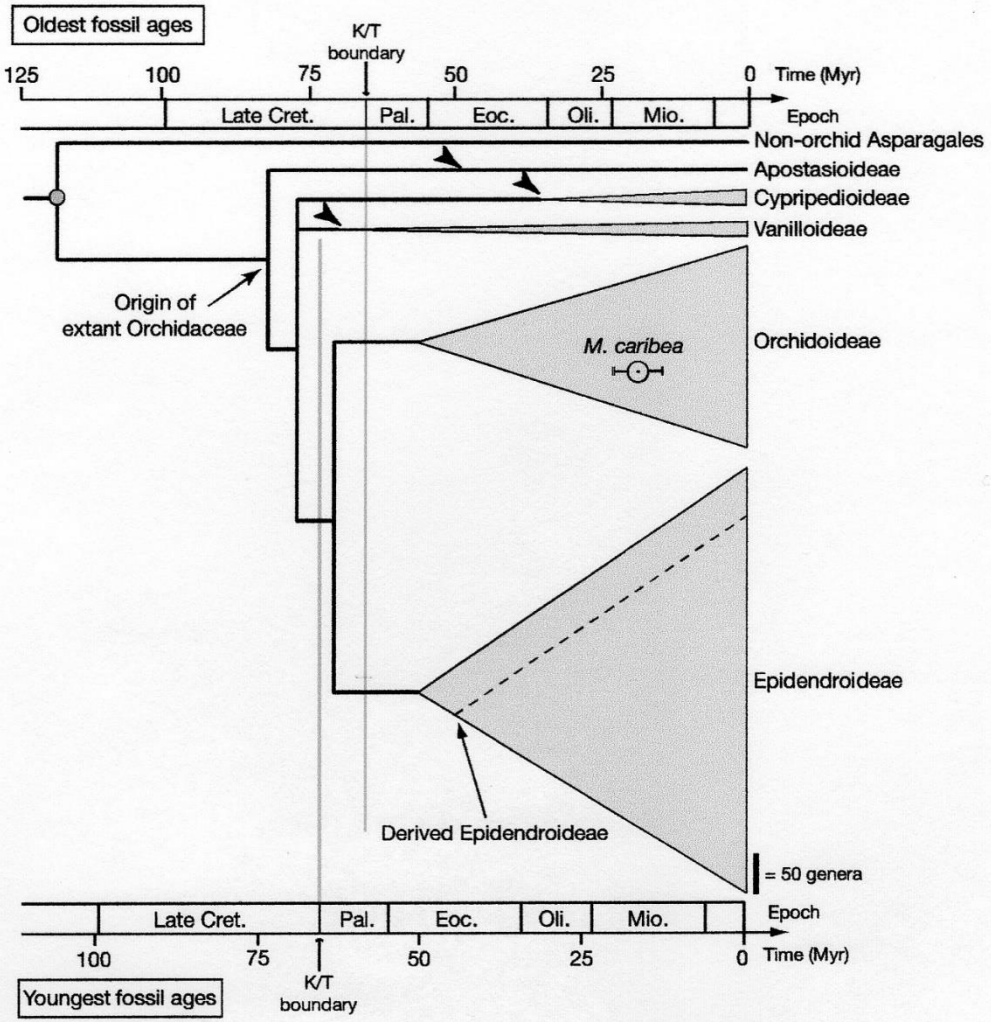

Figure 4 | Fossil-calibrated molecular clock chronogram of the family Orchidaceae, based on ~3 kilobases of plastid DNA (*matK* and *rbcL*). The relative size of each clade is proportional to the number of genera described in each orchid subfamily. Crown ages of small clades are indicated with arrow heads. Two sets of dates were used to calculate orchid divergence times: the oldest and youngest estimates of the ages of the fossils. The age boundaries of *M. caribea* (15–20 Myr old) relative to each timescale correspond to the distance between the circle's centre and the vertical bar. Additional monocot fossil records outside Orchidaceae were used to calibrate the root of the tree (node indicated by filled circle). Branch lengths were optimized under the maximum likelihood model of sequence evolution GTR+Γ+I using a 95% majority-rule consensus tree (see Supplementary Information); node ages were estimated using a penalized likelihood method[29].

Ramirez et al. 2007 Nature 448

Datação Molecular

Calibração do relógio:

2. Evento geológico (Sanderson 1998)

Por exemplo, eventos da deriva continental.

Viés: Risco de circularidade de raciocínio, quando o relógio é usado para testar hipótese biogeográfica envolvendo um evento potencialmente causado por processo geológico.

3. Idade de uma ilha ou da camada estratigráfica de um táxon endêmico

Procedimento muito criticado!
Viés: Ilhas e estratos jovens geralmente têm táxons antigos.

Tectonic Blocks and Molecular Clocks

De Baets et al. 2016

Evolutionary timescales have mainly used fossils for calibrating molecular clocks, though fossils only really provide minimum clade age constraints.

In their place, phylogenetic trees can be calibrated by precisely dated geological events that have shaped biogeography.
However, tectonic episodes are protracted, their role in vicariance is rarely justified, the biogeography of living clades and their antecedents may differ, and the impact of such events is contingent on ecology.

Biogeographic calibrations are no panacea for the shortcomings of fossil calibrations but their associated uncertainties can be accommodated.

Authors provide examples of how biogeographic calibrations based on geological data can be established for (i) the fragmentation of the Pangean Supercontinent: (ii) for the uplift of the Isthmus of Panama, (iii) the separation of New Zealand from Gondwana, and (iv) for opening of the Atlantic Ocean.

Biogeographic and fossil calibrations are complementary, not competing, approaches to constraining molecular clock analyses, providing alternative constraints on the age of clades that are vital to avoiding circularity in investigating the role of biogeographic mechanisms in shaping modern biodiversity.

Calibração do relógio:

2. Evento geológico

Exemplo:
Richardson et al. 2001 – ausência de fósseis em *Inga* = estimativa das taxas de substituição com base no soerguimento do Istmo do Panamá (~3,5 m.a.) = o primeiro momento em que spp de *Inga* (dispersas por primatas) migraram para América Central.

Estima-se a taxa de subst. comparando-se o n° de subst. entre pares de ssp relacionadas da AC-AS e traduzindo a divergência em seqüências para taxa de subst. baseada em 3,5 m.a.:

ITS: *I. allenii* (endêmica da AC) é a sp mais divergente de seu par AS, com 5 subst. do MRCA = taxa de 2,34 x 10^{-9} s/s/ano.

tnrL-F : I. mortoniana* é a sp AC mais divergente, com 3 subst. = taxa de 1,3 x 10^{-9} *s/s/ano

Calibração do relógio:

2. Evento geológico

Exemplo:
Richardson et al. 2001 –

Aplicando essas calibrações para o n° médio de subst. a partir do MRCA de todas as spp atuais de *Inga,* obtém-se estimativa de 9,8 m.a. para ITS e 1,6 m.a. para *trnL-F* .

Mas ambos conjuntos de dados moleculares exibem alta heterogeneidade entre as linhagens, levando à necessidade de obtenção de árvores não paramétricas (NPRS):

calibração de datas com base nessas árvores e nas divergências de seqüências entre táxons de cada lado do Istmo do Panamá levaram a datação de 3,5 m.a. (*trnL-F*) e 5,9 m.a. (ITS).

Calibração do relógio:

Avaliação final:

Exemplo:

Richardson et al. 2001 –

Riscos de as 2 calibrações serem errôneas:

a) *Inga* pode ter dispersado pelo Istmo do Panamá antes de seu fechamento, uma vez que 10 spp. (8 amplas, 2 endêmicas insulares) ocorrem em ilhas do Caribe.

Mas estas representam apenas 3% da diversidade de spp de *Inga.* Por isso, dispersão a longa distância (sobre mar) deve ser rara, hipótese reforçada pelo fato de que as sementes têm viabilidade máxima de 1-2 semanas, reduzida a poucos dias caso retiradas do legume.

b) Pode ser inapropriado aplicar a *Inga* taxas de táxons não relacionados, pois diferentes linhagens com diferentes histórias de vida podem ter taxas de subst. diferentes!

Mas todos as taxas de ITS dos grupos comparados, e a maioria dos de *trnL-F* indicavam que a diversificação de *Inga* ocorreu nos últimos 10 m.a., o que também é consistente com a calibração pelo Istmo!

Calibração do relógio:

Avaliação final:

Exemplo:

Richardson et al. 2001 – *Inga*

Comparações de spp de *Inga* par a par (ITS) indicaram que 30% das spp. divergiram de seu MRCA dentro dos últimos 2 m.a.

Forte evidência de que para *Inga* a região neotropical seja um laboratório ativo de especiação, sugerindo que alta proporção da diversidade específica na Amazônia possa ter aparecido recentemente, promovida por:

1. fases recentes da orogenia andina (~5 m.a.) – o maior centro de diversidade de *Inga* fica no sopé dos Andes na Amazônia Ocidental;

2. conexão pelo Istmo do Panamá;

3. flutuações climáticas do Quaternário.

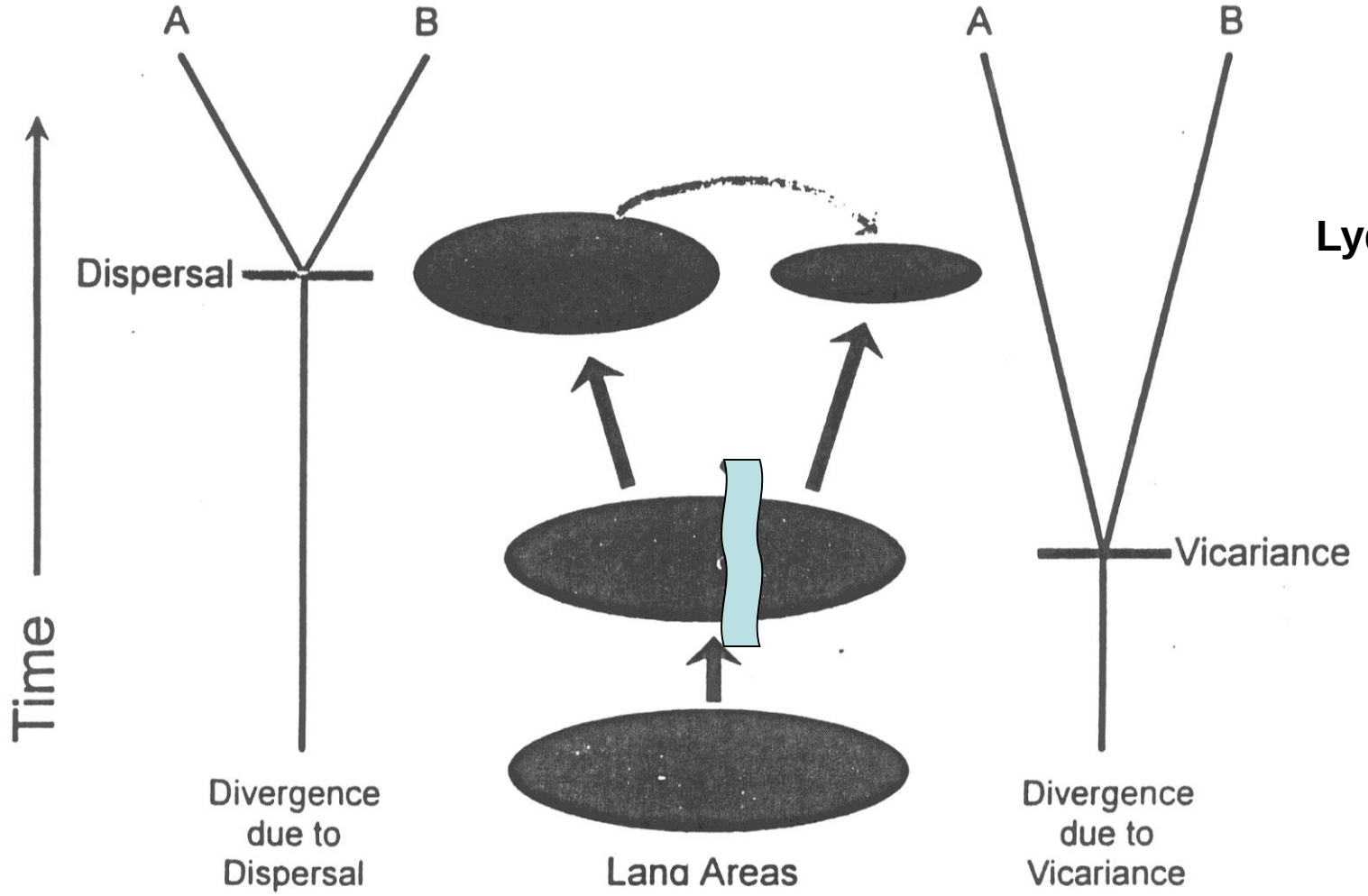

Page & Lydeard 1994

Fig. 1. Application of the time test in biogeographic analysis. Two groups on either side of a barrier are found to be sister taxa. Because the same phylogenetic relationships are expected with both models, examination of divergence times (through fossil evidence or molecular divergence) is necessary to distinguish between vicariance and dispersal. If the time of divergence between the two groups is shown to be significantly more recent than would be predicted by a vicariant event, then that vicariant event is rejected.

Bromham & Penny 2003: The modern molecular clock.

2002-hoje: “Relaxed molecular clocks”

Máxima Verossimilhança Penalizada – Sanderson 2002
(PMLE = Penalized Maximum Likelihood Estimation)

Multidivtime – Thorne & Kishino 2002, Shiguno 2005

PhyBase – Aris-Brosou & Yang 2002

BEAST – Drummond & Rambaut 2005 (http://beast.bio.ed.ac.uk)
BEAST v1.7.5 released 2013!
Critério bayesiano

(Será examinado em aula próxima)

2 tipos de modelos de “relaxed-clocks”:

1) assume que a taxa de evolução molecular varia ao longo do tempo e entre grupos de organisms,
mas que tal variação ocorre em torno de um valor médio estimável.

2) permite taxa evolutionária "evoluir" no tempo,
baseado na suposição de que a taxa de evolução molecular esteja ligada à evolução de outros caracteres biológicos.
Por ex: há evidência de que as taxas de substituição são influenciadas pela taxa de metabolismo do organismo.

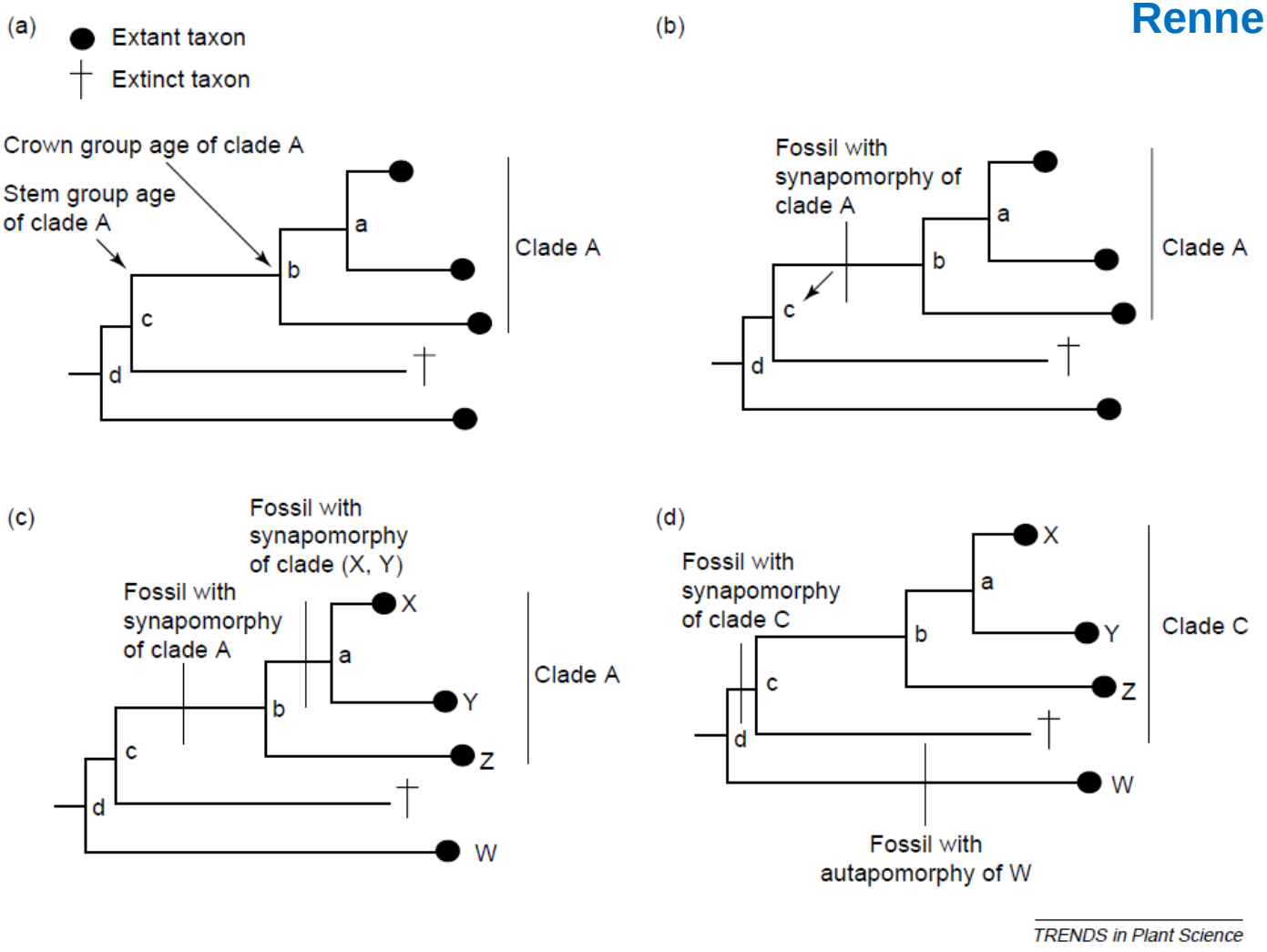

Figure 1. **(a)** Clade A, like every clade, has two ages, the age of its stem lineage and the age of its living 'crown' group. Molecular data concern the age of the crown group. Many seeming contradictions between molecule-based estimates and fossil-based estimates dissolve once the distinction of stem group age and crown group age is understood. Both ages are biologically relevant because each stem group (age) becomes a crown group (age) with the inclusion of phylogenetically more distant outgroups. **(b)** A fossil exhibiting a character that is synapomorphic for clade A could represent any point (time slice) along the stem of clade A. The only objective way to handle this problem is to take the age of the fossil as the minimum age of node c, the split between living representatives whose sequences are the dataset. **(c)** To constrain the crown age of clade A, a fossil with a synapomorphy of a subclade of A, such as (X,Y), is required. **(d)** Two fossils are available to constrain node d, with varying completeness of preservation and unequal reliability of dating. It seems best to use them sequentially and to evaluate the resulting time estimates against independent evidence, such as climate data, geological data, ages of coevolved organisms or biomes, or molecular clock-based estimates that rely exclusively on other calibration fossils, for instance, the fossil of (X,Y) used in (c).

GNETALES

Welwitschia

Ephedra

G. Heiden 2011

P. Fiaschi 2008

Gnetum

RELAXED MOLECULAR CLOCKS

Gnetum

- dados combinados de *rbc* e *matK*

- relógio mol. bayesiano relaxado

- restrito a idade mínima de fósseis nos nós 2 e 9

Won & Renner 2006

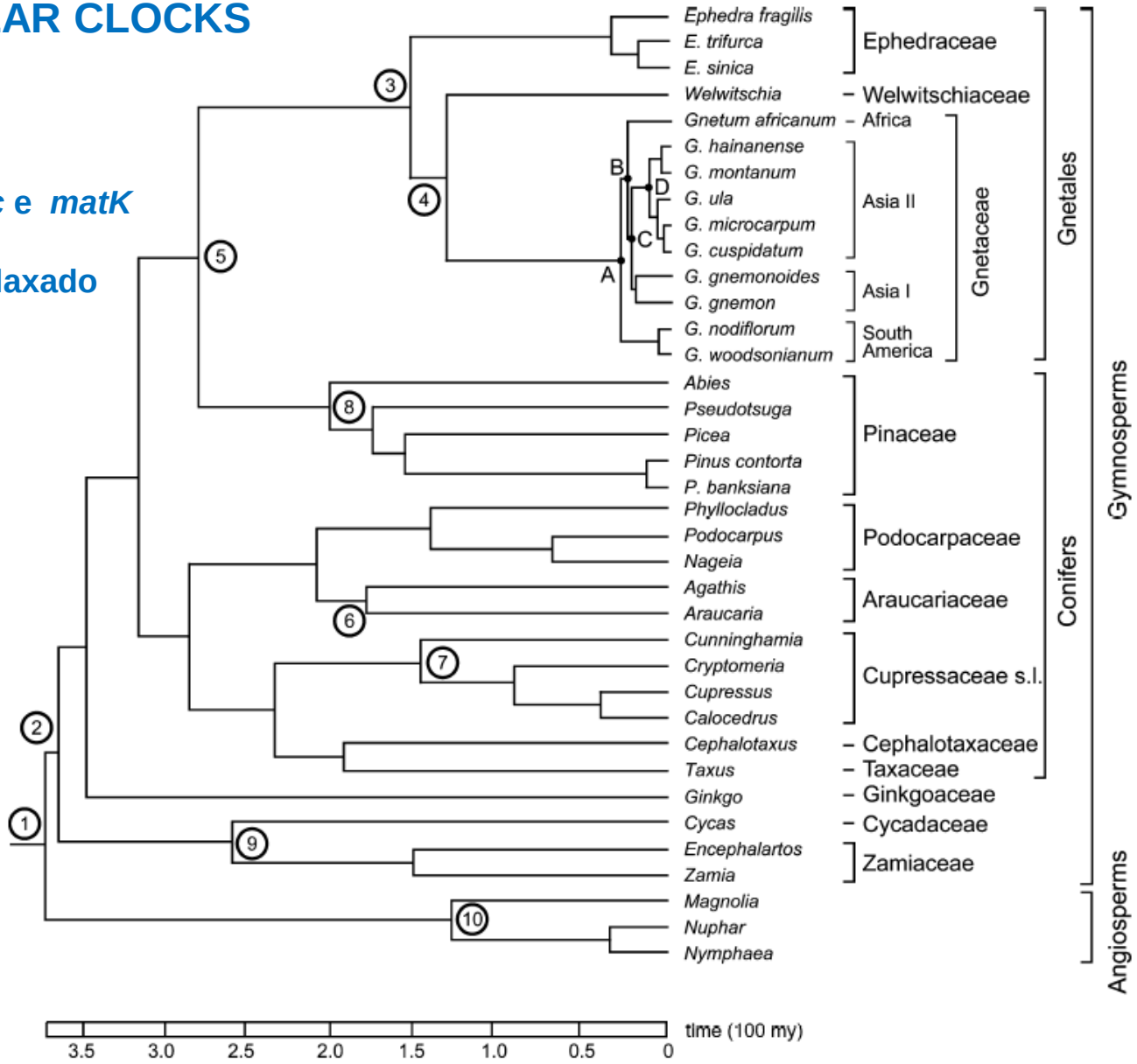

FIGURE 1. Divergence events in *Gnetum* estimated from the chloroplast genes *rbcL* and *matK* analyzed under a Bayesian relaxed clock, constrained by fossil-based minimal ages at nodes 2 to 9 (see Materials and Methods) and assuming that Gnetales are nested in the conifers (the so-called Gnepine topology). For results with four other seed plant topologies see Figures S1A–D. All analyses were rooted with *Psilotum* because the GenBank *matK* sequence of *Marchantia* appears to be a pseudogene. Nodes of particular biogeographic interest are A, the split between the South American clade of *Gnetum* and the remainder of the genus; B, the split between African and Asian *Gnetum*; C, the split between the two main Asian clades of *Gnetum*; and D, the onset of radiation of the most species-rich Asian clade.

RELAXED MOLECULAR CLOCKS

Gnetum **- dados combinados de DNA nuclear, plastidial e mitocondrial;**
máxima verossimilhança, modelo
GTR+G+I
Bootstrap parcimônia / probabilidade posterior bayesiana

Idades dos nós A-D (intervalo de confiança de 95%) baseadas em análise bayesiana em relógio relaxado de *matK* e *rbcL* (ver Tab. 1)

Won & Renner 2006

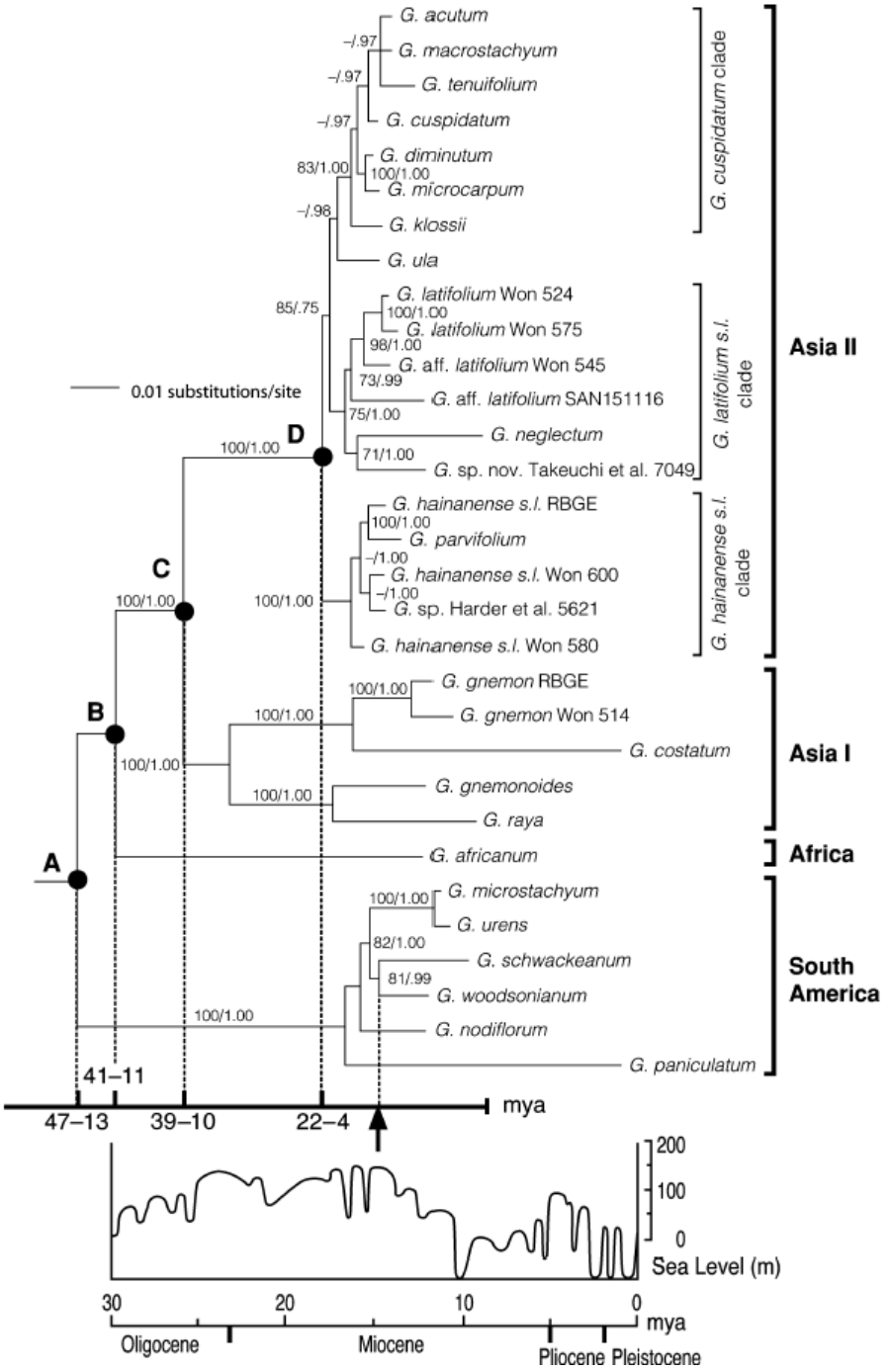

RELAXED MOLECULAR CLOCKS

Gnetum

Estimativas de tempo (m.a. + intervalos de confiança de 95%) dos nós A-D em relógio estrito calibrado com um fóssil no nó 4 (da fig. 1) e relógio relaxado de *matK* e *rbcL* (ver Tab. 1) restrito a 9 idades mínimas baseadas em fósseis.

TABLE 1. Time estimates (in million years, followed by 95% confidence intervals) for nodes A, B, C, D in Figures 1 and 2, and in Figures S1A–D, obtained from combined *matK* and *rbcL* sequences under a strict clock (row 1), calibrated with one fossil (Fig. 1, node 4), or a Bayesian relaxed clock (rows 2 to 7), constrained with 9 fossil-based minimal ages (Fig. 1 and Materials and Methods). Row 7 shows results obtained when 125-My-old *Ephedra* seeds were used as a minimal constraint for crown group *Ephedra*. Alternative input topologies are shown in Figure 1 and Figures S1A–D.

Model	Node A (split: South American vs. remaining *Gnetum*)	Node B (split: African vs. Asian *Gnetum*)	Node C (split: Asia I and II clades of *Gnetum*)	Node D (split: basal divergence within Asia II clade of *Gnetum*)
Strict clock, 13-taxon *matK/rbcL* data set	14	12-11	11	3
Relaxed clock, 38-taxon *matK/rbcL* data				
Constrained as in Figure 1 under the Gnepine topology	26 (13, 47)	22 (11, 41)	21 (10, 39)	11 (4, 22)
Constrained as in Figure S1A under the Gnetifer topology	29 (14, 51)	25 (11, 44)	24 (11, 43)	12 (5, 25)
Constrained as in Figure S1B under the Gnetales-sister topology	38 (19, 66)	33 (15, 58)	31 (15, 56)	17 (7, 34)
Constrained as in Figure S1C under the Anthophyte topology	37 (18, 64)	32 (15, 58)	30 (14, 55)	16 (6, 33)
Constrained as in Figure S1D with basal 4-tomy in gymnosperms	30 (14, 53)	26 (12, 47)	24 (11, 45)	13 (5, 26)
Constrained as in Figure 1 under the Gnepine topology, but *Ephedra* crown min. age set to 125 My	44 (23, 71)	38 (19, 64)	36 (18, 62)	20 (8, 39)

Won & Renner 2006

datações utilizadas na filogenia plotada no mapa

RELAXED MOLECULAR CLOCKS

Renner 2005

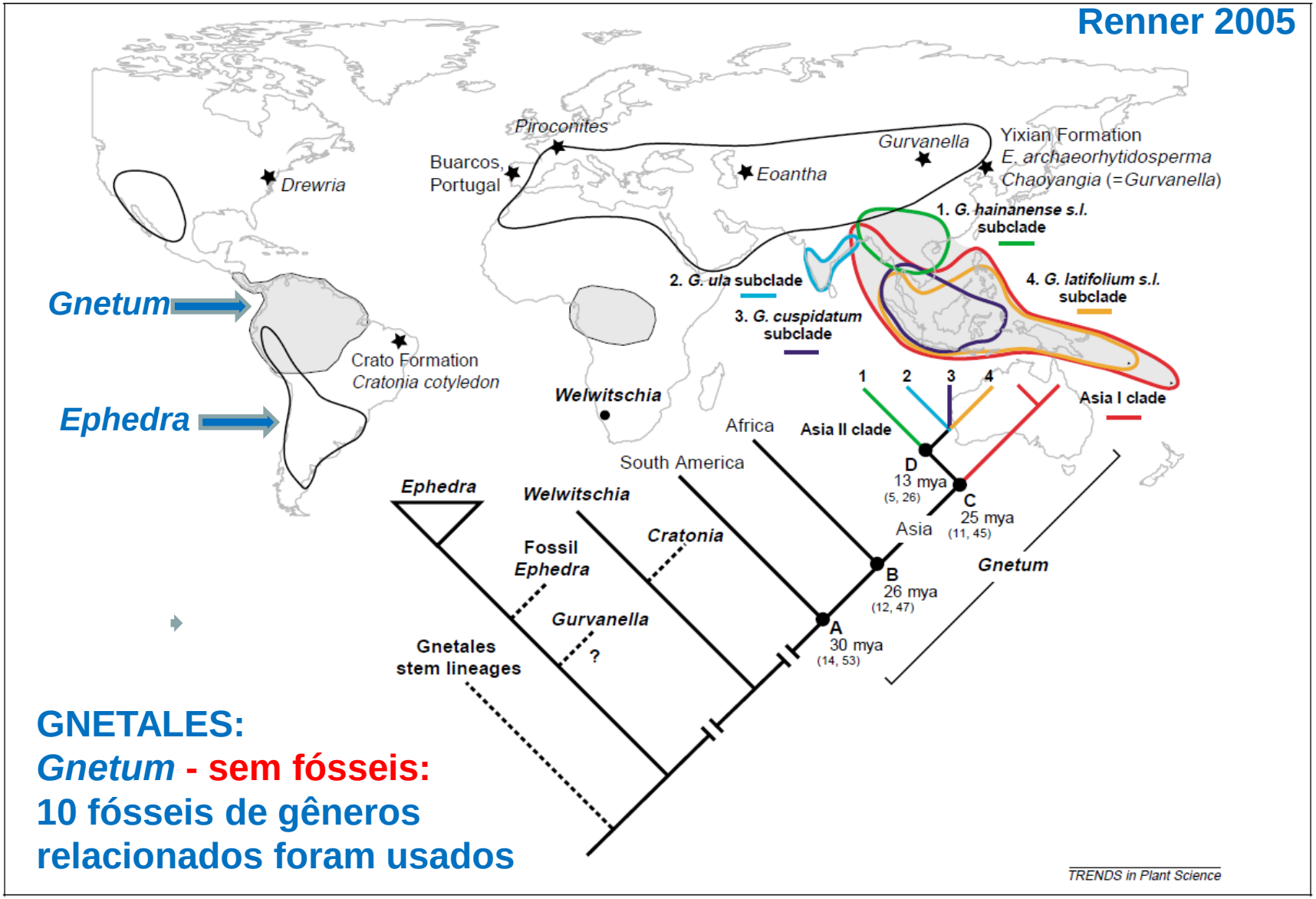

GNETALES:

***Gnetum* - sem fósseis:**

10 fósseis de gêneros relacionados foram usados

Figure 2. Former and current ranges of *Ephedra*, *Gnetum* and *Welwitschia* (Gnetales), and time estimates (with 95% confidence intervals) for major divergences within *Gnetum* from a Bayesian relaxed clock calibrated with ten seed plant fossils [119]. The ten seed plant fossils were needed to estimate divergence times within *Gnetum* because *Gnetum* itself has no fossils. The geographic range of *Gnetum* is indicated by the shaded areas, the non-shaded areas indicate that of *Ephedra*. The range of *Welwitschia* is represented by the black dot. Stars indicate the localities of fossils. Broken lines in the phylogeny indicate a few particularly important extinct lineages of Gnetales.

Viburnum, Adoxaceae

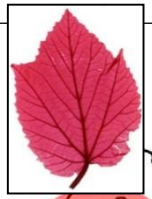

V. acerifolium

V. orientale

V. kansuense

Succodontotinus

Lobodontotinus

Winkworth & Donoghue 2005

ML tree from a combined chloroplast DNA dataset for 30 taxa
Branch-lengths transformed using PL
and calibrated using *Diplodipelta*

Modified from Bell & Donoghue (2005)

Viburnum

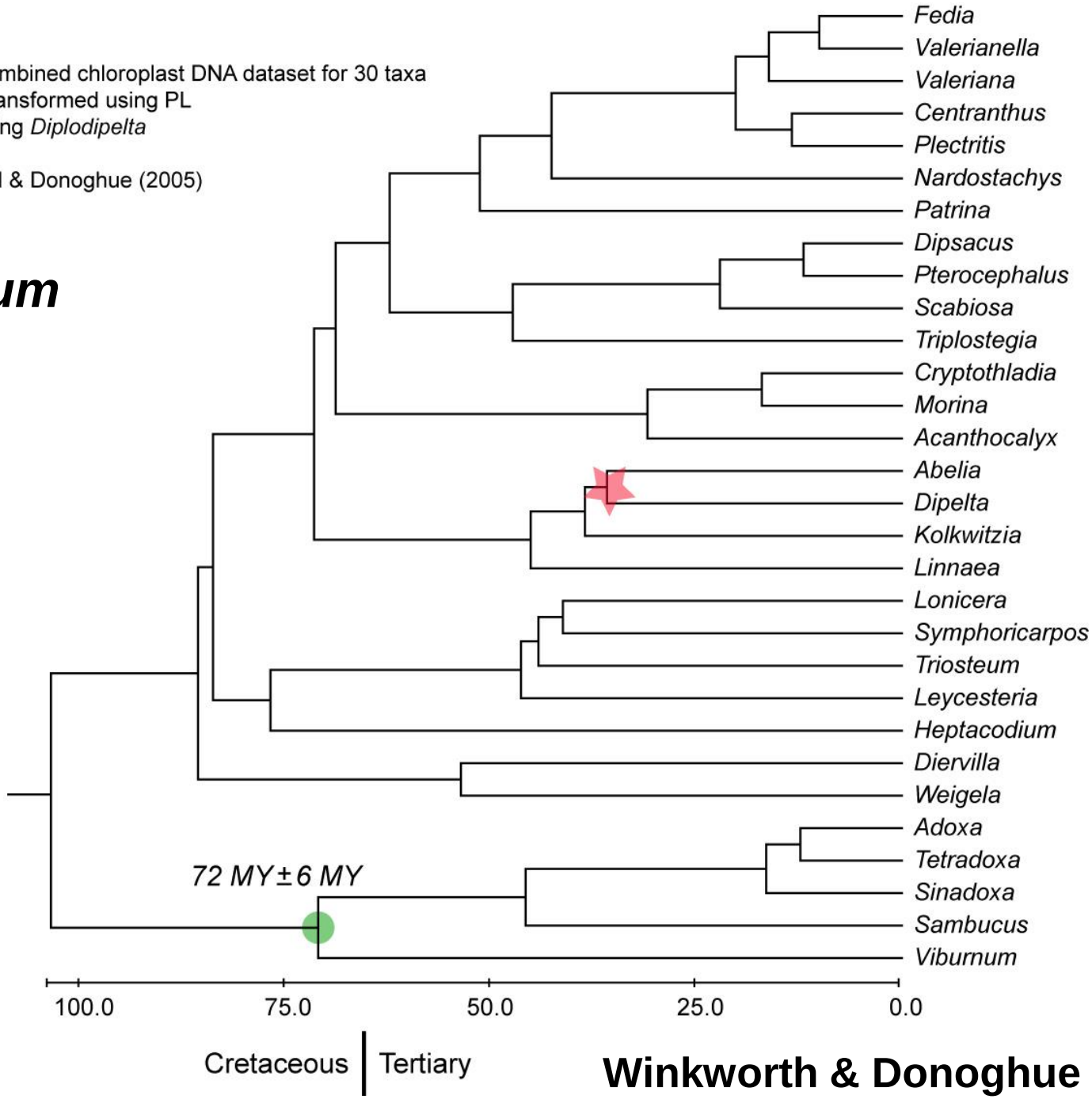

Winkworth & Donoghue 2005

Viburnum

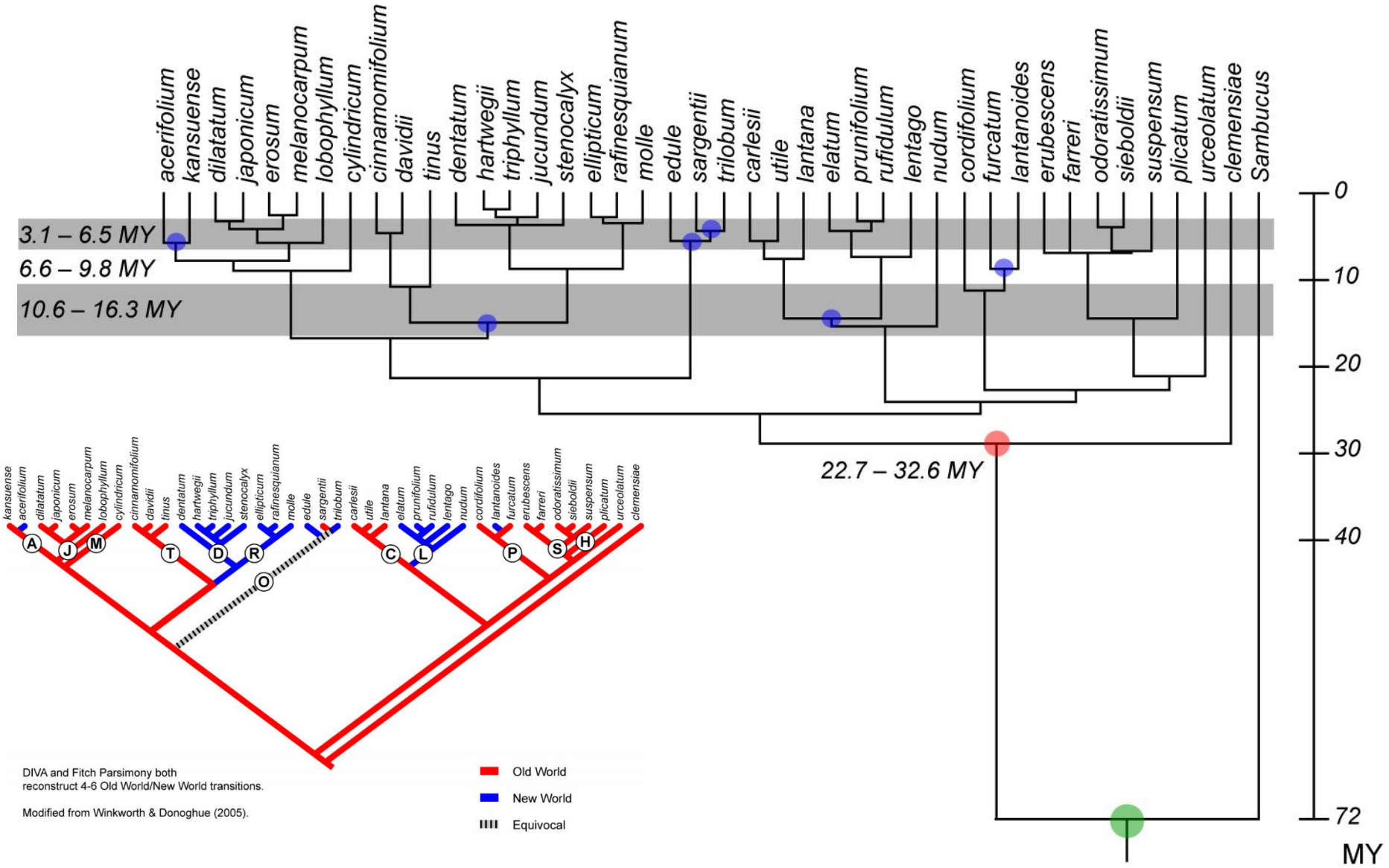

Winkworth & Donoghue 2005

Estimativas das idades relativas da divergência entre spp. de várias famílias tropicais:

na maioria das vezes substancialmente menores que as conhecidas para o afastamento dos blocos gonduânicos!

Isso sugere eventos de dispersão mais recentes, ao invés de vicariância muito antiga:

Lauraceae – Chanderbali et al. 2001
Melastomataceae – Renner et al. 2001
Malpighiaceae – Davis et al. 2002
Bromeliaceae e Rapateaceae – Givnish et al. 2004
Myrtaceae e Vochysiaceae - Sytsma et al. 2004
Poaceae – Bouchenak-Khelladi et al. 2010
***Coprosma* (Rubiaceae) – Cantley et al. 2014**

interpretações distintas

***Nothofagus* – Cook & Crisp 2005**
Proteaceae – Barker et al. 2007
Dicksoniaceae – Noben et al. 2017
Múltiplas linhagens – van den Ende et al. 2017
***Coprosma* (Rubiaceae) – Heads 2017**

em parte vicariância, em parte dispersão.

Estimativas das idades relativas da divergência entre spp. de famílias tropicais

Proteaceae (Barker et al. 2007)

cenário em parte vicariânica, em parte dispersão transoceânica

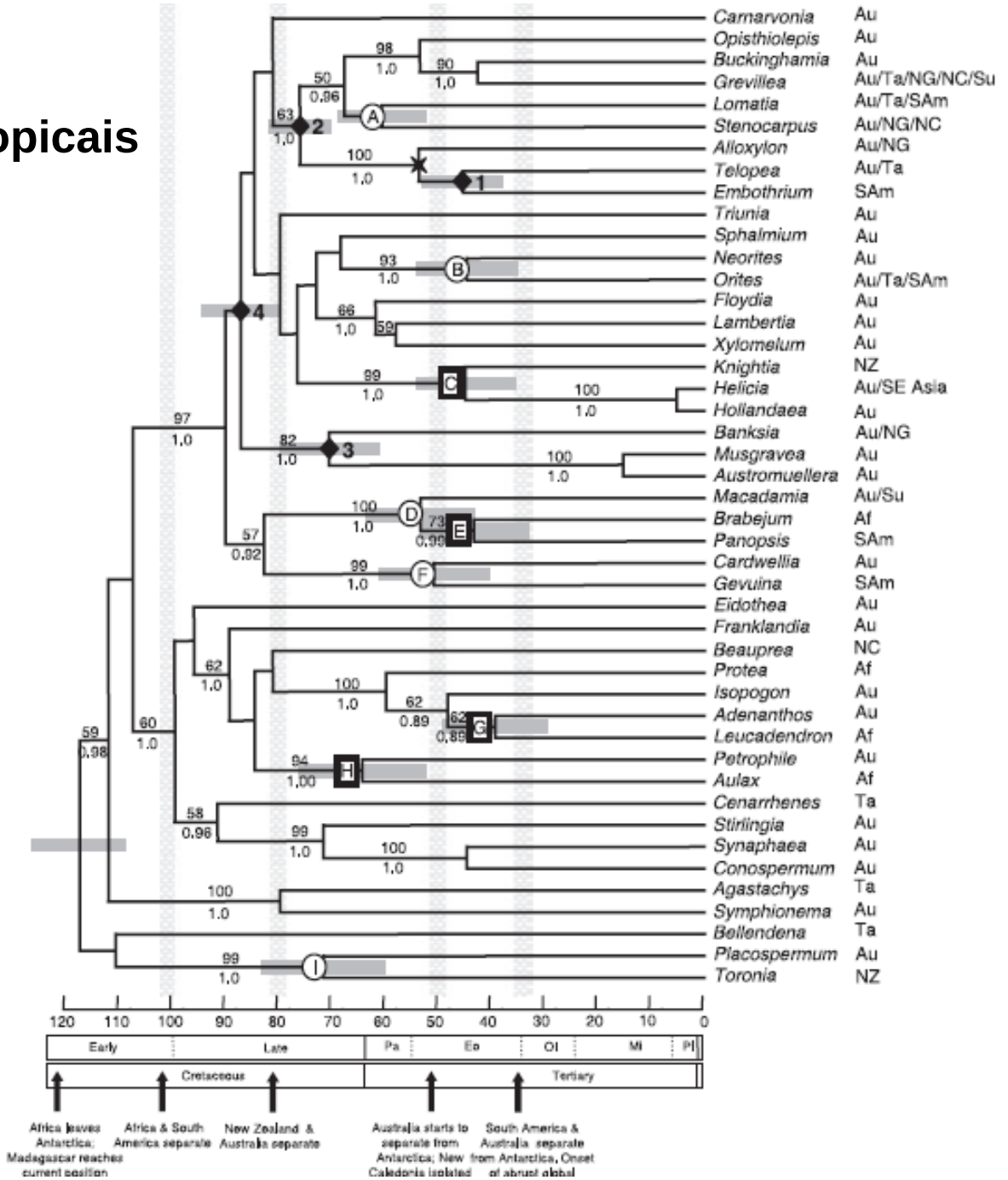

Distribuição atual de **Proteaceae** (isolinha sem preenchimento) e seu grupo-irmão Platanaceae (isolinhas hachuradas em preto)

Ordem Proteales

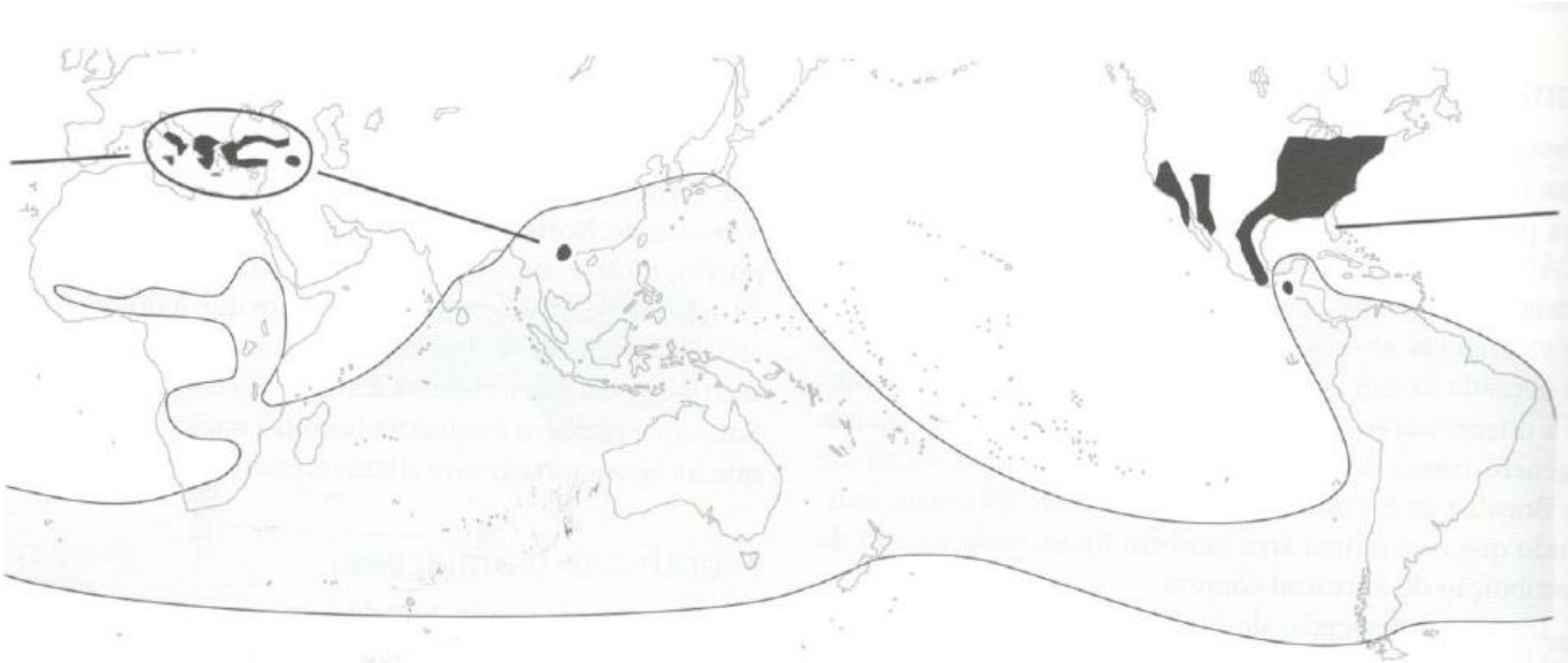

Figura 5.16 Distribuição geográfica de Proteaceae (*cinza*) e seu grupo-irmão, Platanaceae (*preto*).[8]

Heads 2016

ANACARDIACEAE
SAPINDALES

Manchester *et al.* 2007

Anacardium germanicum
Fóssil do Eoceno médio
ca. 47 m.a.

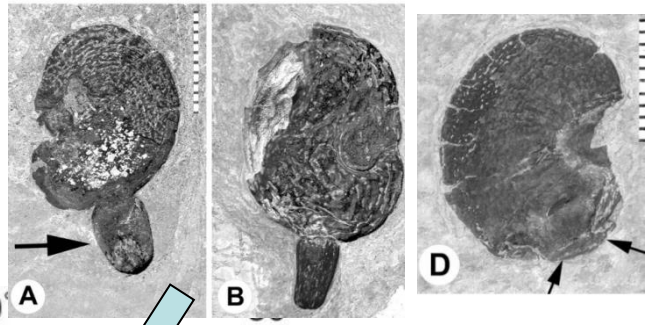

A. excelsum

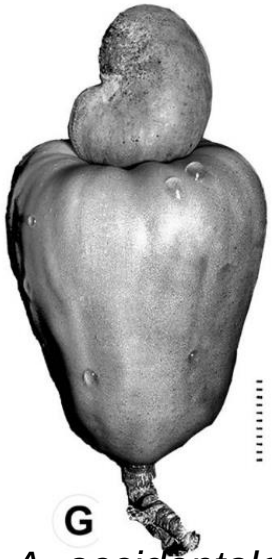

A. occidentale

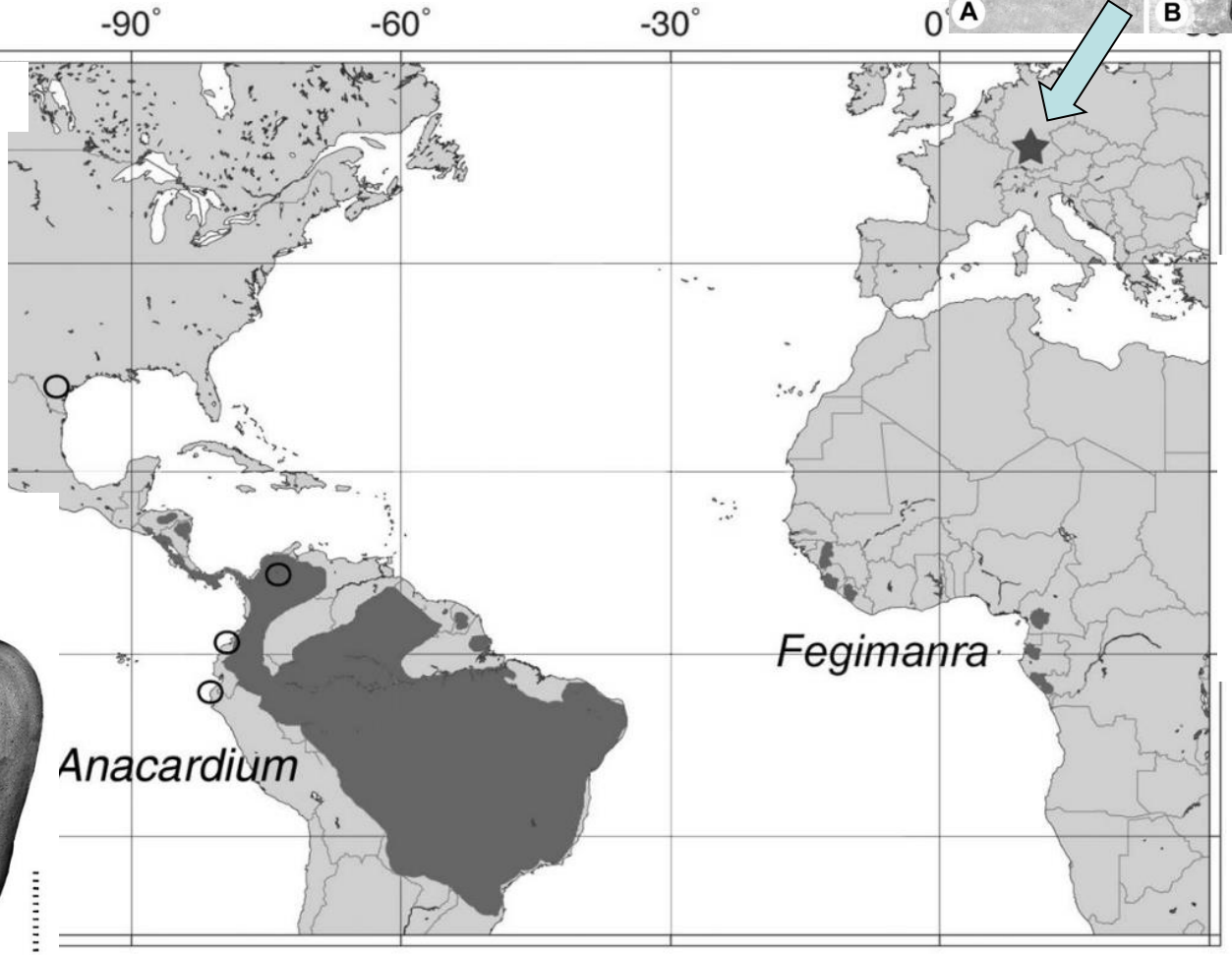

the modern distribution of *Anacardium* and *Fegimanra*, plus the occurrence of fossil *Anacardium germanica* in Germany
Anacardium fossils in the New World (circles in Texas, Peru, Ecuador, and Colombia).

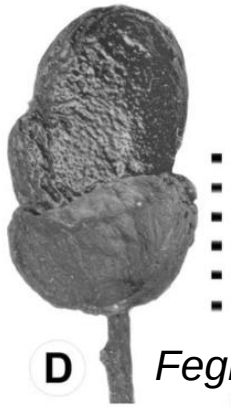

Fegimanra

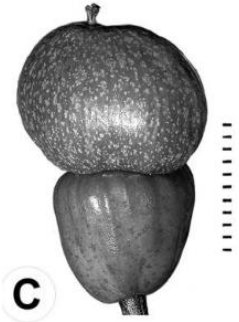

Semecārpus

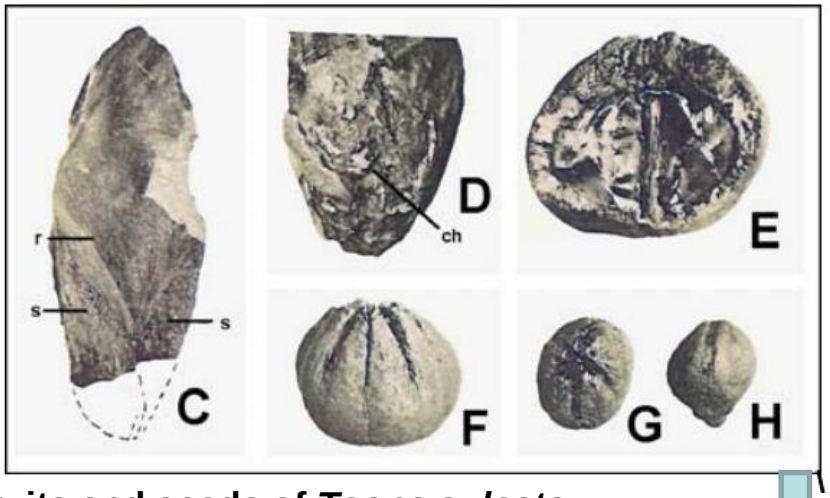

Fruits and seeds of *Toona sulcata*, London Clay, UK, Early Eocene, 49 my of age
(Reid and Chandler, 1933; Chandler, 1964).

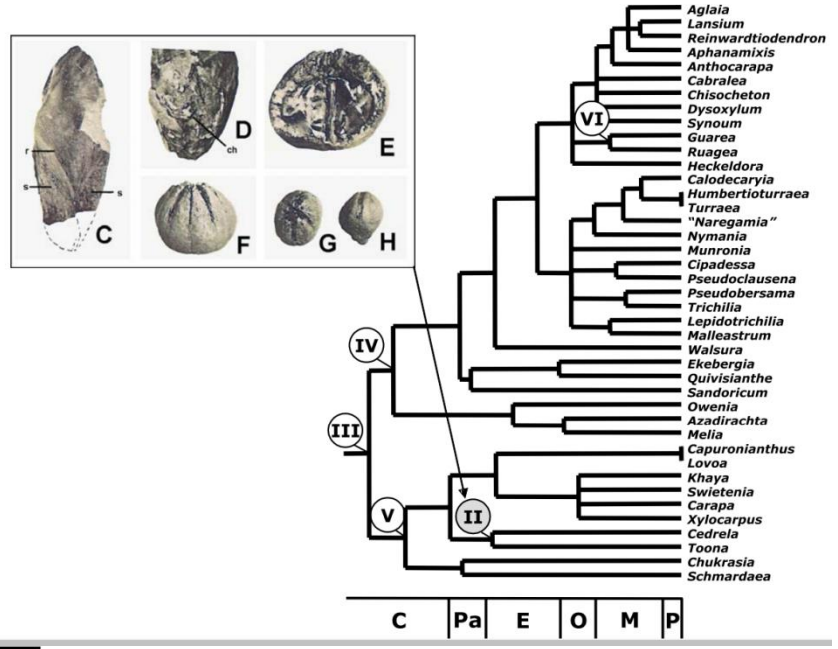

MELIACEAE

Muellner *et al.* 2006

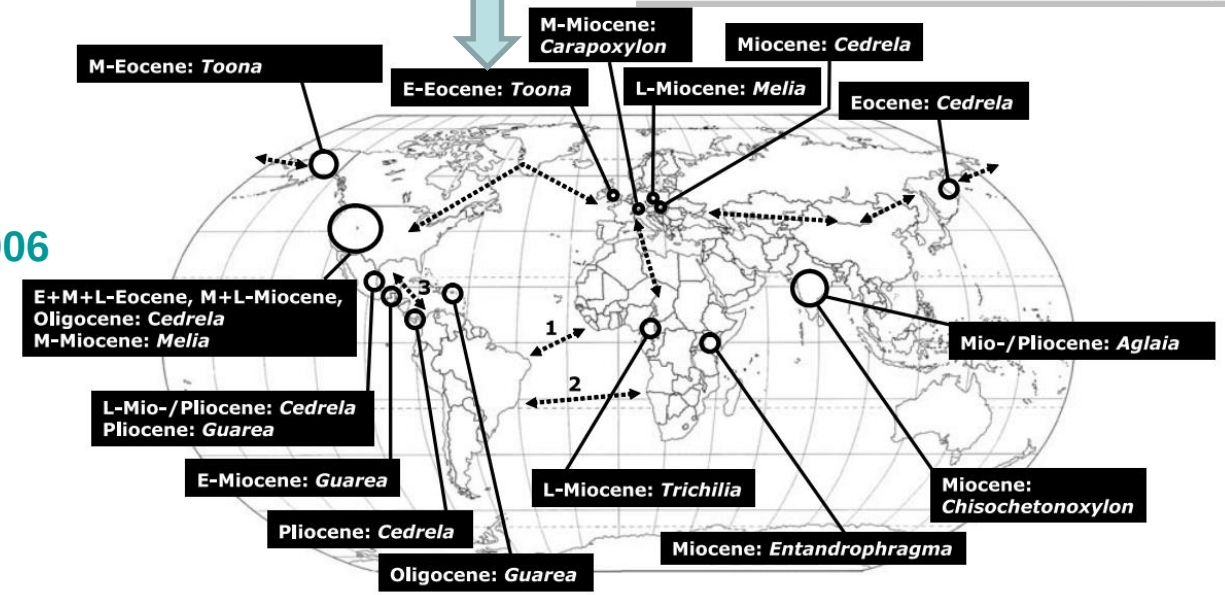

Fig. 2. Map showing the global distribution of Meliaceae fossil findings (Eocene to Quaternary). Dotted arrows indicate interplate dispersal paths and migration routes for megathermal angiosperms from the Late Cretaceous up to the Eocene-Oligocene boundary, modified after Morley (2003). (1) and (2) indicate the approximate position of the Sierra Leone and Walvis ridges (until Maastrichtian); (3) indicates the position of the Proto-Greater Antilles islands (emergent in the Middle Eocene) and GAARlandia (Greater Antilles and Aves ridge; Eocene-Oligocene boundary). E, Early; M, Middle; L, Late.

MALPIGHIACEAE

Davis *et al.* 2002

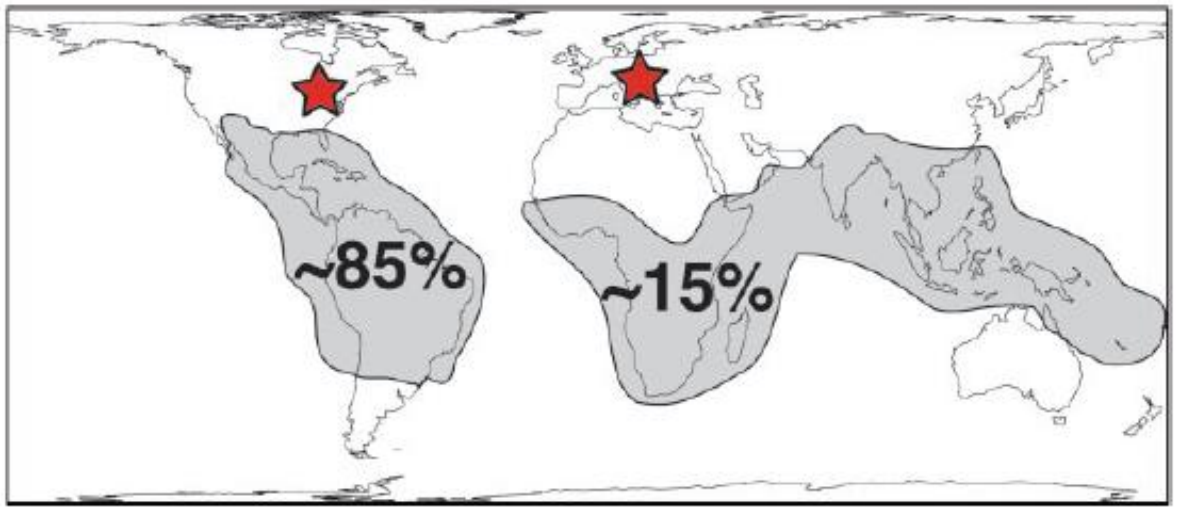

Fig. 1. Current geographic distribution of Malpighiaceae estimated from Arénes (22). Malpighiaceae, with ≈1,250 species (1), are most diverse in northern South America (22). The ≈180 Old World species, belonging to six lineages (see Fig. 2) are variously represented in Africa (47 species), Australasia (17 species), India (43 species), and Madagascar (80 species) [from Arénes (22)]. Red stars indicate fossil localities from Hungary and Slovenia (17), and Tennessee (21).

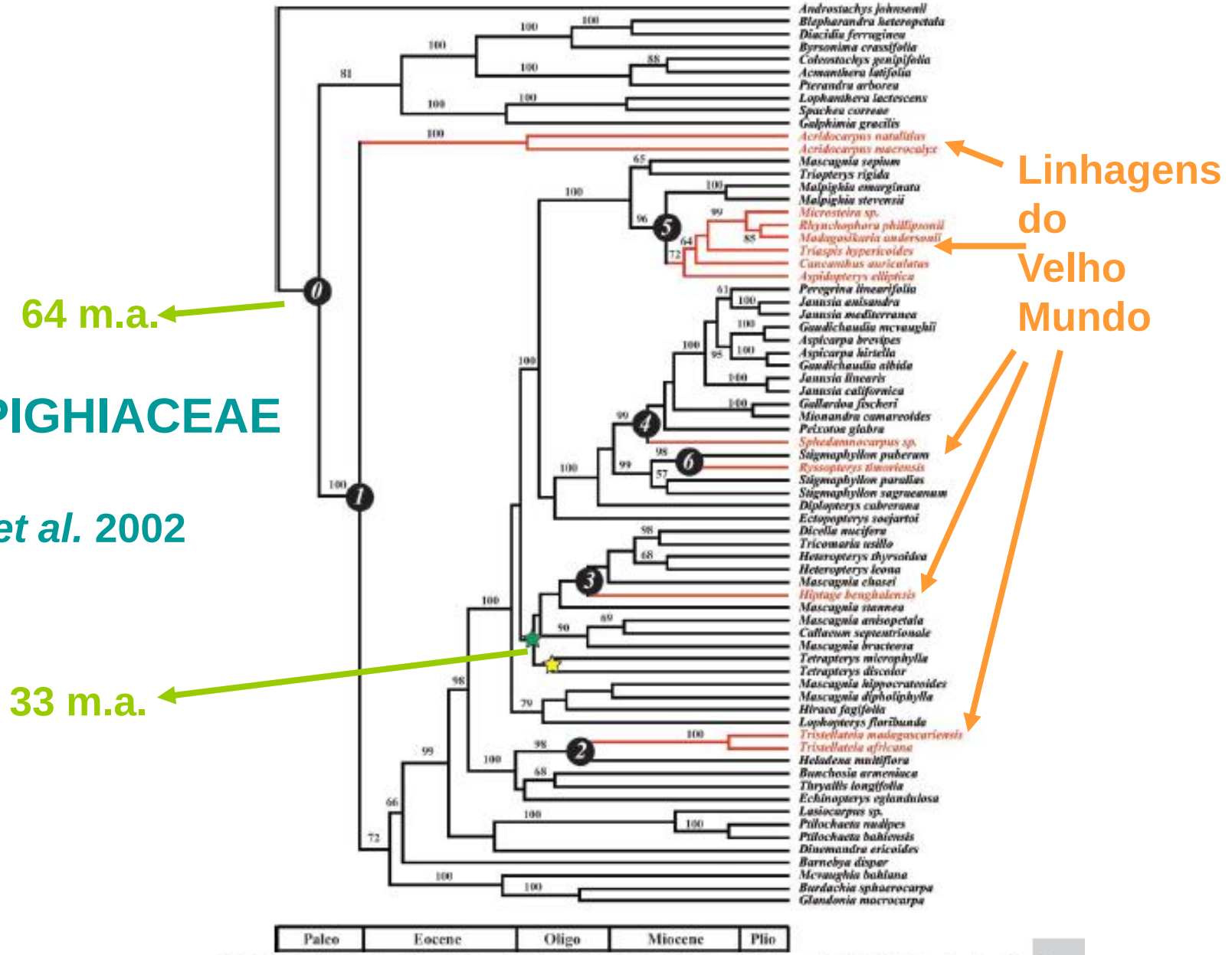

MALPIGHIACEAE

Davis *et al.* 2002

Fig. 2. Maximum likelihood tree topology (−ln *L* = 17,333.97) for combined *ndhF* and *PHYC* data with bootstrap values (>50%) indicated on branches. Old World lineages are shaded red. Divergence times were calculated on the rate-smoothed topology by calibrating the two nodes indicated by the colored stars with a fossil of *Tetrapterys* (33 mya; ref. 17). The origin of Malpighiaceae (node 0) is reconstructed as New World and is estimated at 63.6 ± 5.8 mya. The nodes labeled 1–6 correspond to the New/Old World disjunctions estimated from the DIVA reconstruction. Age estimates for nodes 1 through 6 (calibrated with the fossil placed at the green star) are, respectively: 55.1 ± 6.0 mya, 30.4 ± 2.6, 29.4 ± 2.1, 19.1 ± 1.5, 15.1 ± 1.2, and 12.0 ± 0.85. The scale bar indicates major Tertiary epochs (Paleo = Paleocene; Oligo = Oligocene; Plio = Pliocene).

EVOLUTION

MALPIGHIACEAE: migração laurasiana hipotética de táxons do Gonduana Ocidental (traço verde)

Davis *et al.* 2002

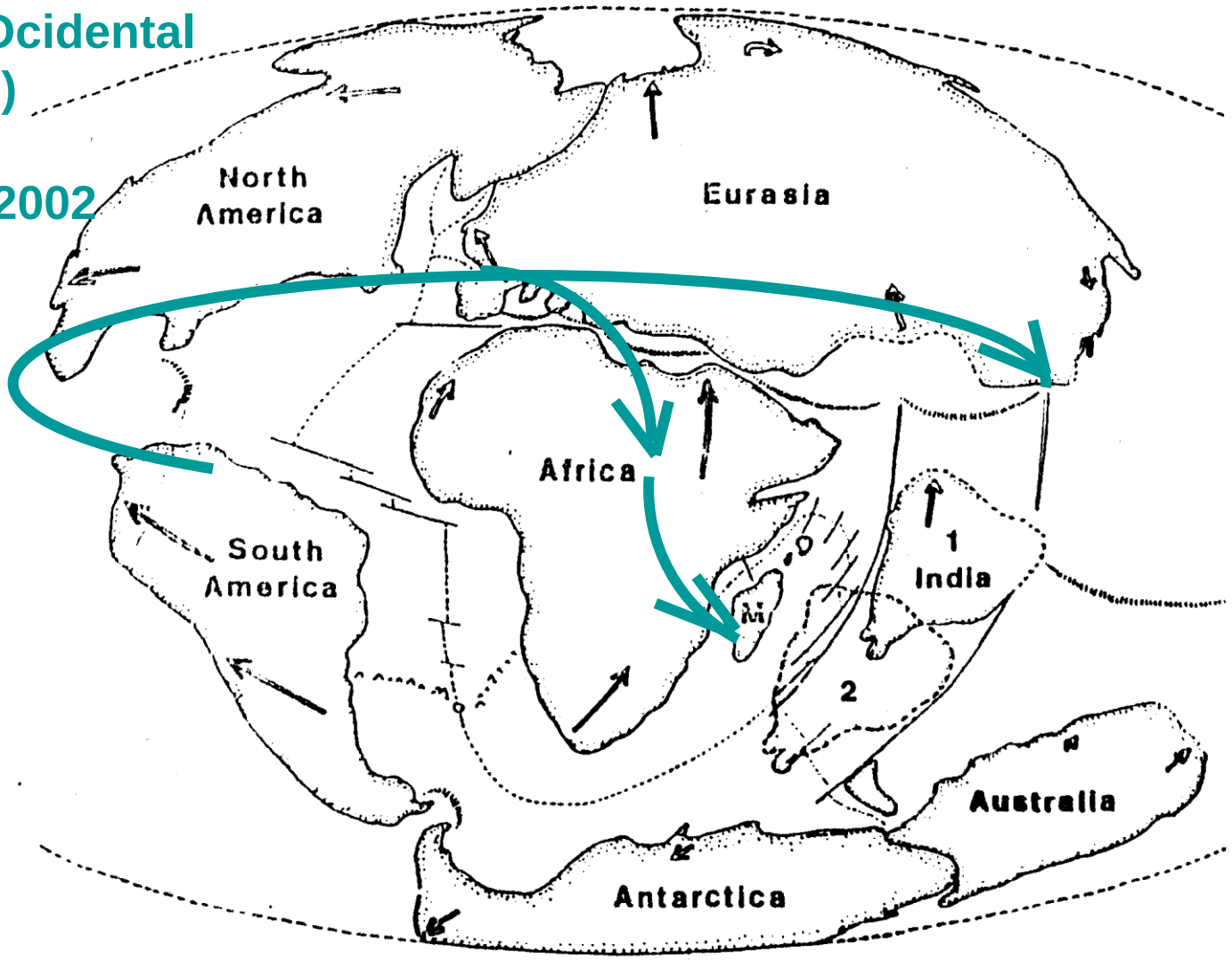

Configuração continental no Terciário inferior (Schuster 1970)

MALPIGHIACEAE:
migração laurasiana hipotética de táxons do Gonduana Ocidental (traço verde)

Davis *et al.* 2002

em vermelho:
outra rota hipotética de clados tropicais de angiospermas.

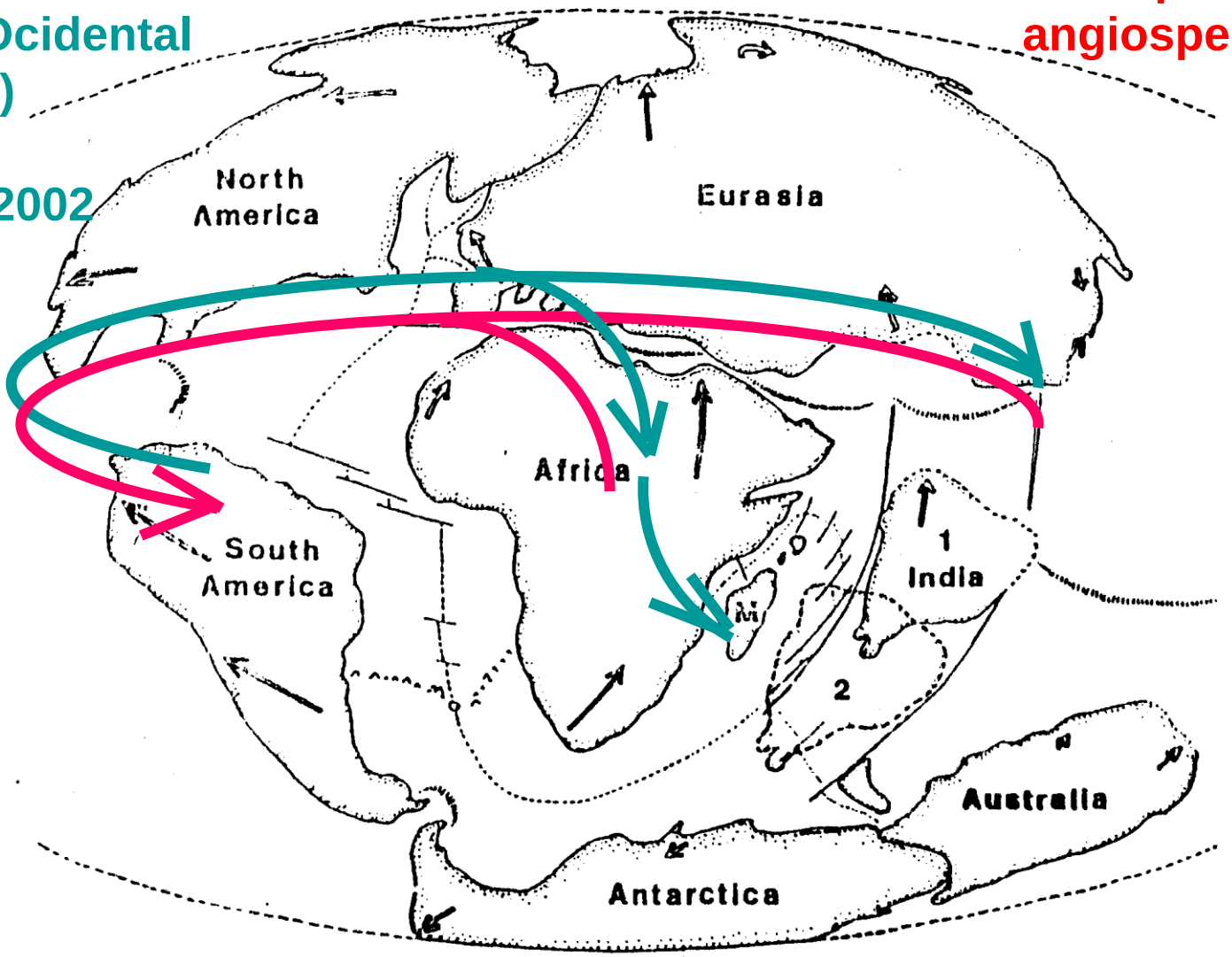

Configuração continental no Terciário inferior (Schuster 1970)

Flora Boreotropical

Nie et al. 2013

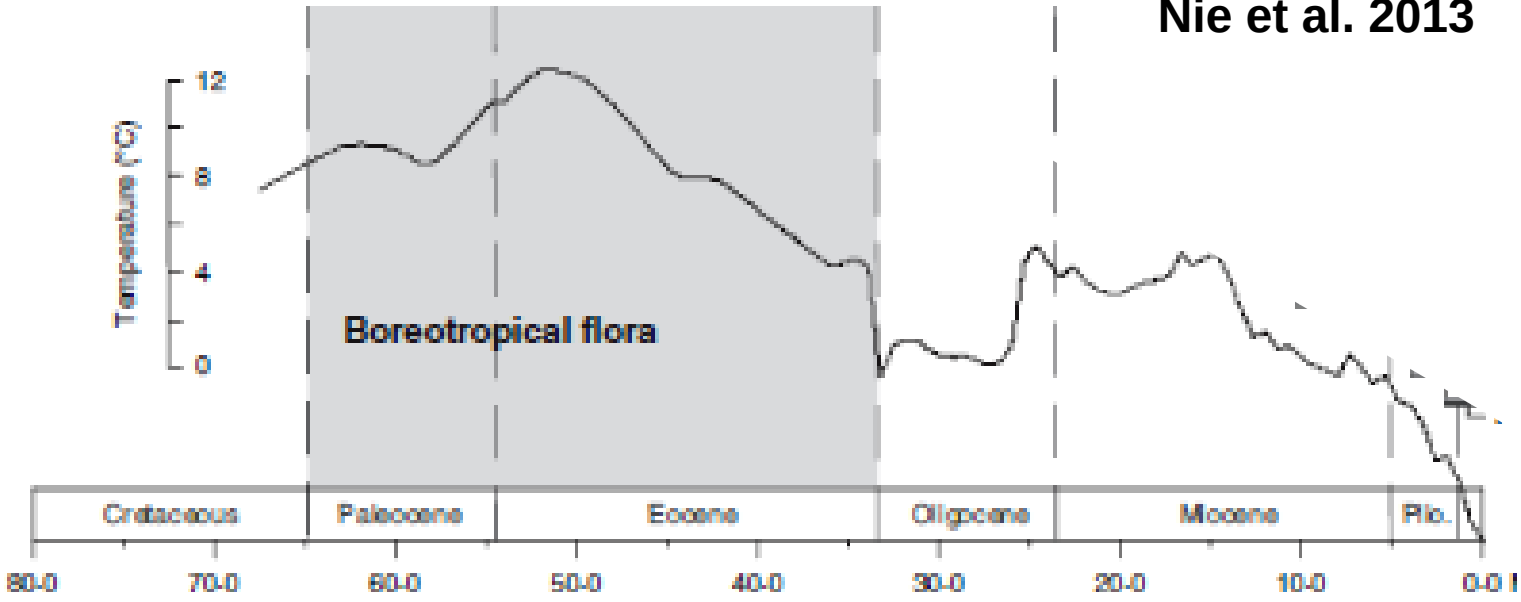

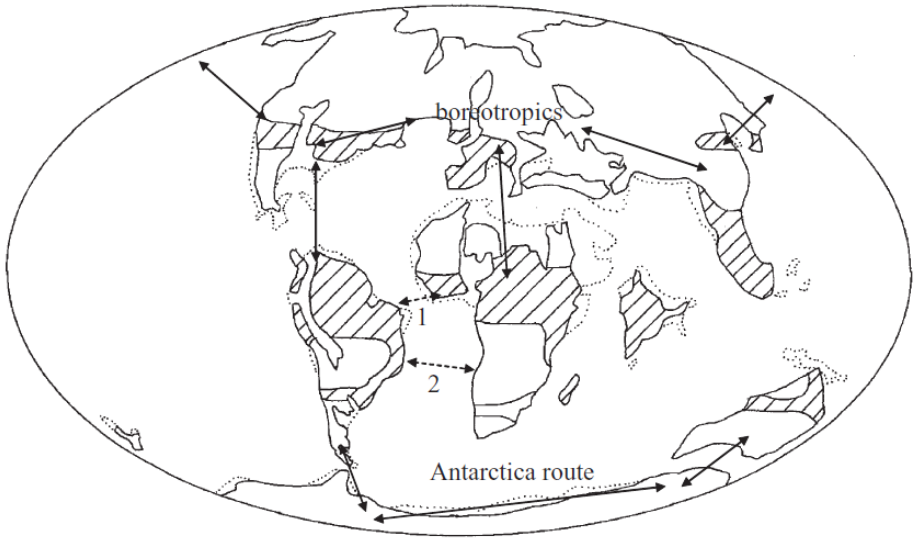

Pennington & Dick 2004

(Baseado nas ideias de Wolfe 1975 e Morley 2003)

Figure 1. Early Tertiary, Early Eocene plate tectonic reconstruction and palaeogeography adapted, with permission, from Morley (2003, fig. 5), indicating closed canopy rainforests (cross hatched). Dotted lines approximate present-day coastlines. Dotted arrows indicate the approximate position of the Sierra Leone (1) and Walvis (2) ridges. Solid arrows indicate migration routes through and from the boreotropics and Antarctica.

MYRTALES:
Sytsma *et al.* 2004

CRONOGRAMA com evolução biogeográfica do grupo

Psidium guajava

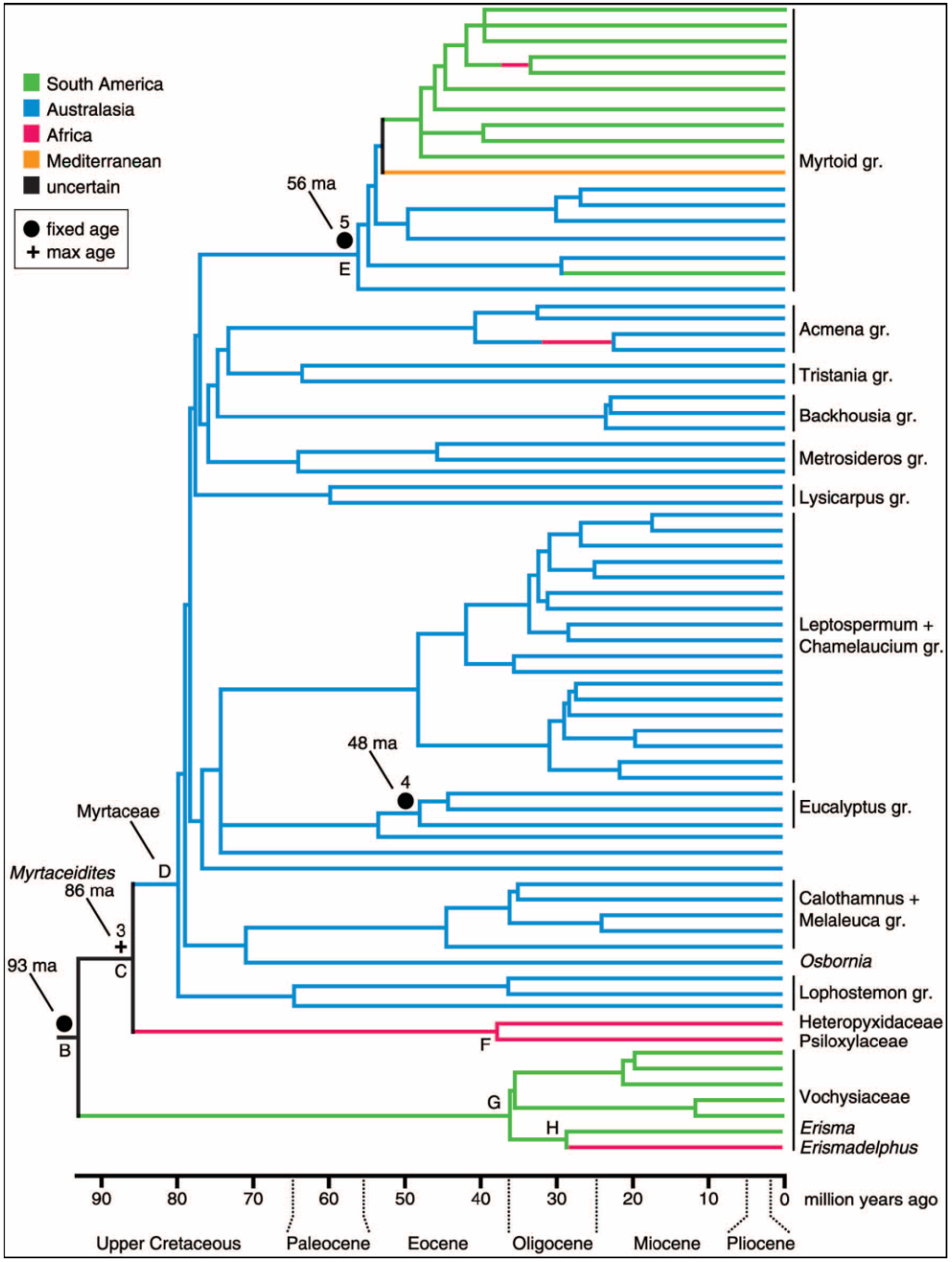

MYRTALES:
Sytsma *et al.* 2004

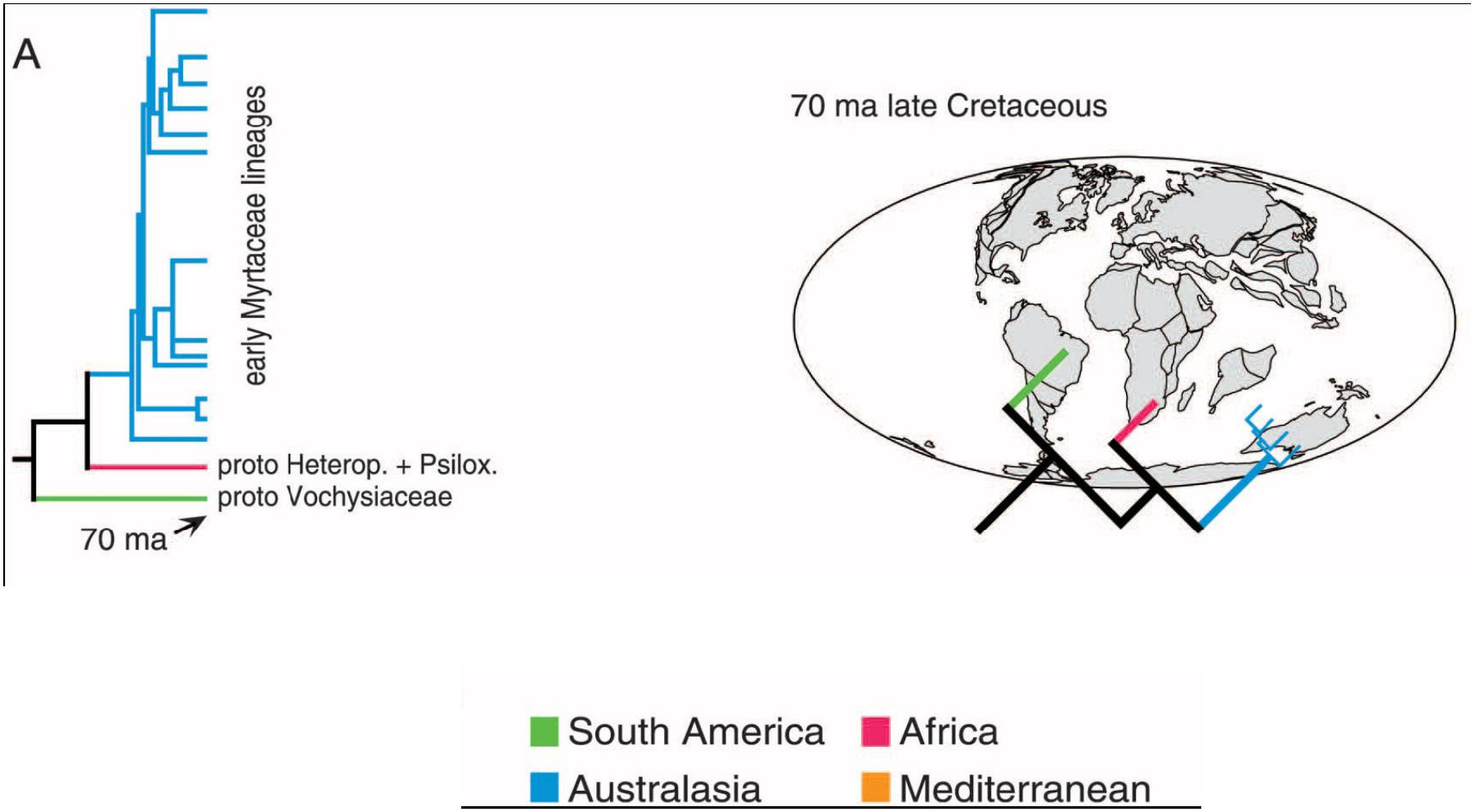

MYRTALES: Sytsma *et al.* 2004

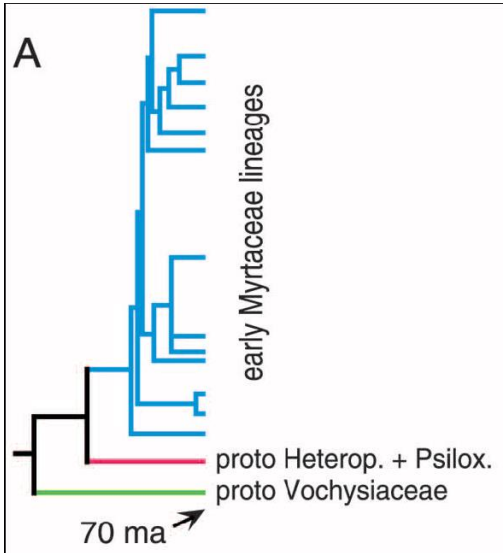

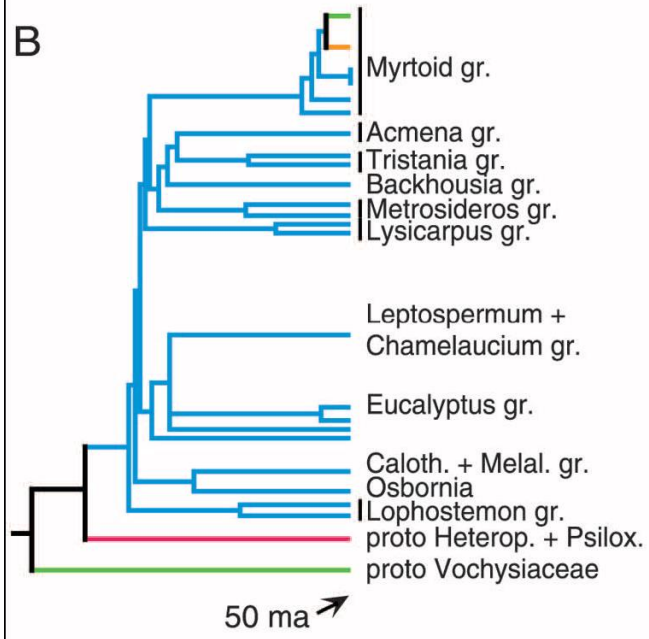

70 ma late Cretaceous

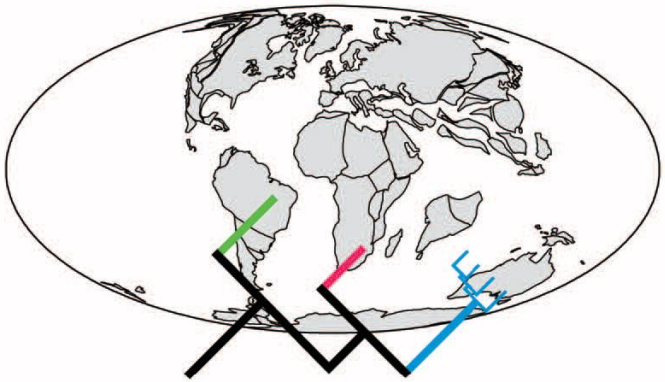

50 ma mid Eocene

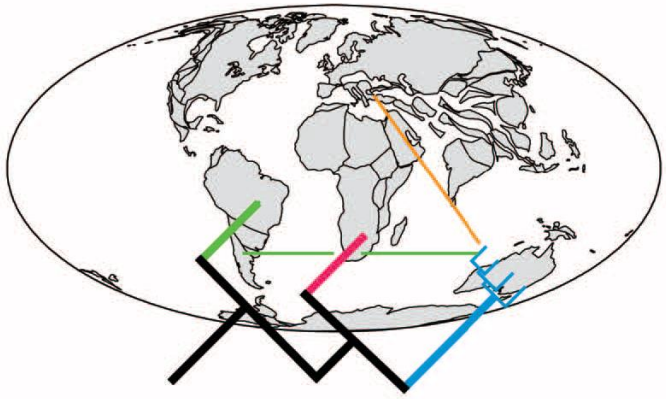

South America
Africa
Australasia
Mediterranean

MYRTALES: Sytsma *et al.* 2004

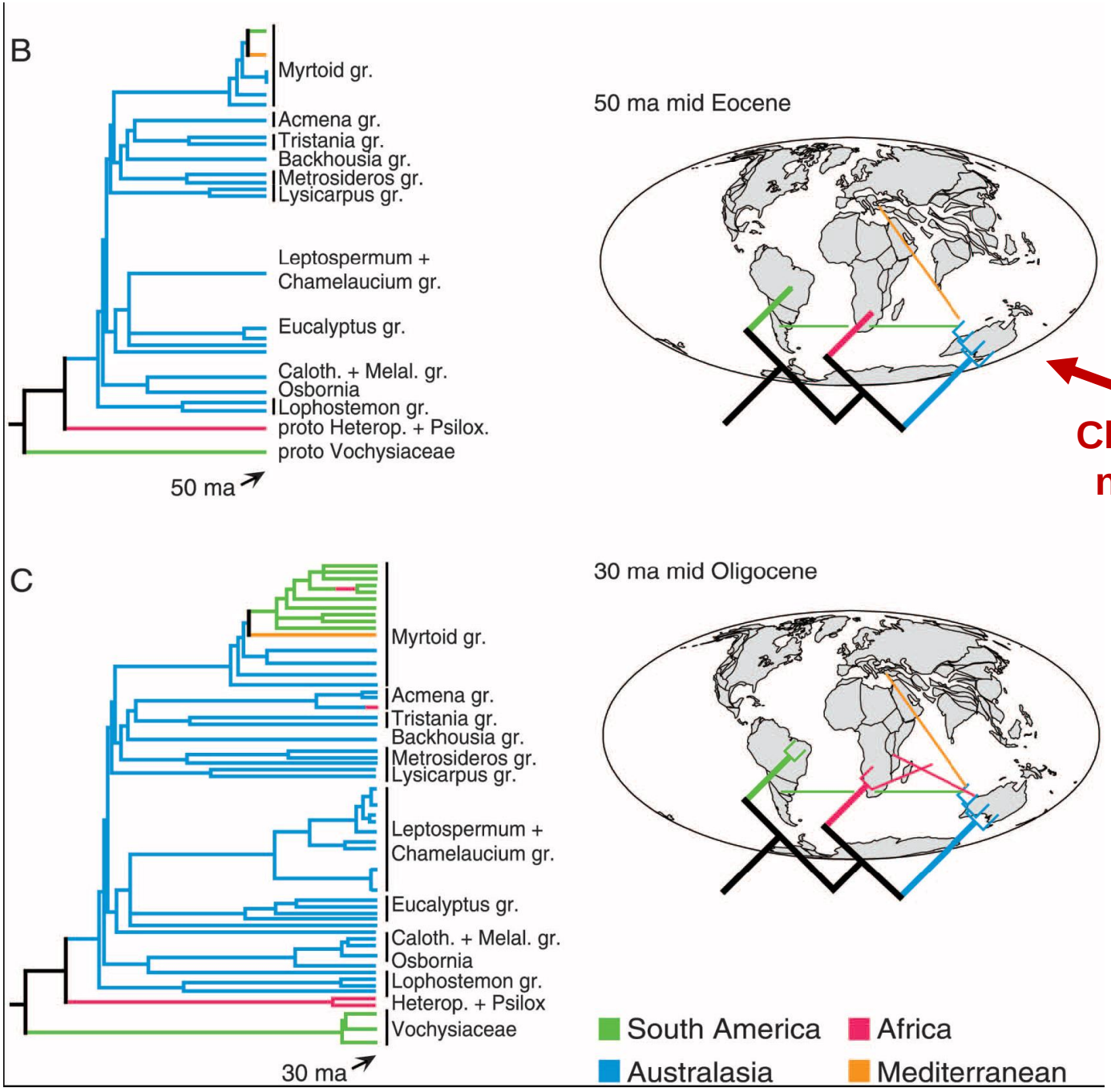

Chegada de Myrtoideae na região Neotropical poderia ter sido por migração via Flora Boreotropical ?

Melicope (Rutaceae)
nDNA + cpDNA

Harbaugh et al. 2008

Havaí como "stteping stone" para dispersão no Pacífico

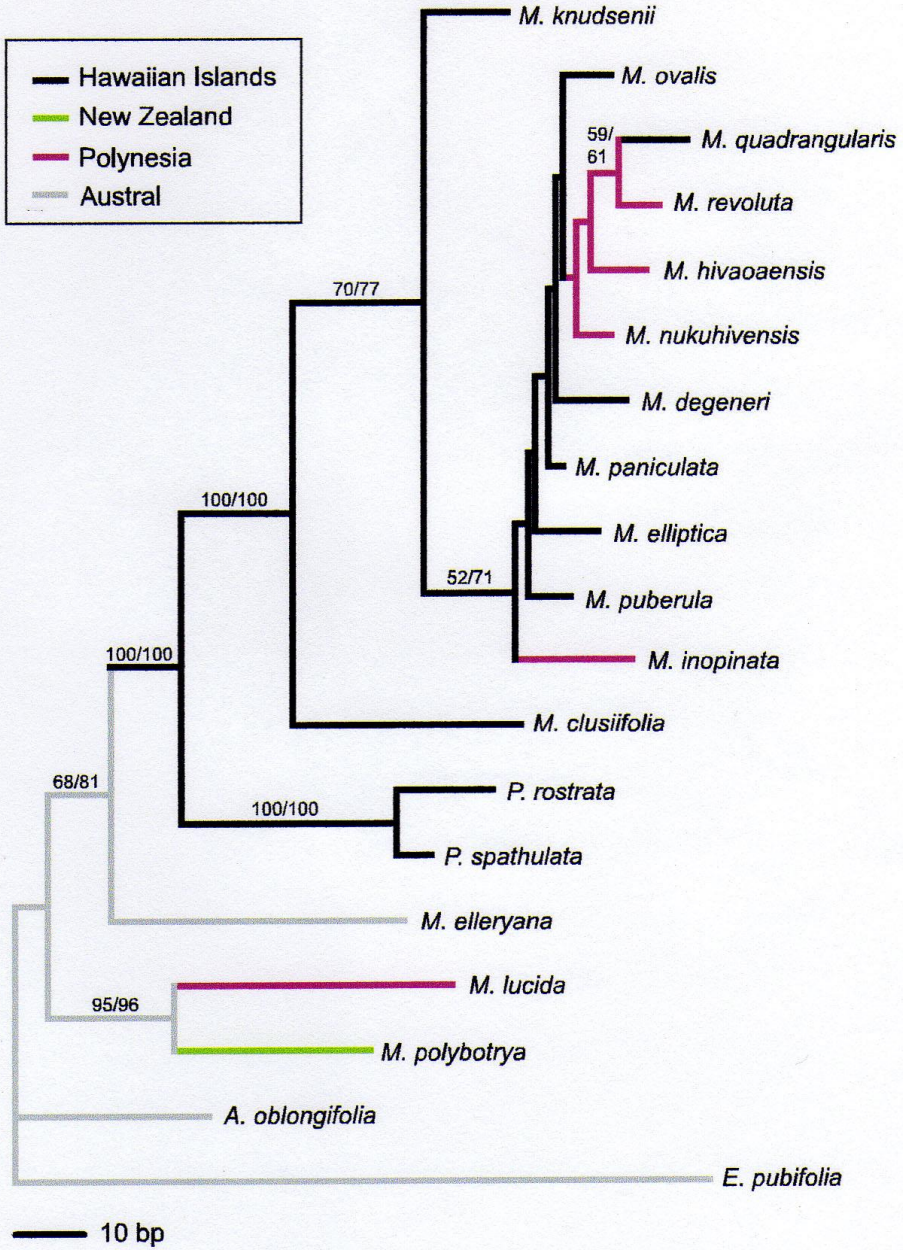

Figure 3 The combined chloroplast and nuclear ribosomal phylogram from the maximum parsimony (MP) analysis using sequences obtained in this study. The topologies of the MP and maximum likelihood (ML) phylogenies are identical. The genera are abbreviated with the following letters: *A. Acronychia*; *E. Euodia*; *M. Melicope* and *P. Platydesma*. Numbers above branches represent MP bootstrap values (first) and ML bootstrap values (second). Geographical areas are mapped onto the phylogeny as described in the Materials and Methods section.

Biogeography of the grasses (Poaceae): a phylogenetic approach to reveal evolutionary history in geographical space and geological time.

BOUCHENAK-KHELLADI et al. 2010

Poaceae

cronograma baseado em dados combinados de **cpDNA** de uma amostragem abrangente: **todos os 800 gêneros da família**

Poaceae tem ca.10.000 spp. (5° fam. mais rica)

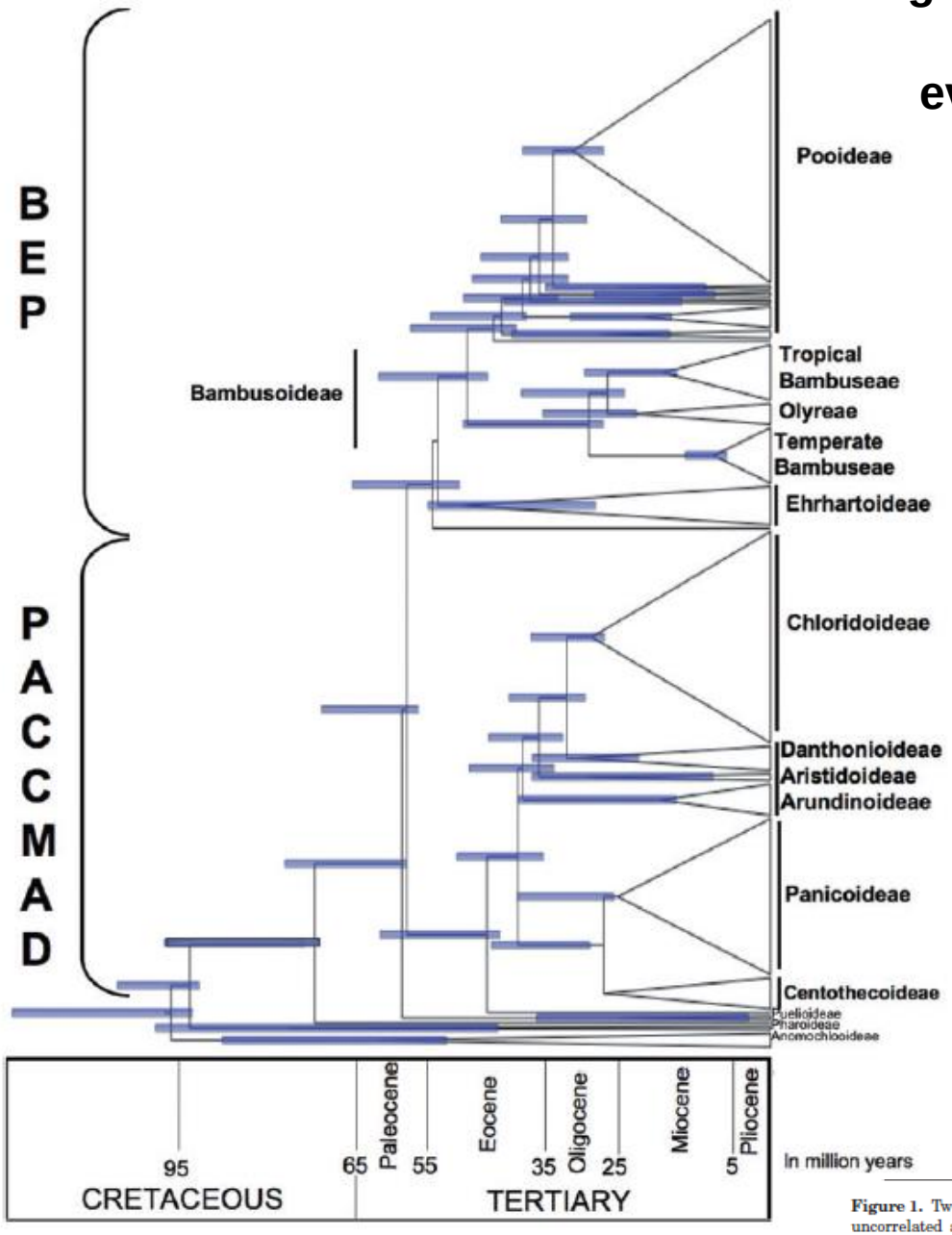

Figure 1. Two hundred and ninety-eight-grass taxa chronogram based on a relaxed Bayesian clock, with rates being uncorrelated and sampled from a lognormal distribution (UCLN as in Drummond *et al.*, 2006). BEP and PACCMAD clades following the GPWG (2001) and Sánchez-Ken *et al.* (2007), respectively. Horizontal thick bars represent 95% confidence intervals of divergence times. Note that the sizes of terminal triangles are proportional to the number of taxa imbedded in the clades.

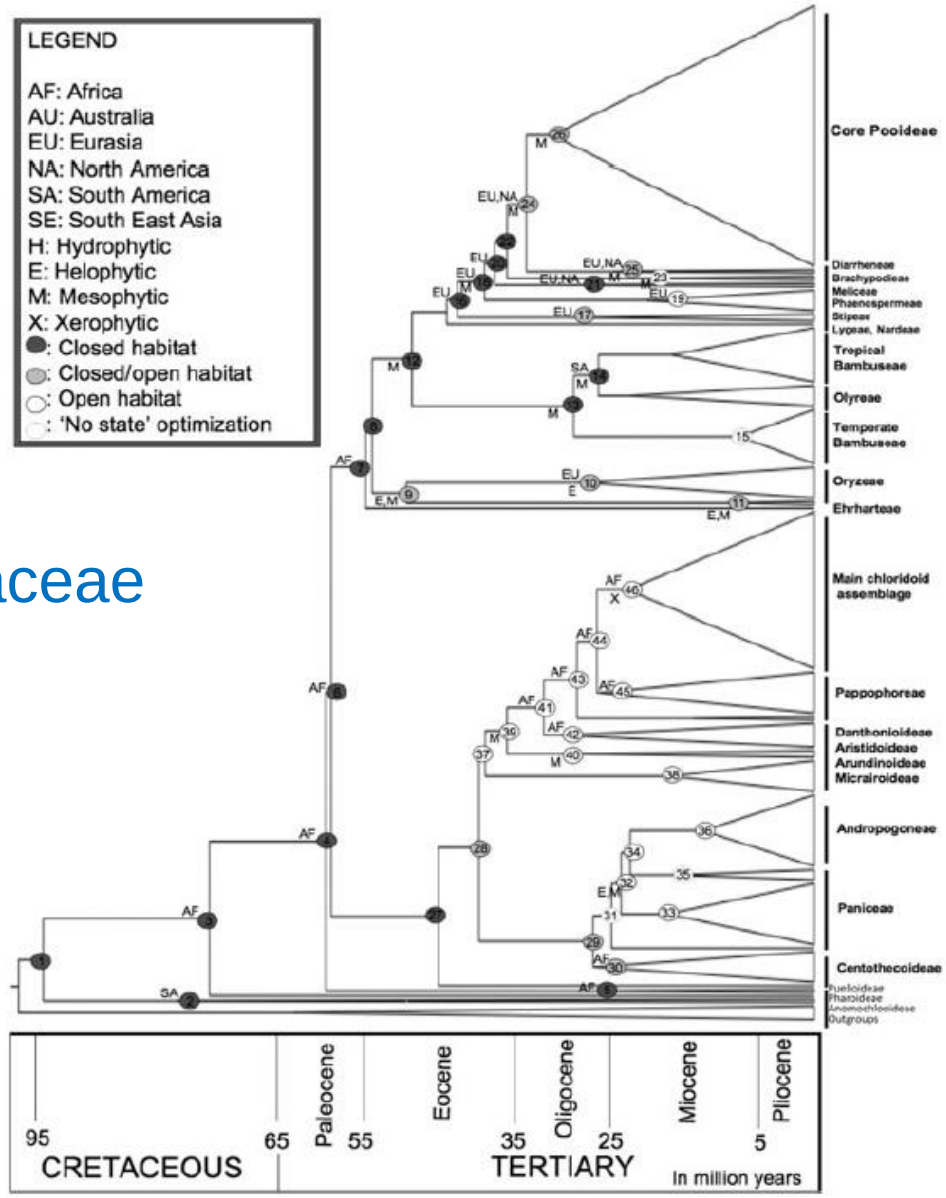

Poaceae

Figure 2. Ancestral reconstructions of geographical areas, vegetation type and habitat moisture using polymorphism coding and maximum likelihood (as shown in Table 1), using a comprehensive generic-level phylogenetic tree of the grasses. Likelihood estimates can be found in Table 2. Main chloridoid assemblage and core Pooideae according to Watson & Dallwitz (1992). Numbers within circles refer to node numbers in Table 2.

Biogeography of the grasses (Poaceae): a phylogenetic approach o reveal evolutionary history in geographical space and geological time.

BOUCHENAK-KHELLADI et al. 2010

additional tree using a **supermatrix of morphological and molecular data that** included all 800 grass genera so that **ancestral biogeography and ecological habitats** could be inferred.

likelihood-based method allows the **estimation of ancestral polymorphism in both biogeographical and ecological** analyses for large data sets.

BOUCHENAK-KHELLADI et al. 2010

POACEAE:
palaeo-biogeographical and palaeo-ecological scenarios
that may have led to present-day distribution and diversity of grasses
at the family level.

The **origin** of Poaceae was retrieved as **African and shade adapted**.
The crown node of the BEP + PACCMAD clade was dated at **57 Mya, in the early Eocene**.
Grasses dispersed to all continents by approximately 60 million years after their Gondwanan origin in the late Cretaceous.

PACCMAD taxa adapted to open habitats as early as the late Eocene,
a date consistent **with recent phytolith fossil data for North America.**

C4 photosynthesis first originated in Africa, at least for Chloridoideae in the Eocene at *c. 30 Mya.*
The BEP clade members adapted to open habitats **later** than PACCMAD members;
this was inferred to occur in Eurasia in the Oligocene.

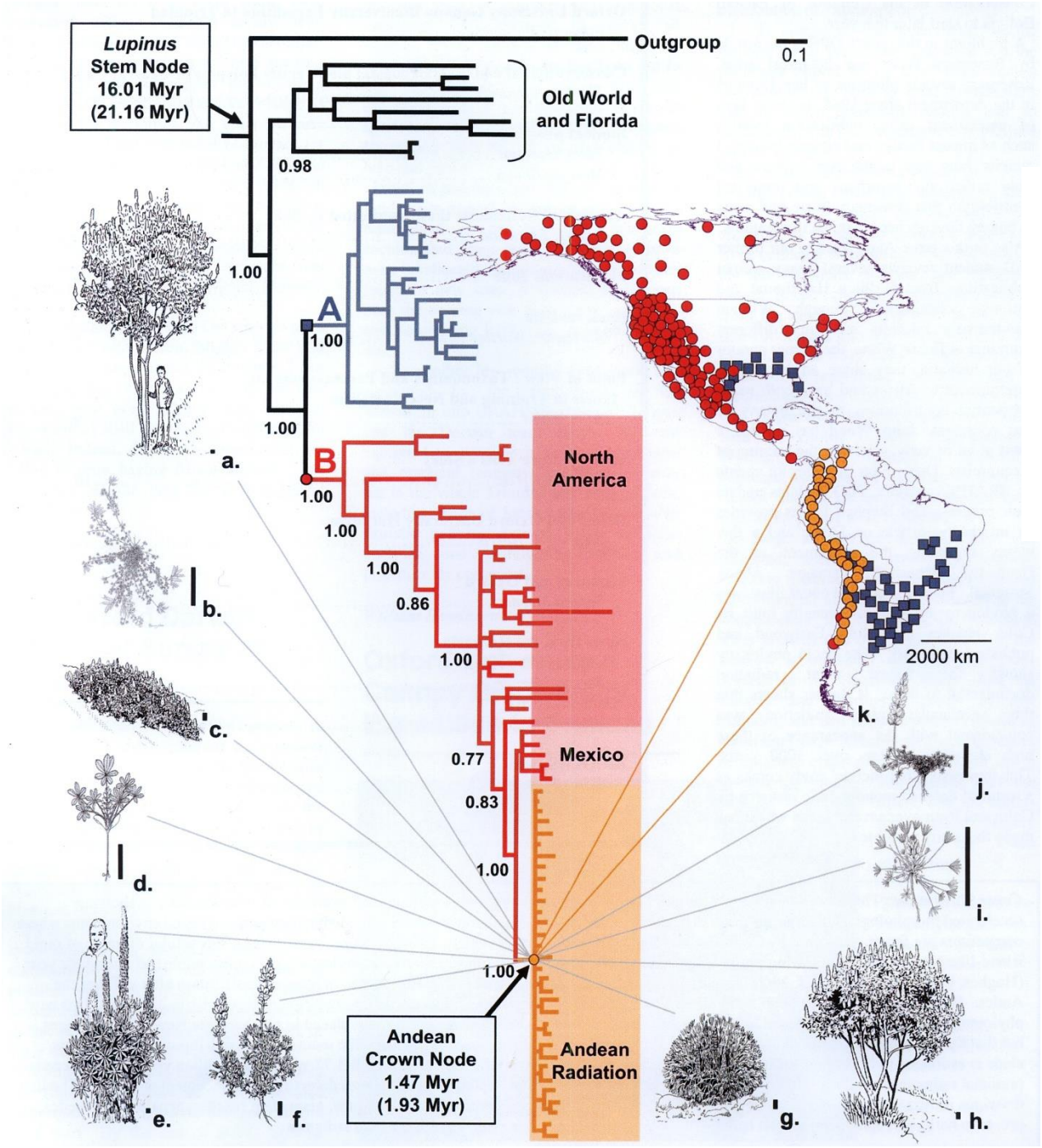

Lupinus

Hughes & Eastwood 2006

PNAS

Cyathostegia - Leguminosae
Andean diversification
Pennington et al. 2010

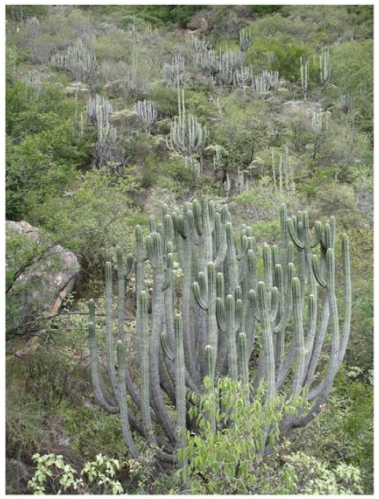

Fig. 1. Cactus-rich seasonally dry tropical forest in the Marañon valley, Peru.

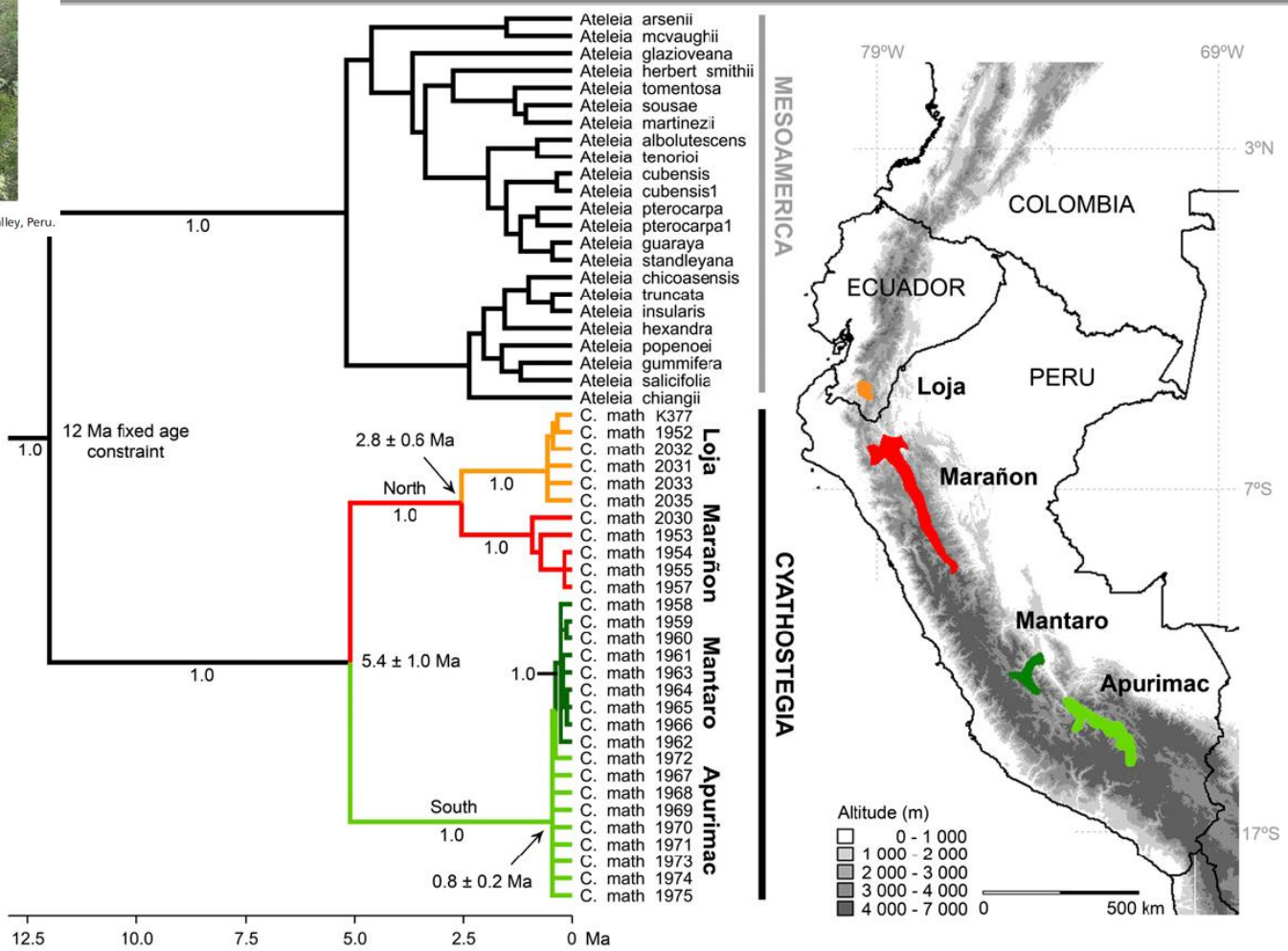

Fig. 3. Chronogram for *Cyathostegia* derived from penalized likelihood rate smoothing of a 50% majority rule Bayesian likelihood tree estimated from the ITS sequence data. Clade labels (Loja, Marañon, Mantaro, Apurimac) indicate the dry inter-Andean valleys where accessions were collected, the locations of which are shown on the map. Numbers (1.0) below branches indicate posterior probabilities.

Cronograma combinado com análise biogeográfica das BROMELIACEAE

Givnish *et al.* 2011

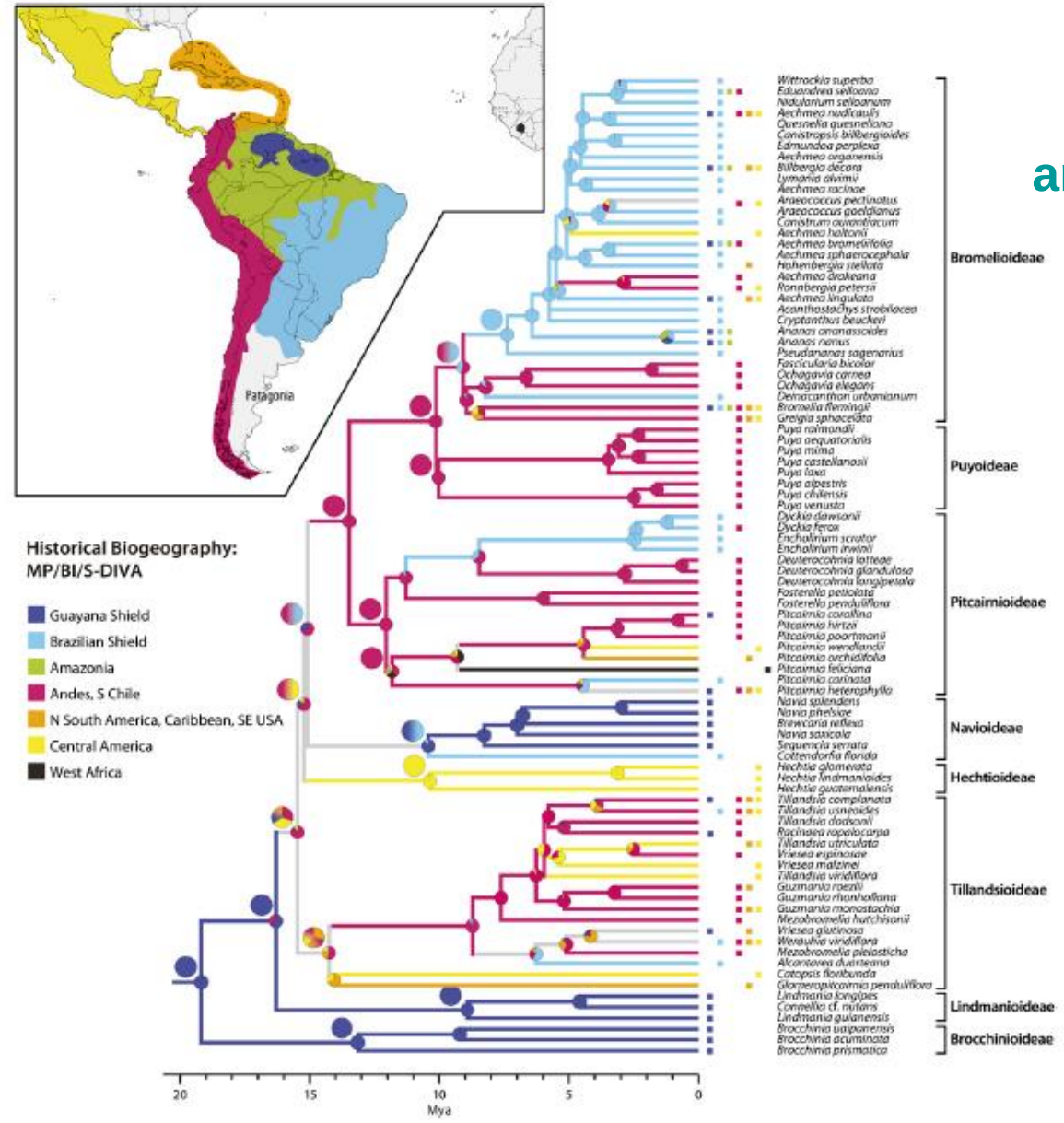

Fig. 8. Geographic evolution of Bromeliaceae calibrated against time. Present-day distribution of individual species (or of genera, in cases where wide-ranging groups are represented by one or two placeholder taxa) indicated by colored boxes. Branch colors indicate the inferred distributions of ancestral taxa under maximum parsimony (MP); gray indicates ambiguity. Pie diagrams at nodes indicate the inferred ancestral distributions under Bayesian inference (BI), with width of wedges delimited by black lines showing likelihood of alternative inferences. Larger pie diagrams displaced northwest of nodes indicate the inferred ancestral distributions under S-DIVA, with wedges delimited by black lines showing likelihood of alternative inferances, and a blend of colors within wedges signifying vicariance involving a fusion of two regions represented by those colors. Analyses involving the possible fusion of more than two areas yield similar results except for a few backbone nodes.

Causes of Plant Diversification in the Cape Biodiversity Hotspot of South Africa

Análise comparativa de várias linhagens da região biogeográfica Capense

Schnitzler *et al.* 2011

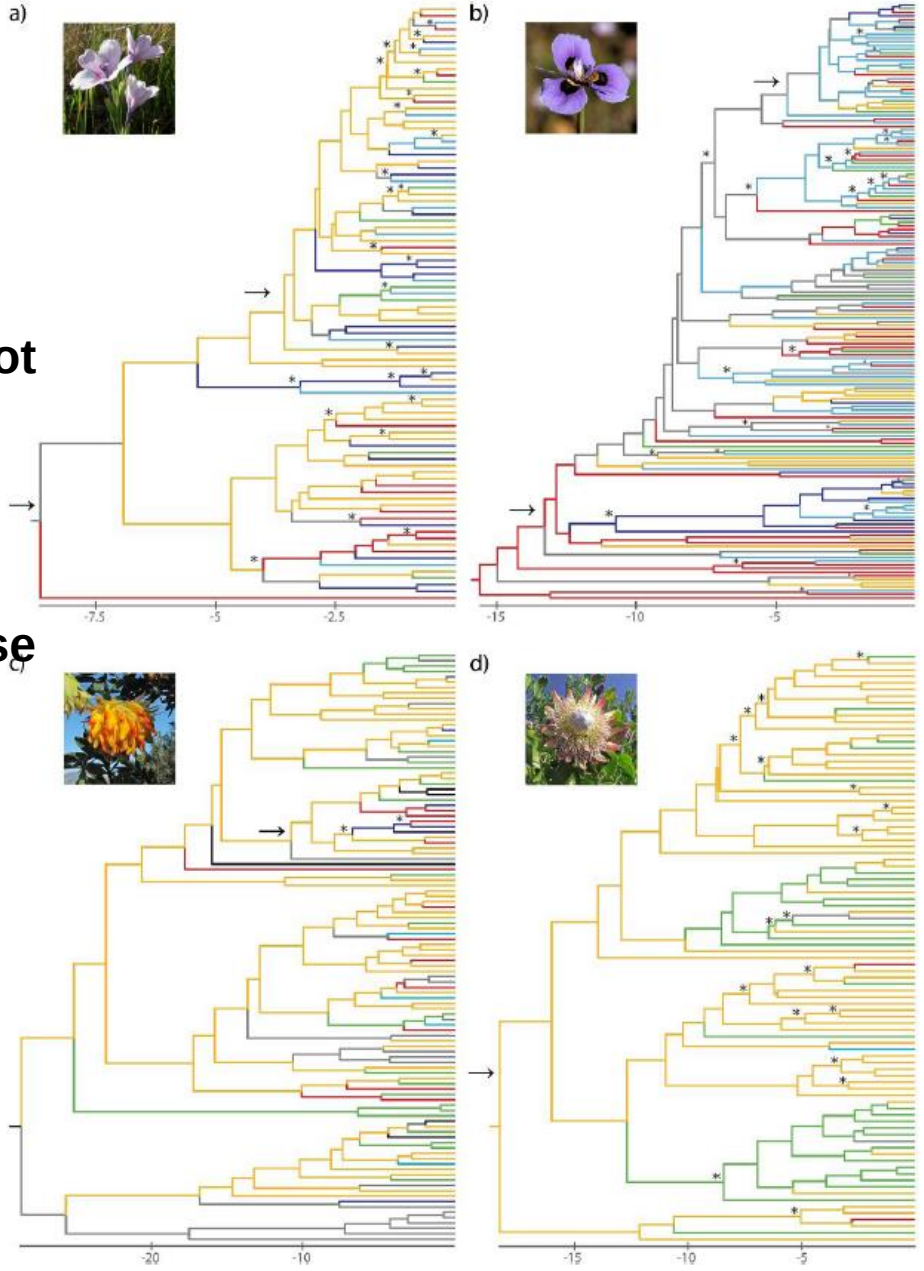

FIGURE 2. Variability of species traits. Maximum clade credibility trees of the BEAST analysis for a) *Babiana*, b) *Moraea*, c) Podalyrieae, and d) *Protea*. Branches are colored according to maximum likelihood reconstructions of soil types (blue—rocky outcrops; red—gravel, yellow—sand; greenloam; cyan—clay; black—marshy soil). Unknown states and/or equivocal reconstructions are colored in gray. Shifts in pollination system are marked with an asterisk. Arrows indicate branches along which a significant increase in diversification rates (Δ_1, Chan and Moore 2005) has been detected, the scales represent time (Ma). Photographs show representatives of the clades included in this study: a) *Babiana patersoniae*

Reconstrução das áreas ancestrais

Lemey et al. 2009

(método bayesiano)

Cronograma combinado com análise biogeográfica das RUBIACEAE neotropicais

Antonelli *et al.* 2009

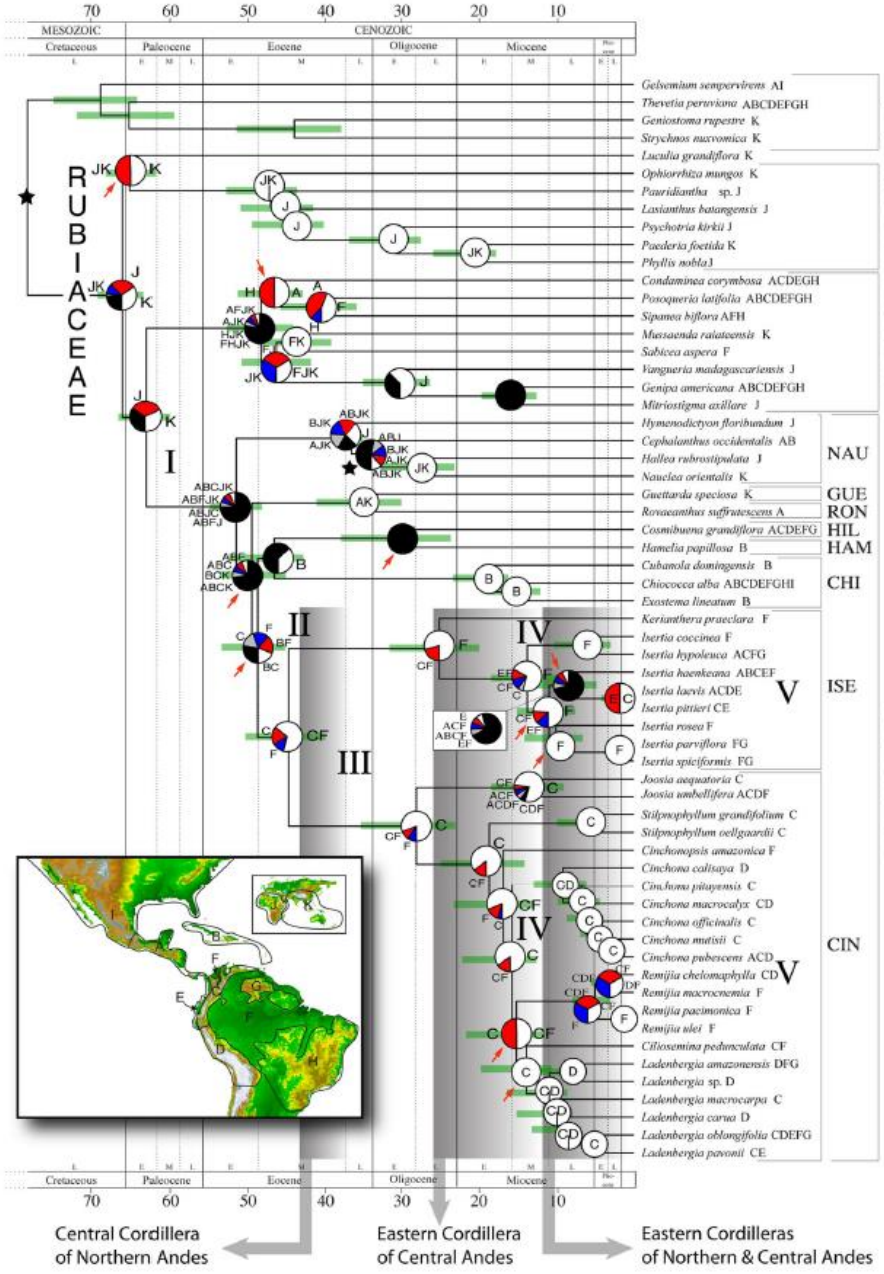

Fig. 1. Combined chronogram and biogeographic analysis of Neotropical Rubiaceae. The tree is the 50% majority-rule consensus (with compatible groups added) from the Bayesian analysis, with branches proportional to absolute ages (in millions of years) calculated from mean branch lengths of 6,000 Bayesian trees. Green bars indicate 95% confidence intervals of node ages estimated from 1,000 trees randomly sampled from the Bayesian stationary distribution. Node charts show the relative probabilities of alternative ancestral distributions obtained by integrating dispersal-vicariance analysis (DIVA) optimizations over the 1,000 Bayesian trees; the first 4 areas with highest probability are colored according to their relative probability in the following order: white > red > blue > gray; any remaining areas (usually frequencies <0.01) are collectively given with black color. Stars indicate calibration points. Red arrows indicate clades with a posterior probability <0.90. Present ranges for each species are given after the species name. Brackets identify subfamilies and tribes: CHI, Chiococceae; CIN, Cinchoneae; GUE, Guettardeae; HAM, Hamelieae; HIL, Hillieae; ISE, Isertieae; NAU, Naucleeae; RON, Rondeleticae. Shaded boxes indicate approximate periods of Andean uplift phases. The biogeographic interpretation of events I–V is summarized in Fig. 2. (*Inset*) Areas used in the biogeographic analysis. A, Central America, B, West Indies; C, Northern Andes; D, Central Andes; E, Chocó; F, Amazonia; G, The Guiana Shield; H, Southeastern South America; I, Temperate North America; J, Africa; K, Australasia. Topographic map from the National Geophysical Data Center (www.ngdc.noaa.gov).

Evolução espaço-temporal das RUBIACEAE neotropicais

Antonelli *et al.* 2009

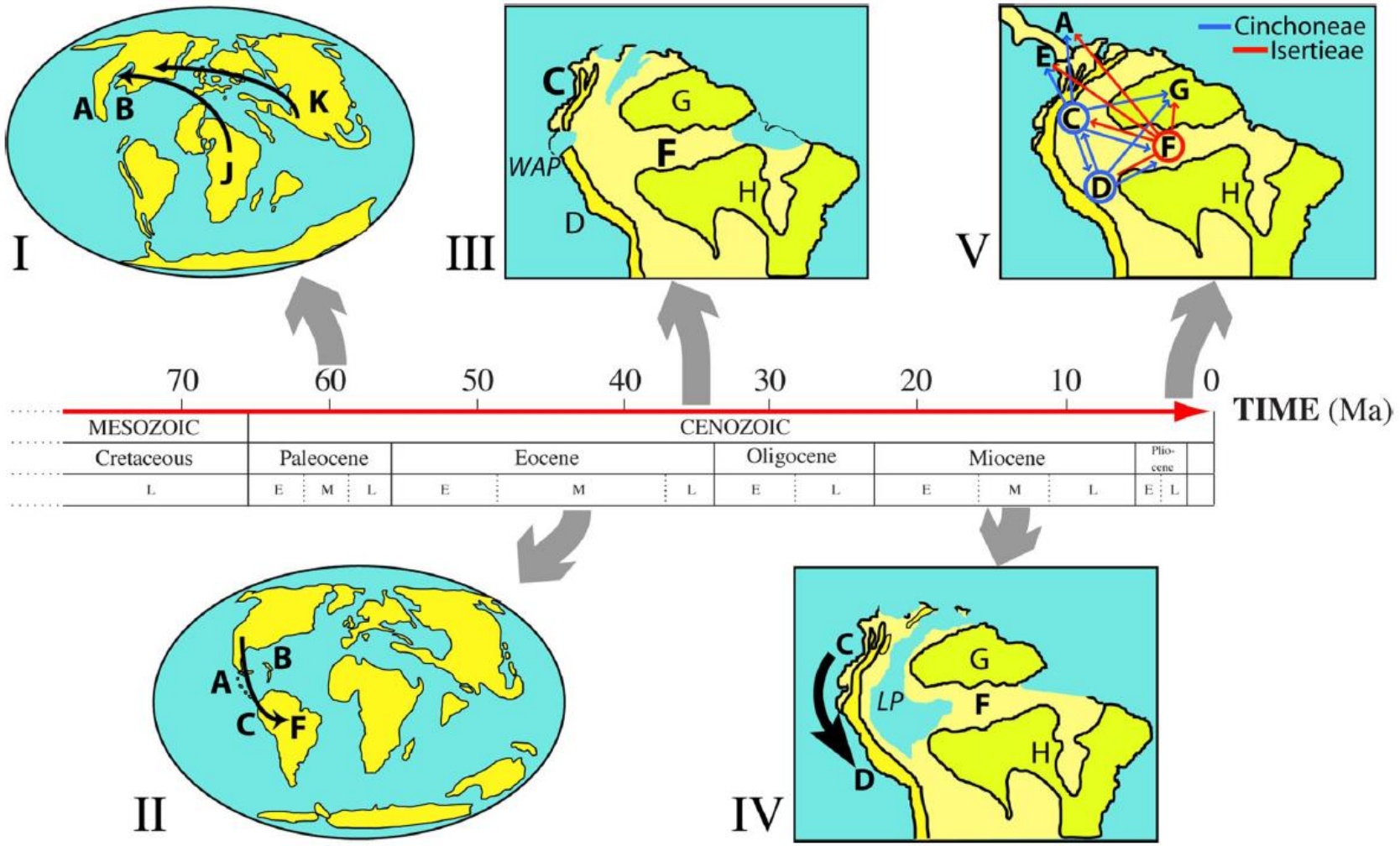

Fig. 2. Spatiotemporal evolution of the Neotropical Rubiaceae. (I) Paleocene: Rubiaceae ancestors use the boreotropical route to reach North America from the Paleotropics. (II) Early Eocene: Dispersal into South America, presumably facilitated by occasional island chains. (III) Late Eocene: North Andean and Amazonian lineages become isolated by marine incursions such as the Western Andean Portal (WAP). (IV) Middle Miocene: The gradual uplift of the Eastern Cordillera creates a huge watershed, Lake Pebas (LP). It also closes the WAP, enabling dispersal of plant lineages from the Northern to the Central Andes. (V) The Pebas system drains, promoting land dispersal of several lineages and rapid speciation of terrestrial plants in western Amazonia. Area codings as in Fig. 1. (Maps I–II are based on C. R. Scotese's PALEOMAP project (www.scotese.com); maps III–V modified from refs. 2 and 28).

Reconstrução das áreas ancestrais:

- **método bayesiano CTMC: *standard continuous time Markov chain* (implementado usando BEAST, Lemey et al. 2009)**
- **método de máxima verossimilhança** incorporando explicitamente dispersão – extinção – cladogênese (**DEC**, Ree et al. 2005) a um modelo de rotas de dispersão disponíveis em cada intervalo histórico correlacionando eventos estocásticos com persistência de linhagem: Programa **Lagrange 2010** (Ree & Smith 2008).
- **Exemplo empregando ambas abordagens: *Paederia* (Rubiaceae) - Nie te al. 2013:**

Post-Boreotropical dispersals explain the pantropical disjunction in *Paederia* (Rubiaceae)

Ze-Long Nie[1], Tao Deng[1], Ying Meng[1,2], Hang Sun[1,*] and Jun Wen[3,*]

Table 1. *Posterior age distributions of major nodes of* Paederia *in Rubiaceae, with results of ancestral reconstruction using the Bayesian CTMC and Lagrange*

	Age estimates		Bayesian CTMC		Lagrange	
Node	Mean (Mya)	95 % HPD (Mya)	Five-area	Six-area	Five-area	Six-area
C1: Rubiaceae stem	78·57	76·64–80·54				
C2: *Cephalanthus* stem	33·48	31·59–35·47				
C3: *Scyphiphora* stem	22·88	20·98–24·82				
C4: *Faramea* stem	36·84	34·94–38·8				
C5: *Morinda* crown	43·36	41·46–45·27				
1: *Paederia* stem	30·73	22·84–39·67	A (0·83)	A (0·86)	A | A (0·43)	A | A (0·44)
2: *Paederia* crown	24·21	16·41–32·5	A (0·83)	A (0·86)	A | A (0·40)	A | A (0·41)
3: *Paederia* clade I crown	15·92	5·11–26·21	A (0·77)	A (0·81)	B | A (0·65)	B | A (0·49)
4: Asian – African disjunction	15·99	10·28–22·68	A (0·80)	A (0·83)	C | A (0·68)	C | A (0·43)
5: *Paederia* clade II crown	8·68	4·59–14·43	C (0·74)	C (0·23) D (0·22) F (0·23)	C | C (0·49) CD | C (0·49)	D | C (0·39) F | C (0·39)
6: African–Central American disjunction	6·08	1·87–11·33	C (0·74)	C (0·30) D (0·30)	C | D (0·86)	F | D (0·60)
7: *Paederia* clade III crown	12·13	7·9–17·93	A (0·95)	A (0·96)	A | A (0·78)	A | A (0·81)
8: Asian–South American disjunction	10·01	5·57–15·47	A (0·95)	A (0·96)	E | A (0·65)	E | A (0·65)

Node numbers correlate with those in Figs 2 and 3 (C1–C5, calibration nodes). Letters represent results of ancestral reconstruction (as defined in Fig. 3).

Reconstrução das áreas ancestrais:

- **método bayesiano CTMC e**
- **método de máxima verossimilhança (DEC)**
- **Exemplo empregando ambas abordagens: *Paederia* (Rubiaceae) - Nie te al. 2013:**

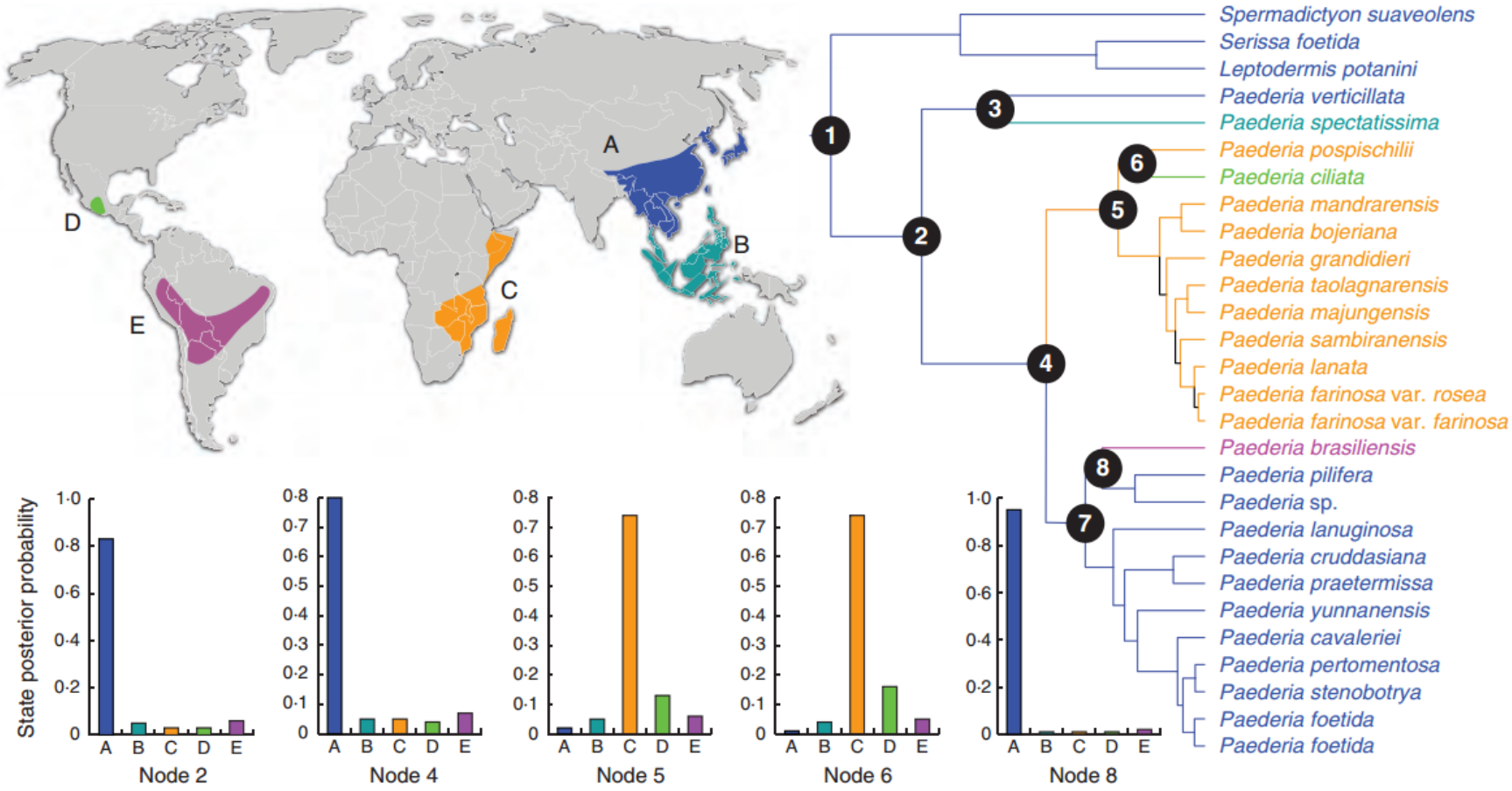

FIG. 3. Bayesian CTMC ancestral area reconstruction from the BEAST tree (right) with branches coloured according to the most probable location state of their descendent nodes. The letter and colour coding for areas are indicated on the map (left upper). Left below are state posterior probability distributions for selected nodes as shown on the right-hand tree (see Fig. 2 and Table 1 for details).

DEC - DISPERSAL-EXTINCTION-CLADOGENESIS MODEL

Ree & Smith 2008

estimating dispersal and extinction parameters and ancestral range inheritance scenarios

(abordagem usando máxima verossimilhança)

software package ***Lagrange:*** *http://code.*google.com/p/lagrange

Taxas de DISPERSÃO

Taxas de EXTINÇÃO LOCAL

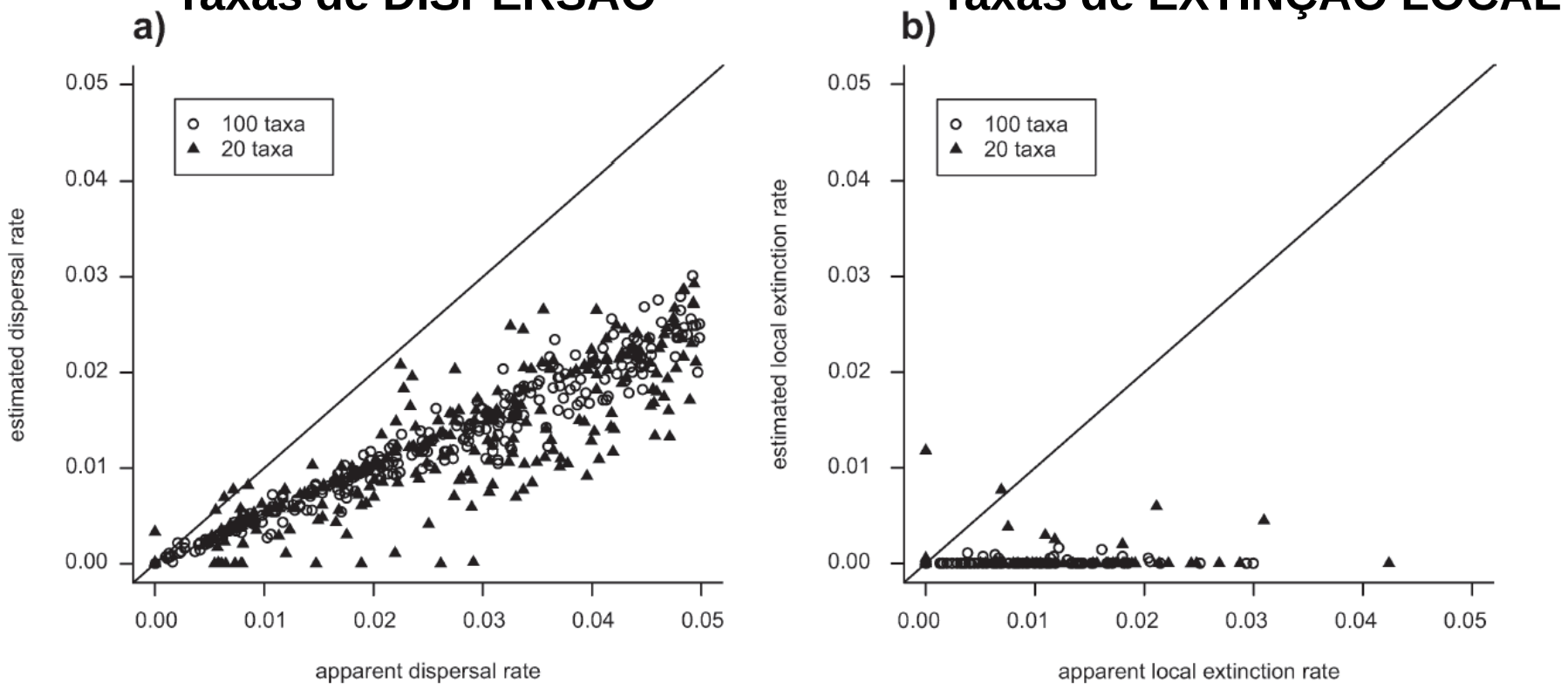

FIGURE 1. Maximum likelihood parameter estimates for rates of dispersal (a) and local extinction (b) under the DEC model from trees of two size categories simulated according to a geographic birth-death model (see text), then pruned of extinct branches. For each size, a random sample of 300 out of 2000 trees are shown. Apparent rates (the number of actual events simulated on a pruned tree divided by tree length) are plotted against estimated rates, with points below the diagonal representing underestimates. Bias toward underestimation is evident for both dispersal and local extinction, with estimates of the latter consistently being close to zero.

DEC - DISPERSAL-EXTINCTION-CLADOGENESIS MODEL

Ree & Smith 2008

lagrange: *http://code.*google.com/p/lagrange

Estudo de caso: *Psychotria* (Rubiaceae) no Havaí

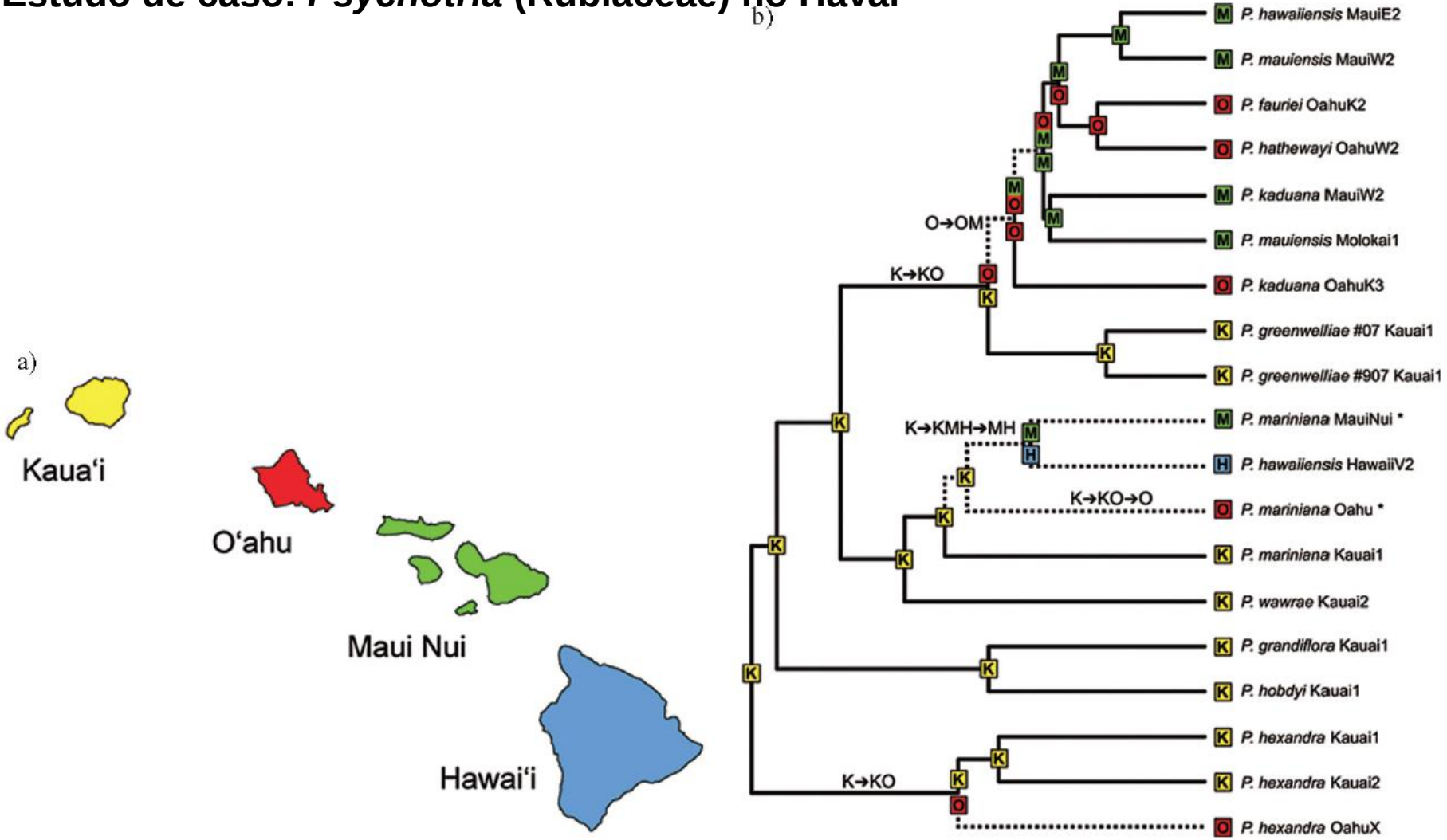

TABLE 1. Inferences about the ancestral area and range evolution parameters of Hawaiian *Psychotria* under DEC models. The unconstrained model (M0) allows geographic ranges to include any combination of islands in the archipelago and permits direct dispersal between any pair of islands. M1 and M2 restrict ranges to include a maximum of two adjacent islands. M2 further limits dispersal to be eastward between adjacent islands. The stratified model permits dispersal to islands only after their time of geological origin, thus with a root age of 5.1 Ma, the only ancestral area possible is Kaua'i.

Model	Area	$-\ln(L)$	Dispersal	Extinction
M0	Kaua'i	35.758	0.040	0.0358
	O'ahu	40.700	0.041	0.024
	Maui Nui	44.378	0.054	0.076
	Hawai'i	45.323	0.058	0.085
M1	Kaua'i	34.636	0.093	0.017
	O'ahu	38.877	0.112	0.052
	Maui Nui	48.683	0.207	0.164
	Hawai'i	55.396	0.377	0.280
M2	Kaua'i	32.434	0.132	0.009
	O'ahu	106.018	0.174	0.103
	Maui Nui	107.701	0.216	0.101
	Hawai'i	118.930	0.173	0.066
Stratified	Kaua'i	40.777	0.075	0.082

DEC - DISPERSAL-EXTINCTION-CLADOGENESIS MODEL

Ree & Smith 2008

Lagrange: *http://code.*google.com/p/lagrange

Estudo de caso:
Psychotria (Rubiaceae) no Havaí

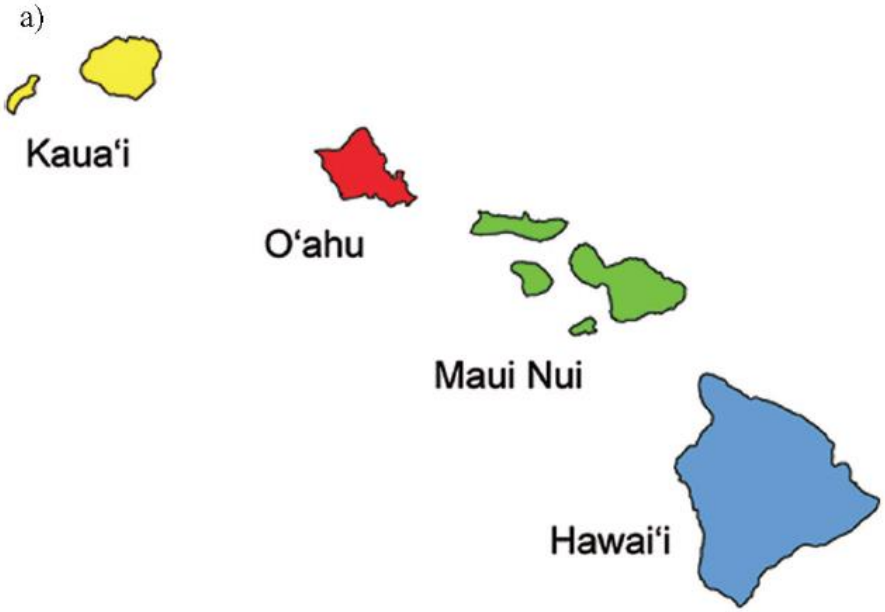

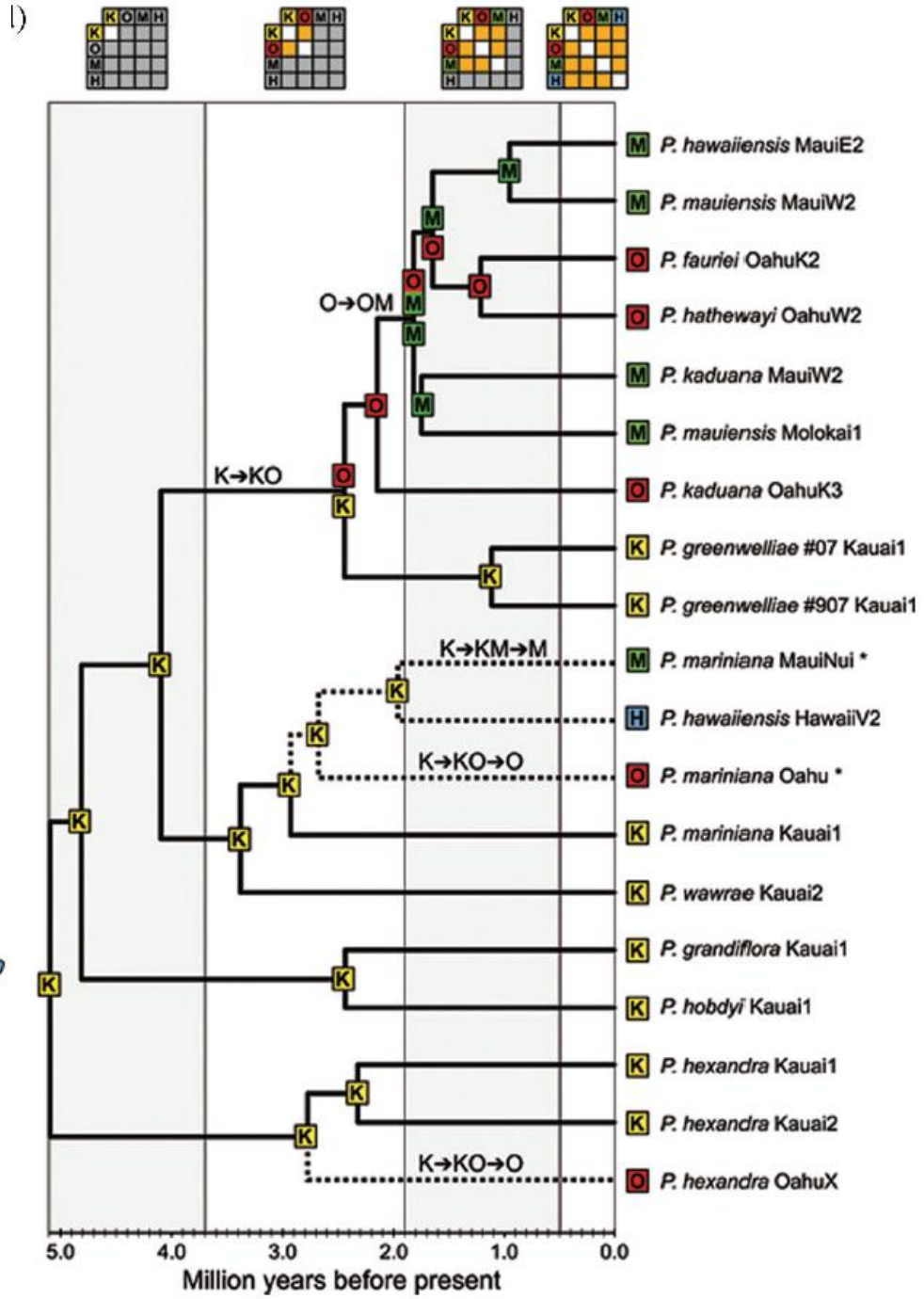

Global biogeography and diversification of palms sheds light on the evolution of tropical lineages. II. Diversification history and origin of regional assemblages

William J. Baker[1]* and Thomas L.P. Couvreur[2]

ARECACEAE

Baker & Couvreur 2013

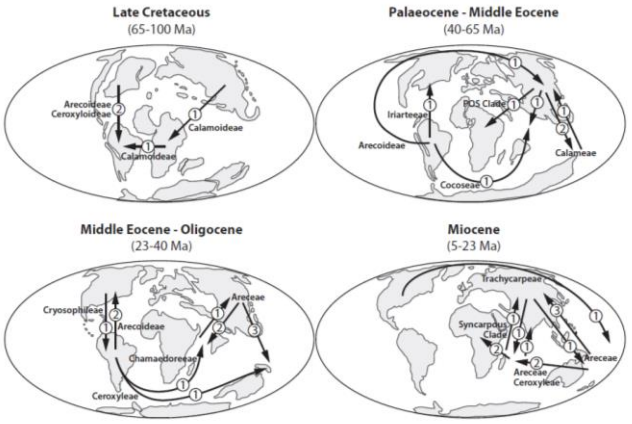

Figure 2 Summary of the dispersal history of palms. Four time frames were chosen to represent the history of the major dispersal events in palms. Arrows represent inferred dispersal events (*not* specific dispersal routes) above the genus level following Fig. 1. Circles on arrows indicate the number of dispersal events that took place in the same direction. Subfamily, tribe or major clade names are indicated on certain arrows (Dransfield *et al.*, 2008). Base maps are derived from Buerki *et al.* (2011).

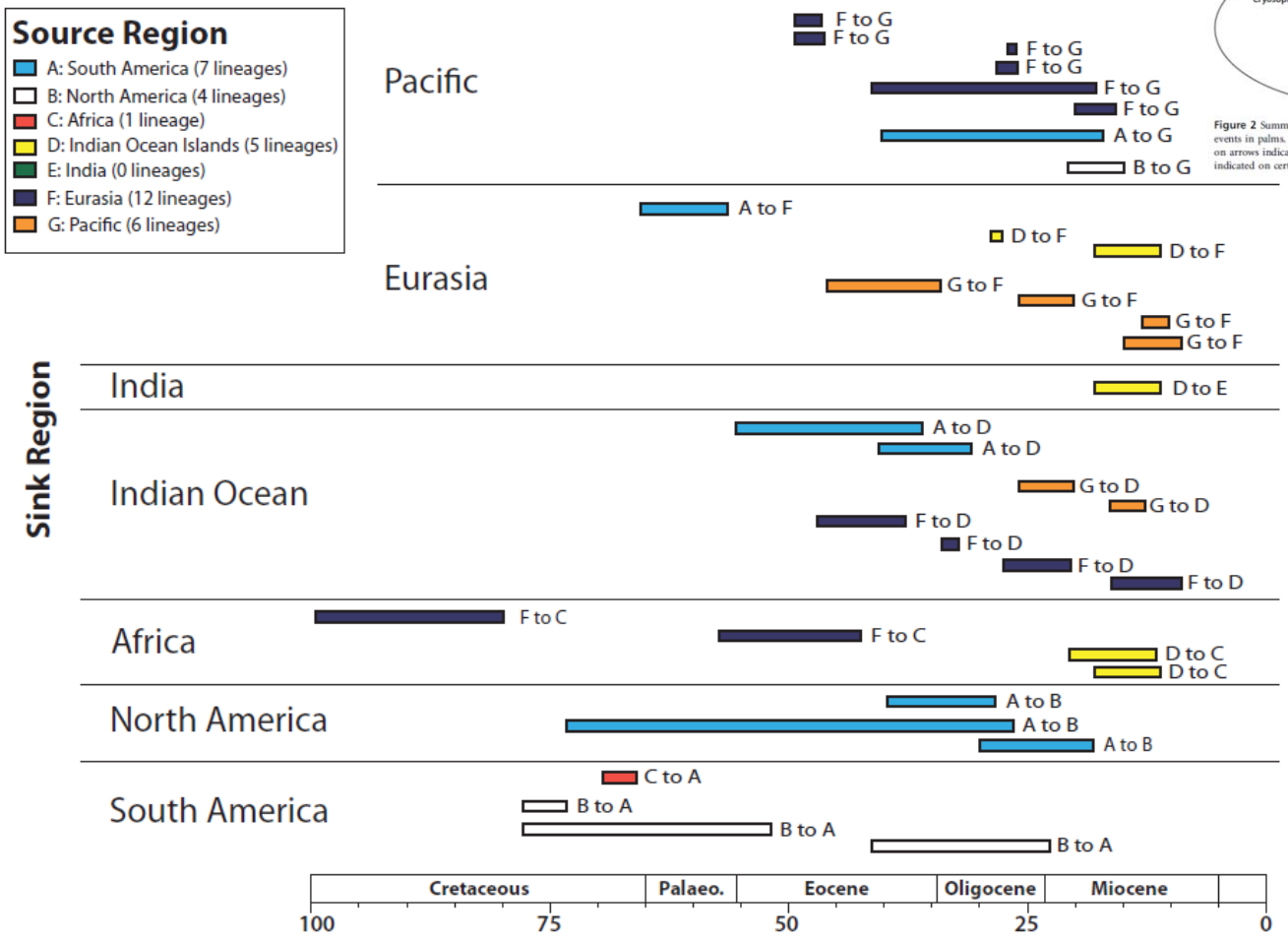

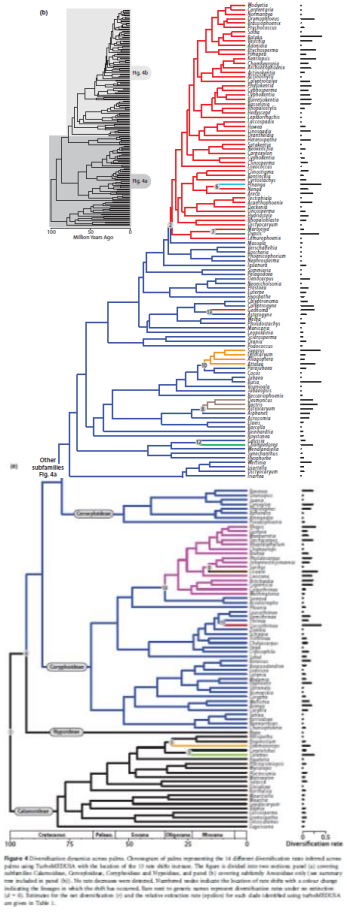

Figure 1 Temporal history of dispersal events in palms. All 35 dispersal events inferred from the most likely ancestral area reconstructions determined by LAGRANGE are illustrated, grouped into sink regions (see Fig. 1 of Baker & Couvreur, 2013 and raw LAGRANGE output at the Dryad data repository: doi:10.5061/dryad.vb25b35j). Each event spans the stem and crown node age of the branch along which it was inferred.

Post-Boreotropical dispersals explain the pantropical disjunction in *Paederia* (Rubiaceae)

Cronograma de *Paederia* e grupos relacionados (Rubiaceae)

4 marcadores plastidiais:
rbcL, rps16, trnT-F and atpB-rbcL

Inferido com BEAST.

Barras cinza = 95 % highest posterior density intervals for node ages.

C1 –C5 = calibrations points

Nie et al. 2013

Paederia foetida

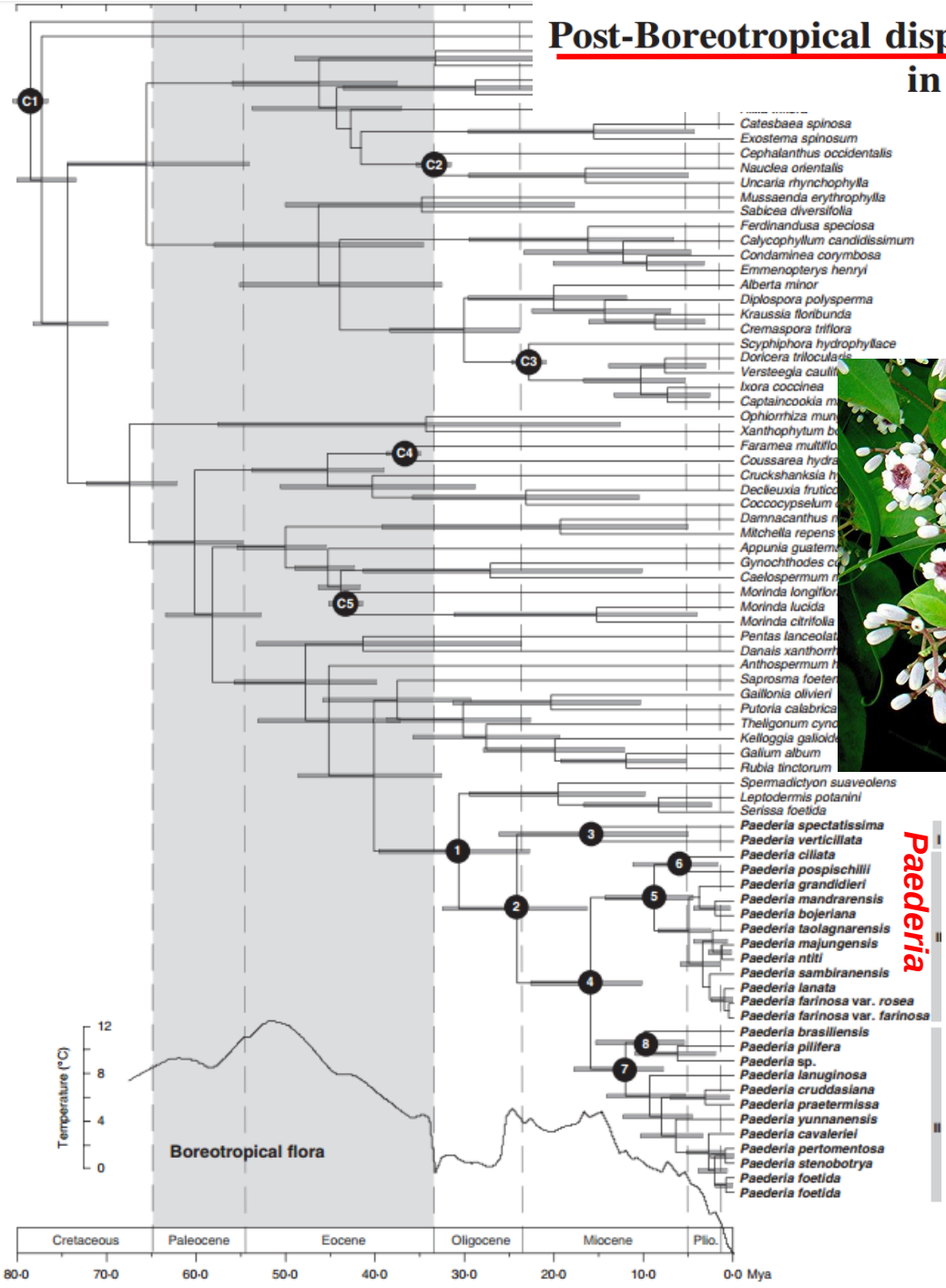

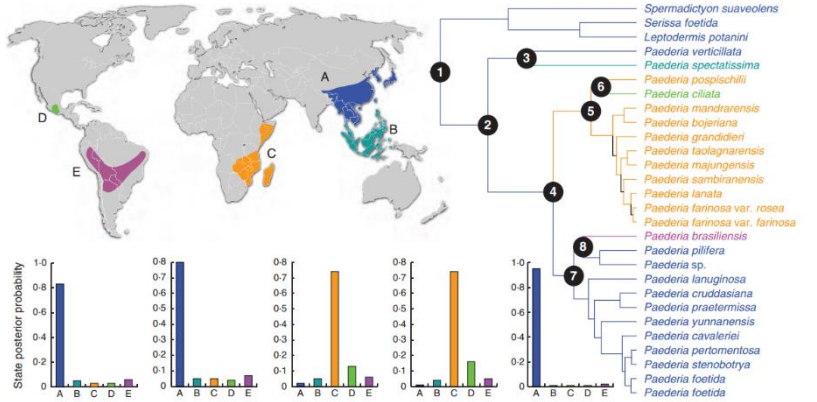

FIG. 3. Bayesian CTMC ancestral area reconstruction from the BEAST tree (right) with branches coloured according to the most probable location state of their descendent nodes. The letter and colour coding for areas are indicated on the map (left upper). Left below are state posterior probability distributions for selected nodes as shown on the right-hand tree (see Fig. 2 and Table 1 for details).

Cantley et al. 2014

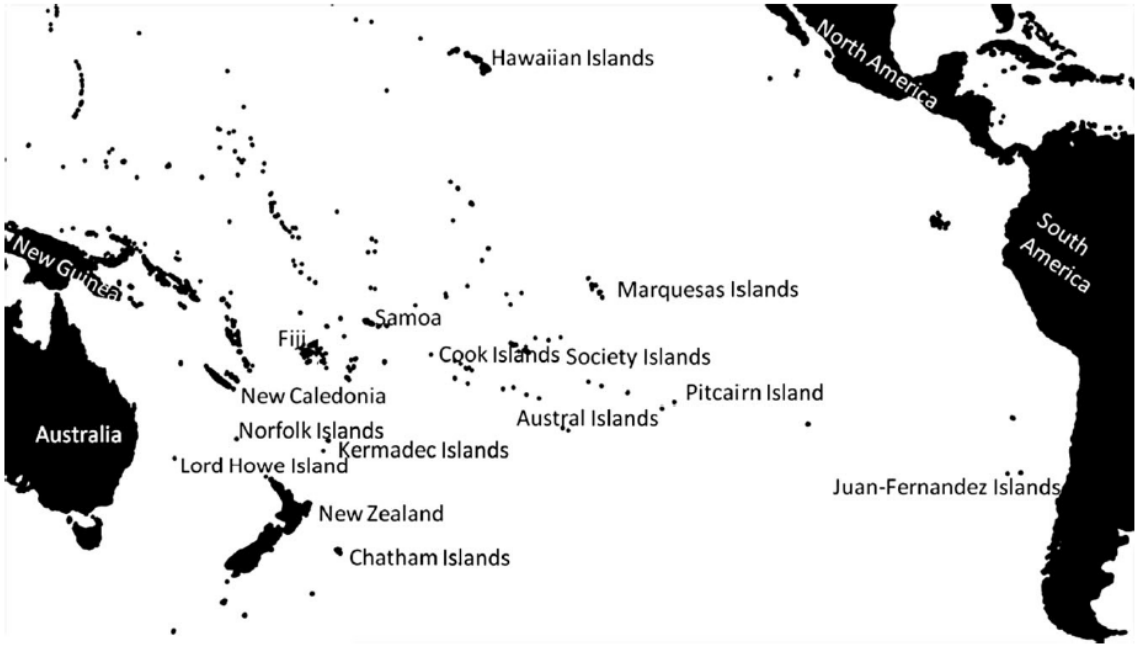

Figure 1. Map of the Pacific Ocean indicating selected island archipelagos and continental land masses discussed in the text. Note that island borders were thickened to better display their locations.

Anthospermae (Rubiaceae)

Heads 2017

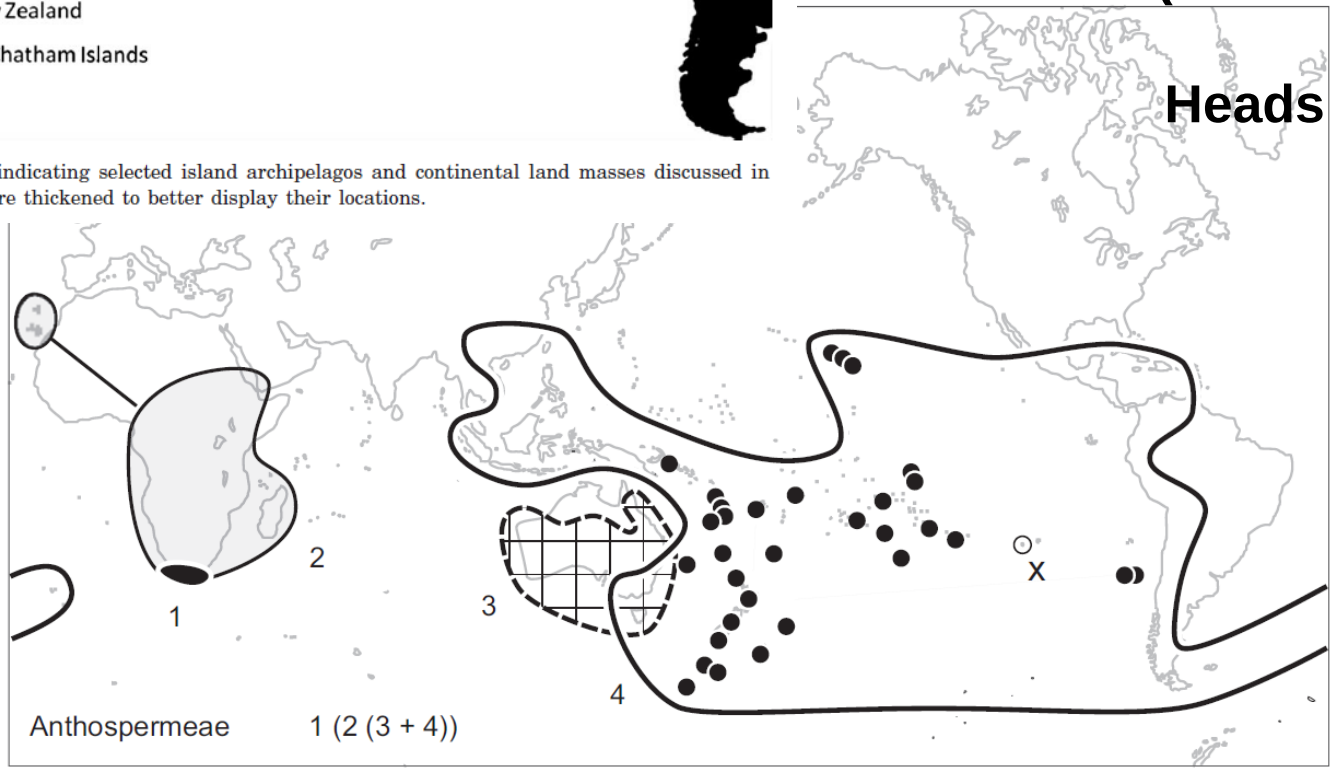

Fig. 8. Distribution of tribe Anthospermeae (Rubiaceae) and its four main clades. 1 = *Carpacoce*; 2 = Anthosperminae; 3 = Opercullariinae; 4 = Coprosminae (Rydin et al., 2009). The phylogeny is: 1 (2 (3 + 4)). Black dots = localities of Coprosminae on Pacific islands east of Australia. Open circle with "x" = fossil pollen on Easter Island.

Biogeographic insights on Pacific *Coprosma* (Rubiaceae) indicate two colonizations to the Hawaiian Islands

JASON T. CANTLEY[1]*, NATHAN G. SWENSON[2], ADRIENNE MARKEY[3] and STERLING C. KEELEY[1]

Cantley et al. 2014

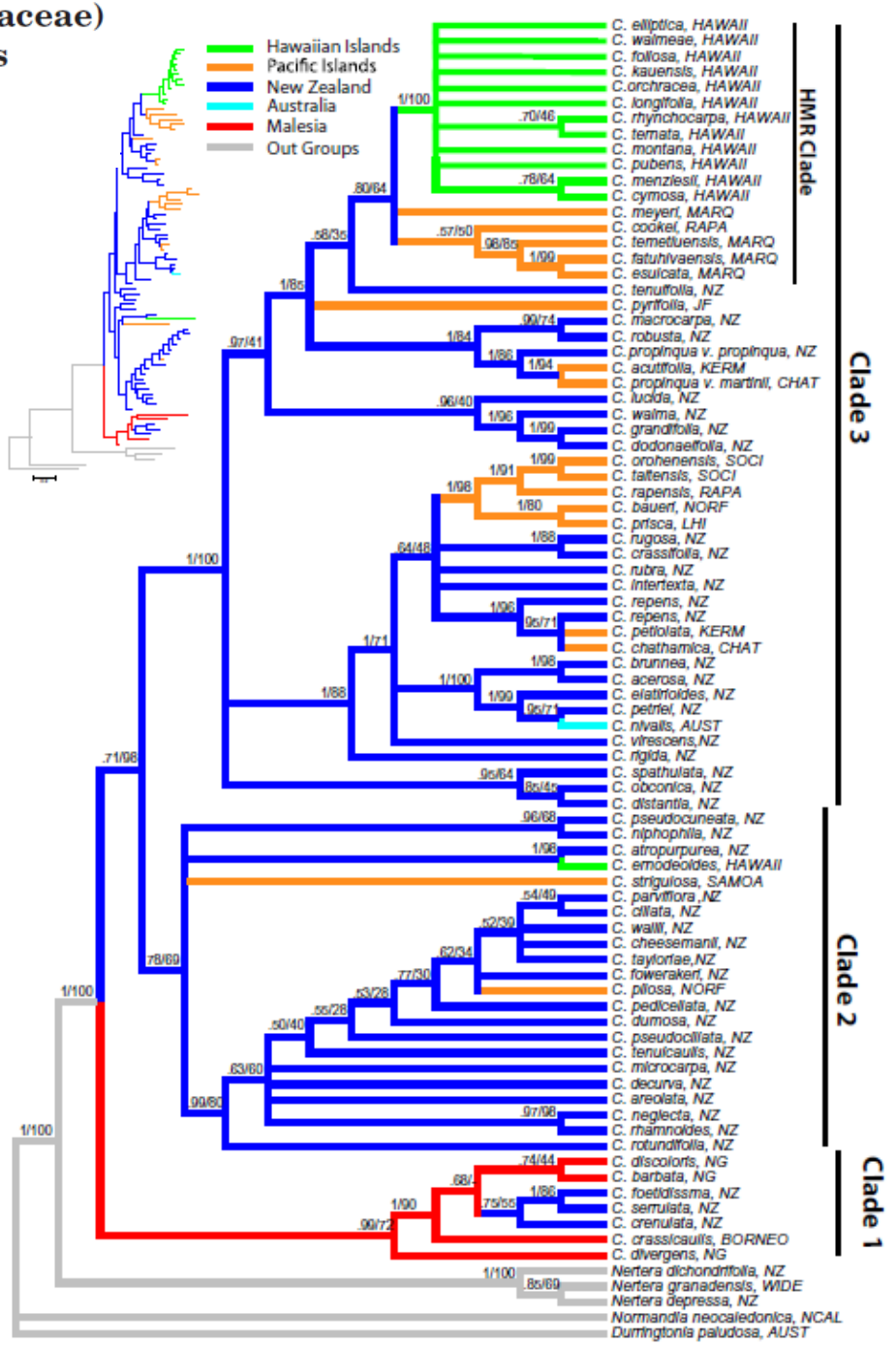

Metapopulation vicariance explains old endemics on young volcanic islands

Michael Heads*

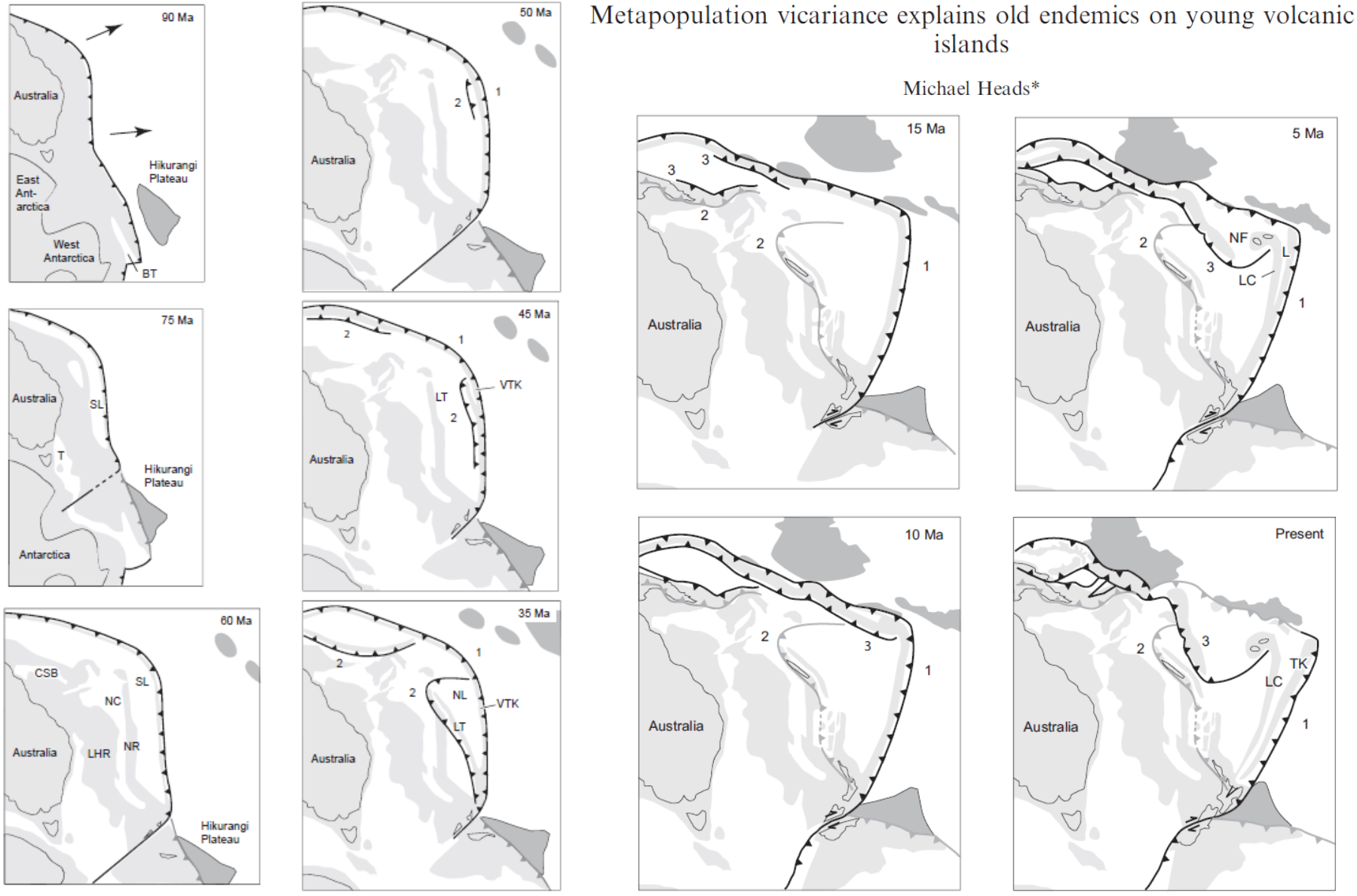

Heads 2017

Fig. 3. Tectonic reconstruction of the south-west Pacific, from the Late Cretaceous to the Present. The reference frame is Australia-fixed. Light grey = continental crust and island arc crust; dark grey = oceanic plateaus. Geographical outlines are shown to help identify the location of the crustal blocks but have no palaeogeographical significance. Arrows in the 90-Ma reconstruction = migration of subduction zone by slab rollback. 1, 2, 3 = 1st, 2nd and 3rd generation subduction zones. BT, Bounty Trough; CSB, Coral Sea Basin; LC, Lau–Colville Ridge; LHR, Lord Howe Rise; LT, Loyalty–Three Kings Ridge; NC, New Caledonia Basin; NL, North Loyalty Basin; NR, Norfolk Ridge; SL, South Loyalty Basin; T, Tasman Basin; TK, Tonga–Kermadec Ridge; NF, North Fiji Basin; VTK, Vitiaz–Tonga–Kermadec Ridge. Simplified from Schellart et al. (2006).

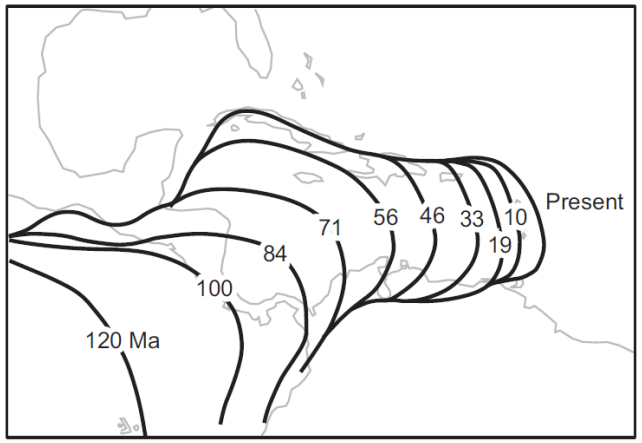

Fig. 6. Former relative positions of the Caribbean Trench from 120 Ma to the Present. The base map has no palaeogeographical significance; over the time period shown, North and South America have drifted apart (Pindell and Kennan, 2009).

Heads 2017

Metapopulation vicariance explains old endemics on young volcanic islands

Michael Heads*

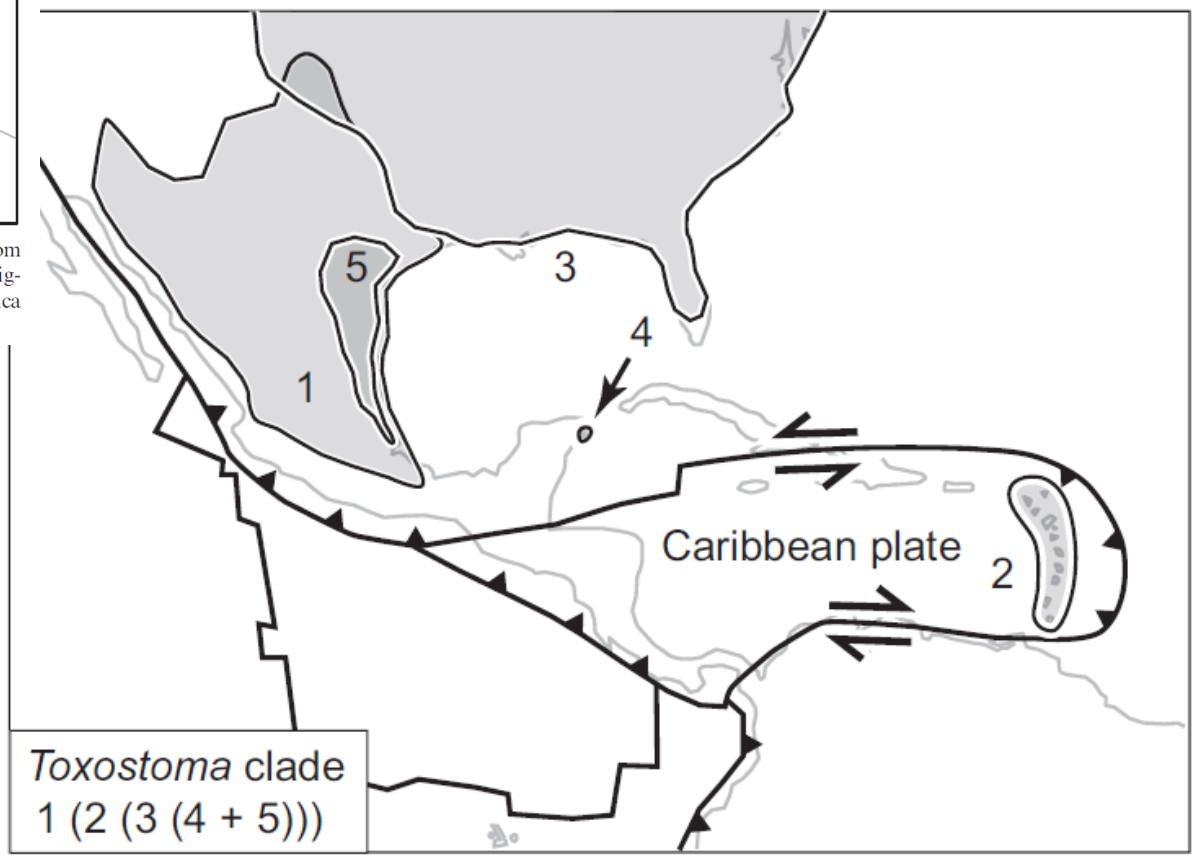

Fig. 5. Distribution of a clade in *Toxostoma* (Mimidae). 1 = *T. curvirostre*, 2 = *T. ocellatum*, 3 = *T. rufum*, 4 = *T. guttatum*, 5 = *T. longirostre*. Phylogeny from Lovette et al. (2012); distributions from IUCN (2016). Continuous lines = divergent and transform plate margins. Lines with barbs = subduction zones (barbs on over-riding plate). Plate boundaries simplified.

PAPEL DOS DADOS MOLECULARES NA HISTÓRIA BIOGEGRÁFICA

Crisci et al. 2003

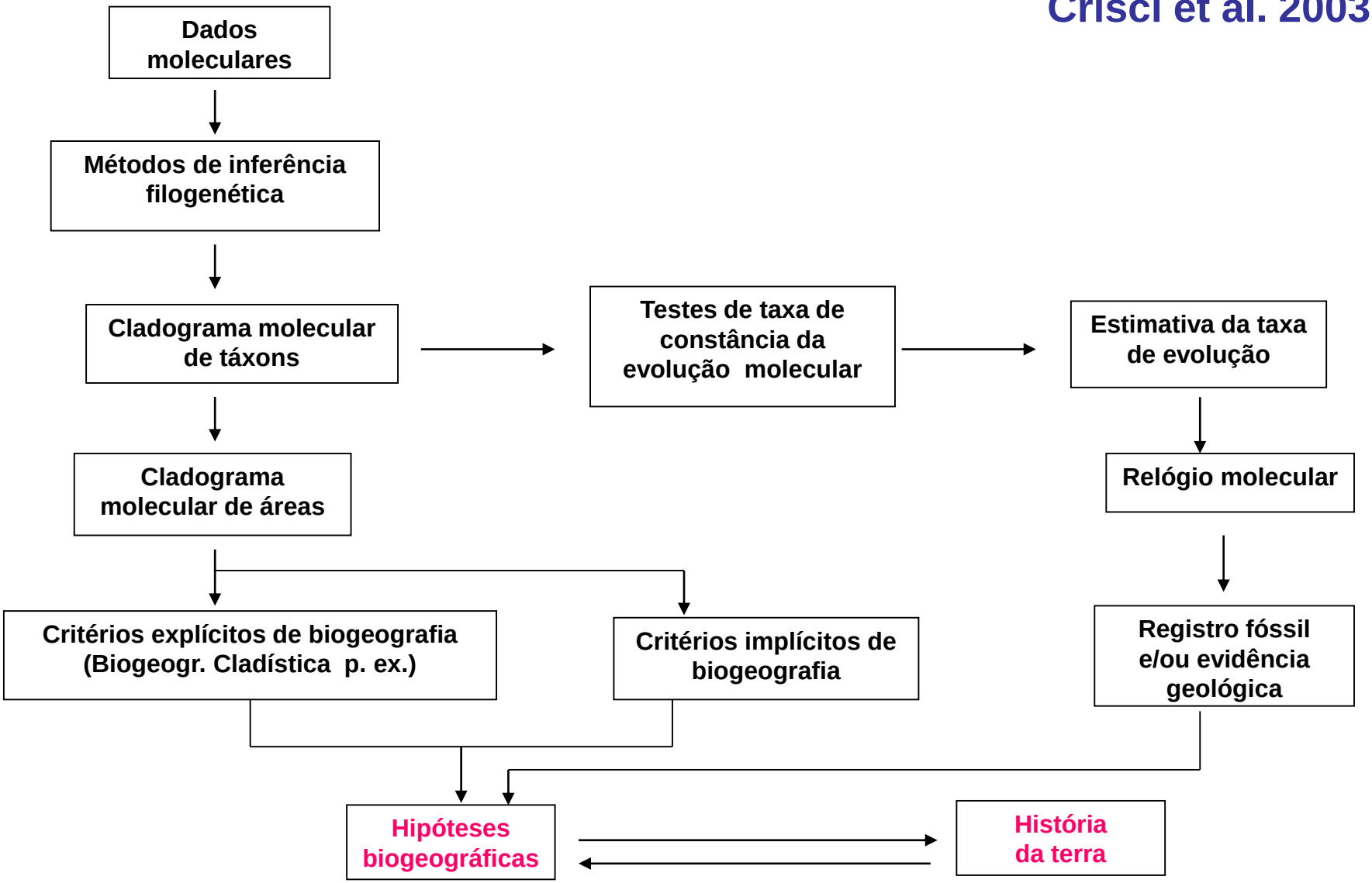

Limitações das datações nas filogenias moleculares: idades do grupo-copa (*crown-group*) e do grupo-tronco (*stem-group*)

*Viés: o fóssil só fornece a **idade mínima** do grupo (Heads 2012)*

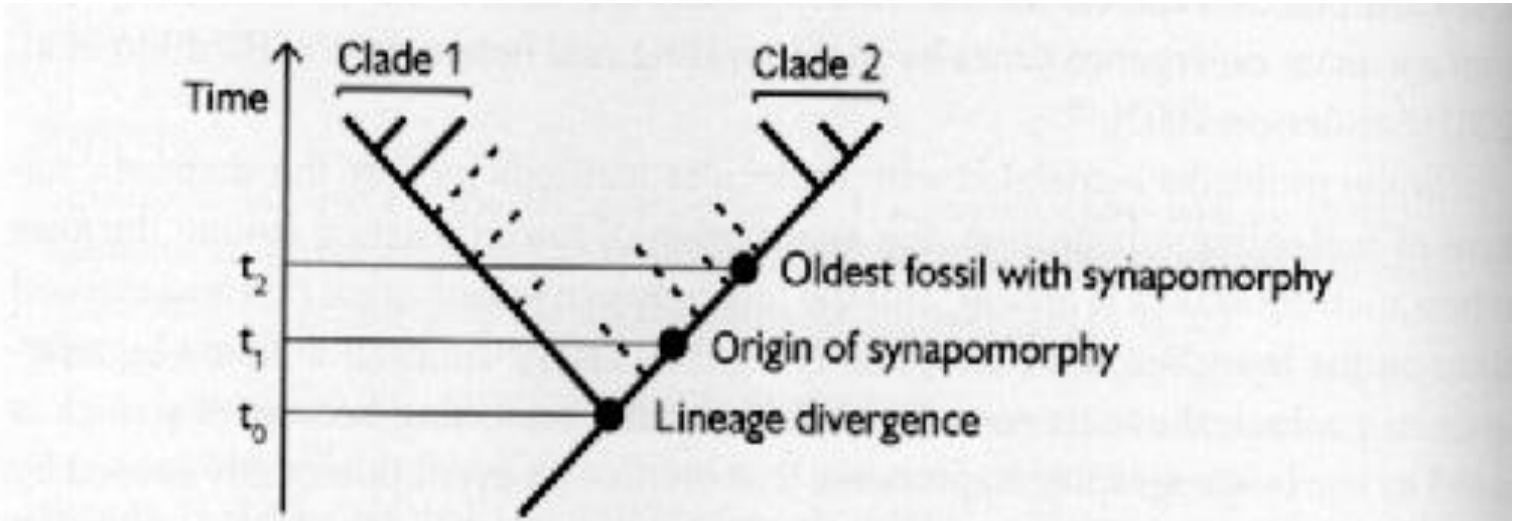

Figure 7.9 Relationship of lineage divergence, origin of a synapomorphy, and occurrence of the oldest fossil with the synapomorphy, according to Magallón (2004). There is a temporal gap between the divergence of a taxon and its sister taxon (t_0), the origin of the synapomorphy (t_1), and the occurrence of the oldest fossil bearing such synapomorphy (t_2).

Morrone 2009

Limitações das datações nas filogenias moleculares

História evolutiva das famílias de marsupiais sul-americanos

Patterson & Pascual 1972 apud Lomolino et al. 2006

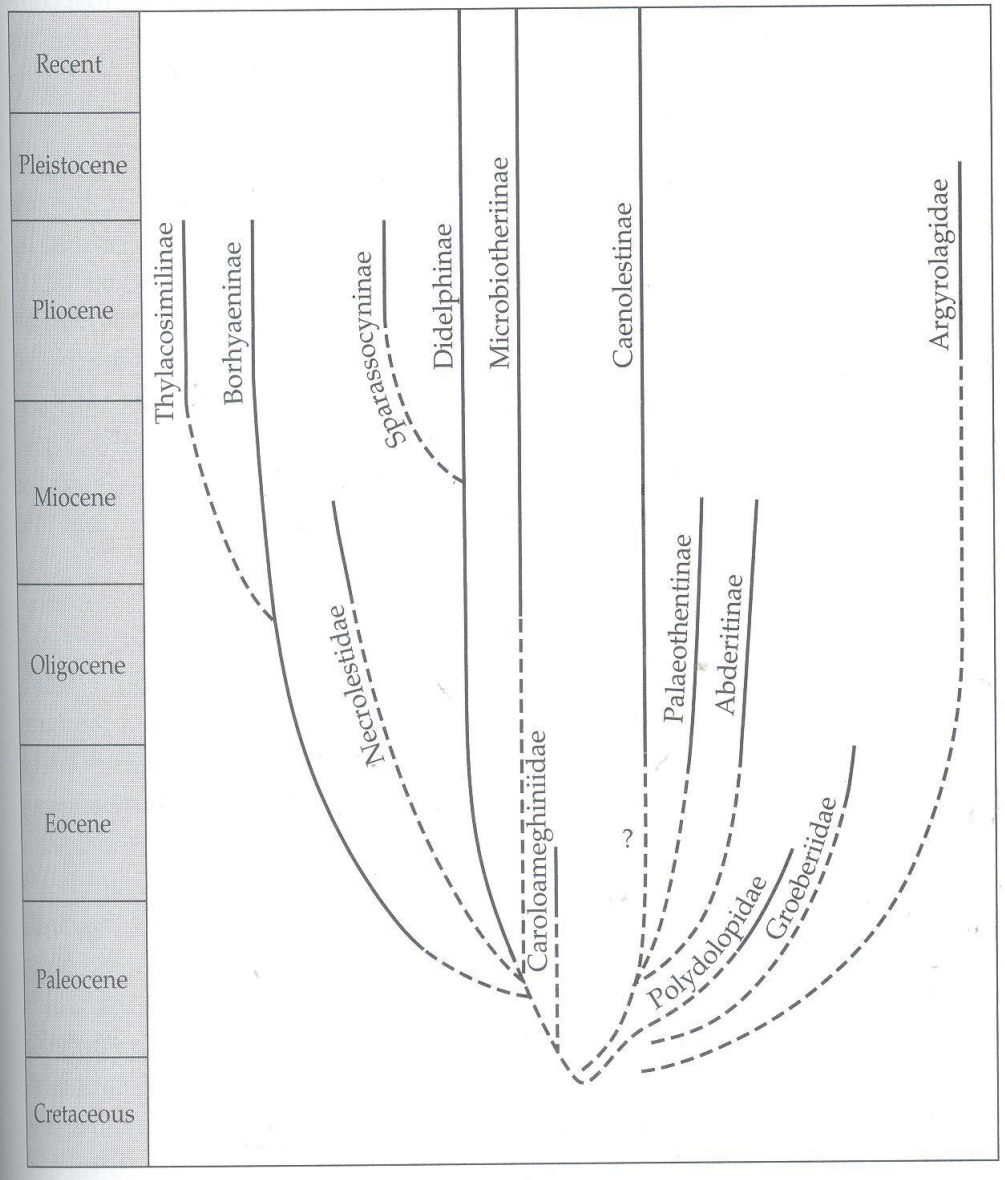

FIGURE 11.16 A phylogenetic hypothesis for the family-level relationships and evolutionary history of South American marsupials. The fossil record shows that this group had a wide radiation on the isolated South American continent during the early Cenozoic, but only three families have survived to the present. The solid lines show the known time spans of the families in the fossil record; the dashed lines show their inferred durations and relationships to other families. This hypothetical reconstruction uses a modification of cladistic methods, based on detailed information on the living forms supplemented by limited data on morphology and dates obtained from the fossils. A classification that employed molecular and strict cladistic techniques would show only the relationships among the three extant families, missing much of the rich history of this groups of South American mammals. (After Patterson and Pascual 1972.)

"GIMNOSPERMAS"

- provavelmente é um grupo parafilético

  - **Dados moleculares:** Chase *et al.* 1993, Doyle *et al.* 1994, Rydin *et al.* 2002, Soltis *et al.* 2002
  - **Dados morfológicos:** Crane 1985, Doyle *et al.* 1994, Loconte & Stevenson 1990

- hipóteses recentes de monofilia do grupo

  - **Dados moleculares:** Samigullin *et al.* 1999, Bowe *et al.* 2000, Chaw *et al.* 1997, Chaw *et al.* 2000, Soltis *et al.* 2002, Simpson 2006, Won & Renner 2006


Carbonífero - Permiano


Triássico


Cretáceo inferior

Acesso à informação paleontológica
(campo praticamente exclusivo da morfologia)

Medullosa

ARCHAEOPTERIS
LYGINOPTERIS
MEDULLOSANS
CYCADS] viventes
CORDAIXYLON
MESOXYLON
LEBACHIA
EXTANT CONIFERS] viventes
GINKGO
CALLISTOPHYTON
PELTASPERMS
GLOSSOPTERIDS
CAYTONIA
CORYSTOSPERMS
BENNETTITALES
PENTOXYLON
GNETUM
WELWITSCHIA
EPHEDRA
ANGIOSPERMS
viventes

Crane 1985

PTERIDOSPERMALES - Carbonífero ao Permiano

CAYTONIALES - Permiano ao Triássico

GLOSSOPTERIDALES - Triássico ao Cretáceo

BENNETTITALES – Triássico ao Cretáceo

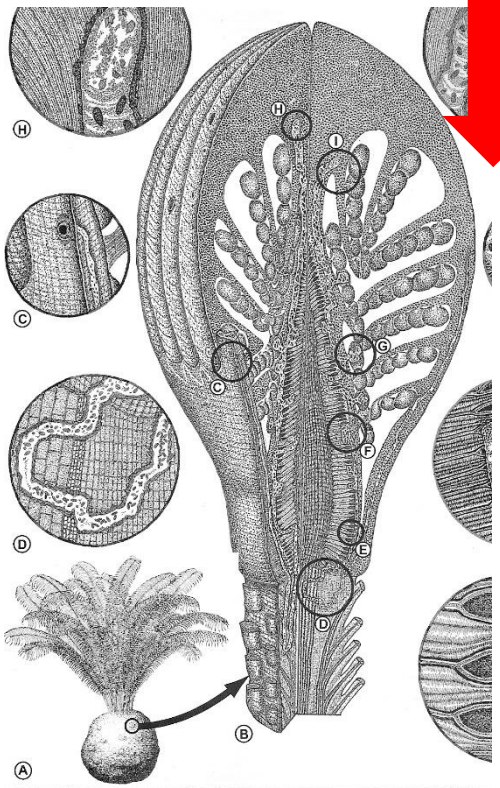

Cycadeoidea

Labandeira *et al.* 2007

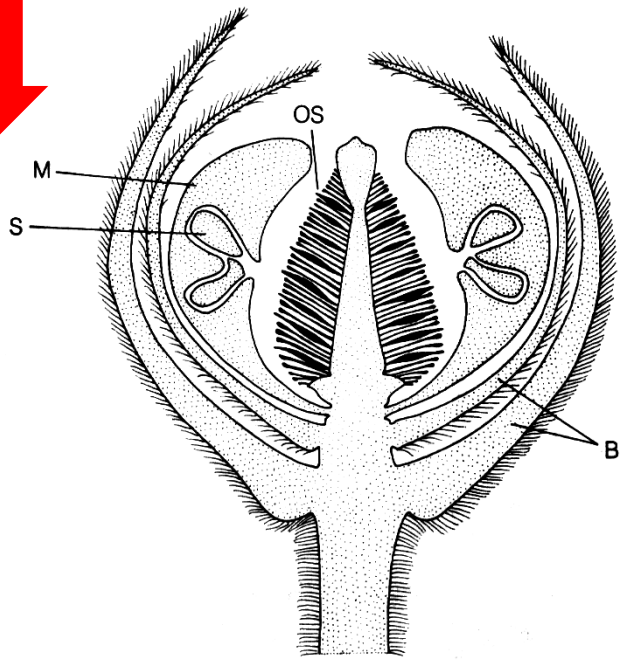

Williamsoniella

Gifford & Foster 1989

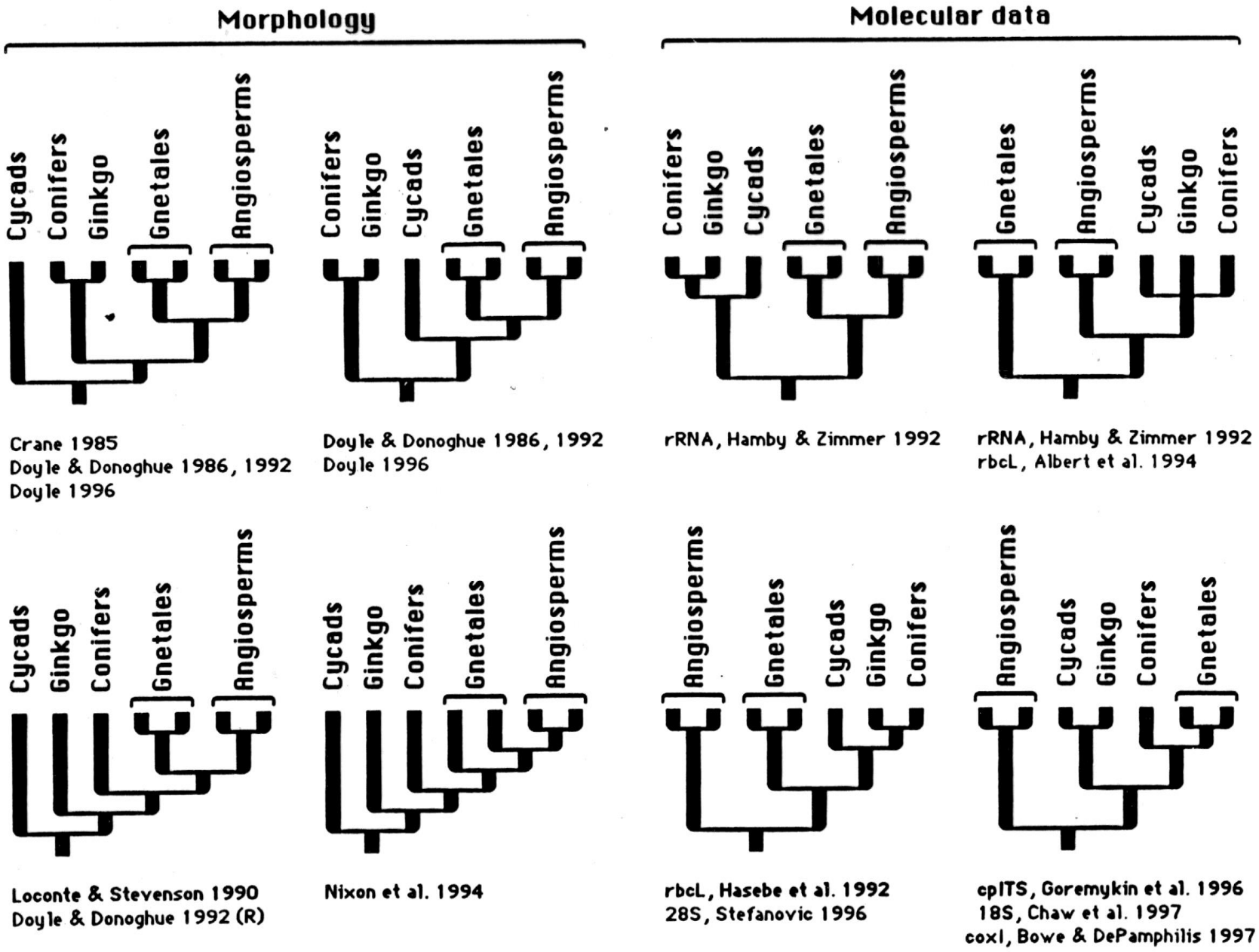

Figure 3 Relationships among living groups of seed plants found in different analyses of morphological and molecular data

Doyle 1998

Won & Renner 2006

rbcL + matK
Bayesian relaxed clock

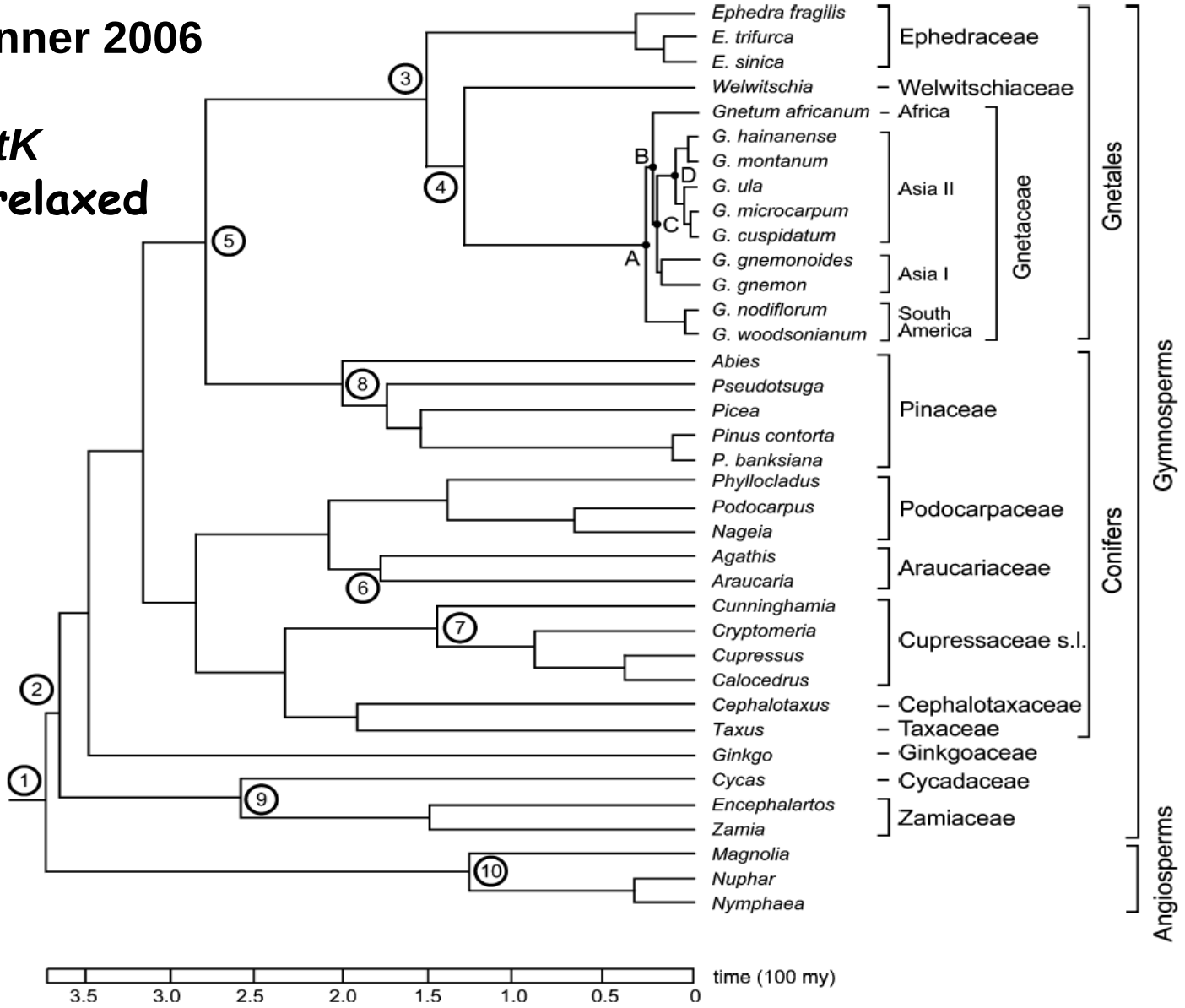

FIGURE 1. Divergence events in *Gnetum* estimated from the chloroplast genes *rbcL* and *matK* analyzed under a Bayesian relaxed clock, constrained by fossil-based minimal ages at nodes 2 to 9 (see Materials and Methods) and assuming that Gnetales are nested in the conifers (the so-called Gnepine topology). For results with four other seed plant topologies see Figures S1A–D. All analyses were rooted with *Psilotum* because the GenBank *matK* sequence of *Marchantia* appears to be a pseudogene. Nodes of particular biogeographic interest are A, the split between the South American clade of *Gnetum* and the remainder of the genus; B, the split between African and Asian *Gnetum*; C, the split between the two main Asian clades of *Gnetum*; and D, the onset of radiation of the most species-rich Asian clade.

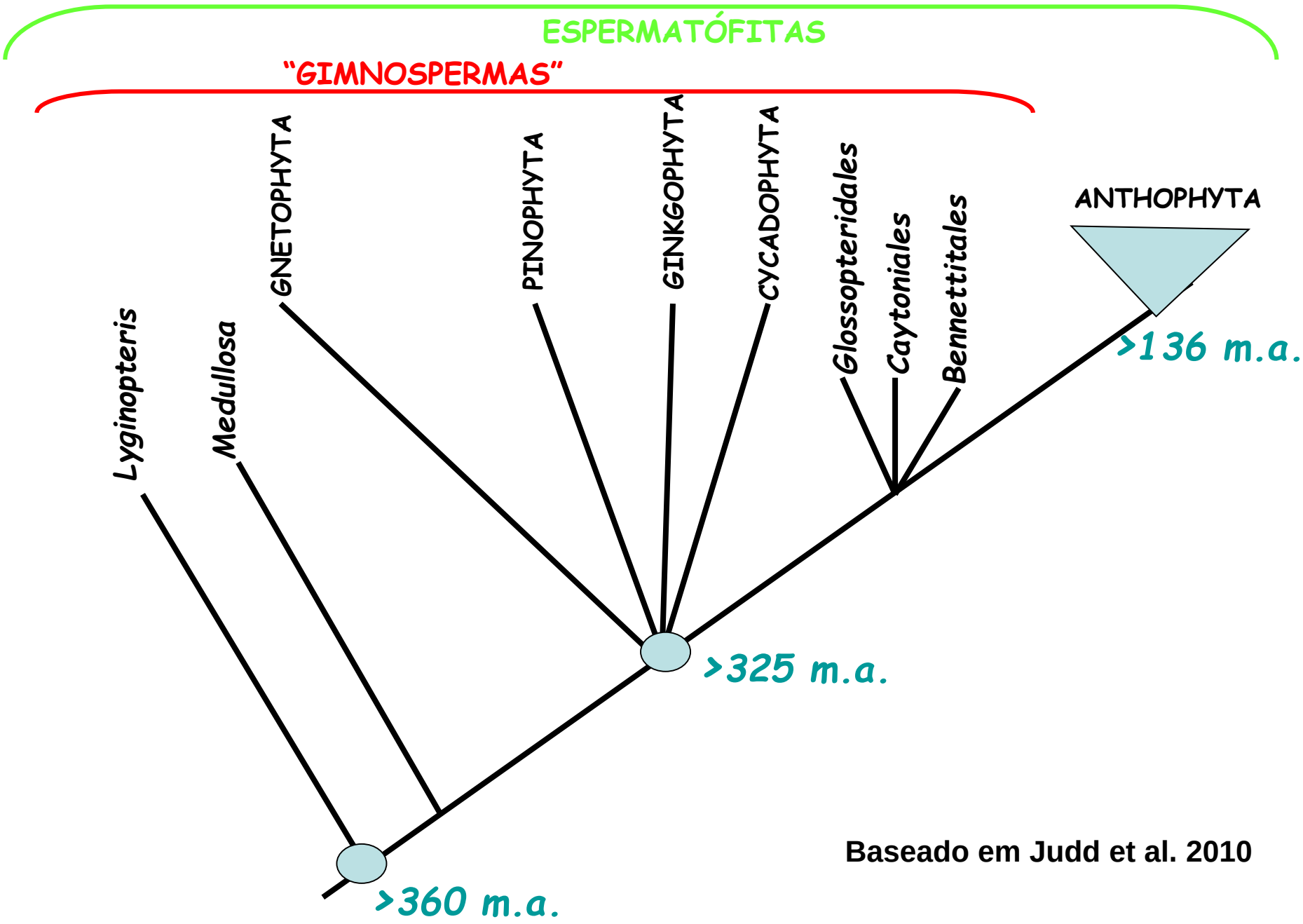

Baseado em Judd et al. 2010

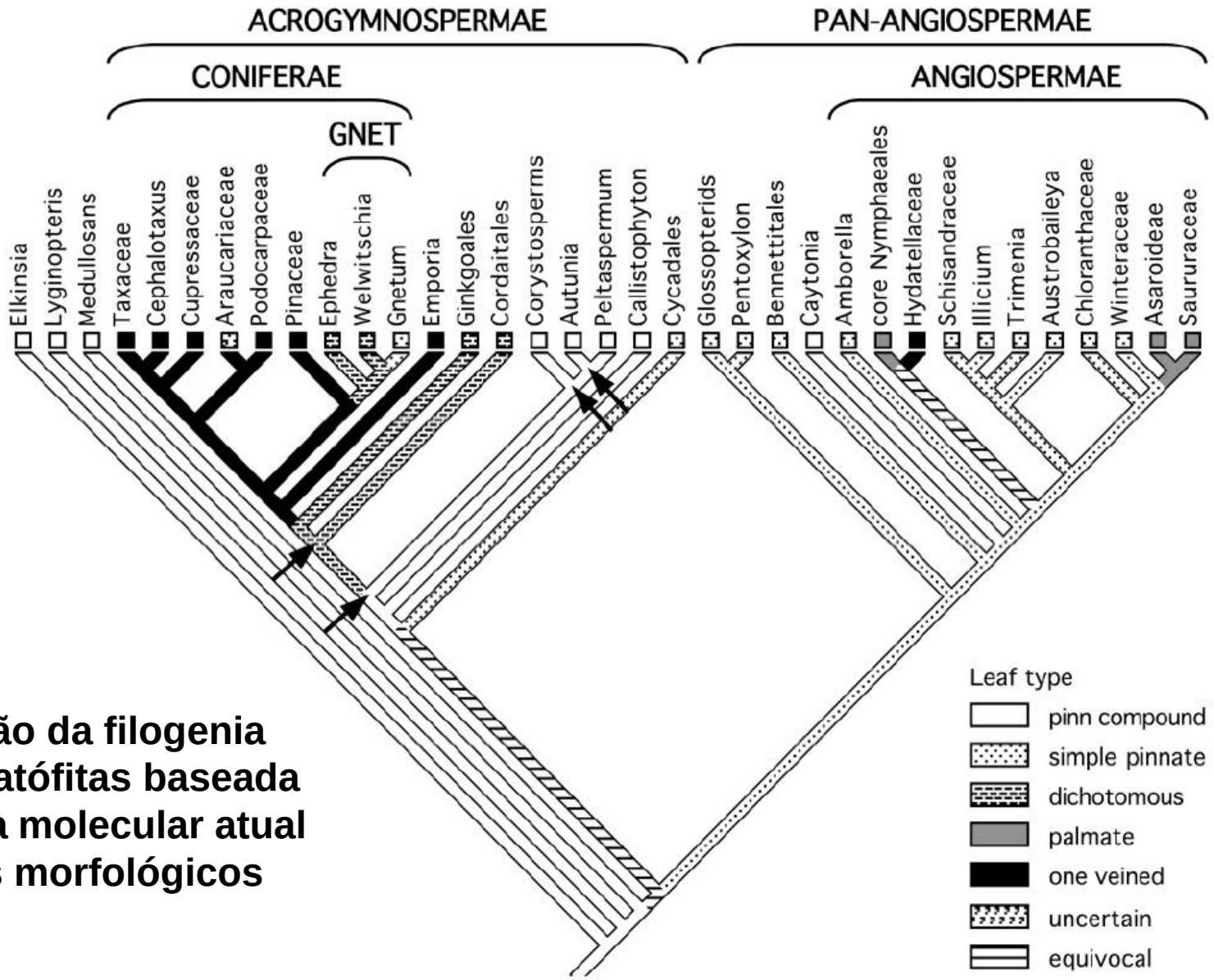

Reconstrução da filogenia das espermatófitas baseada na topologia molecular atual e nos dados morfológicos de fósseis

Doyle 2008

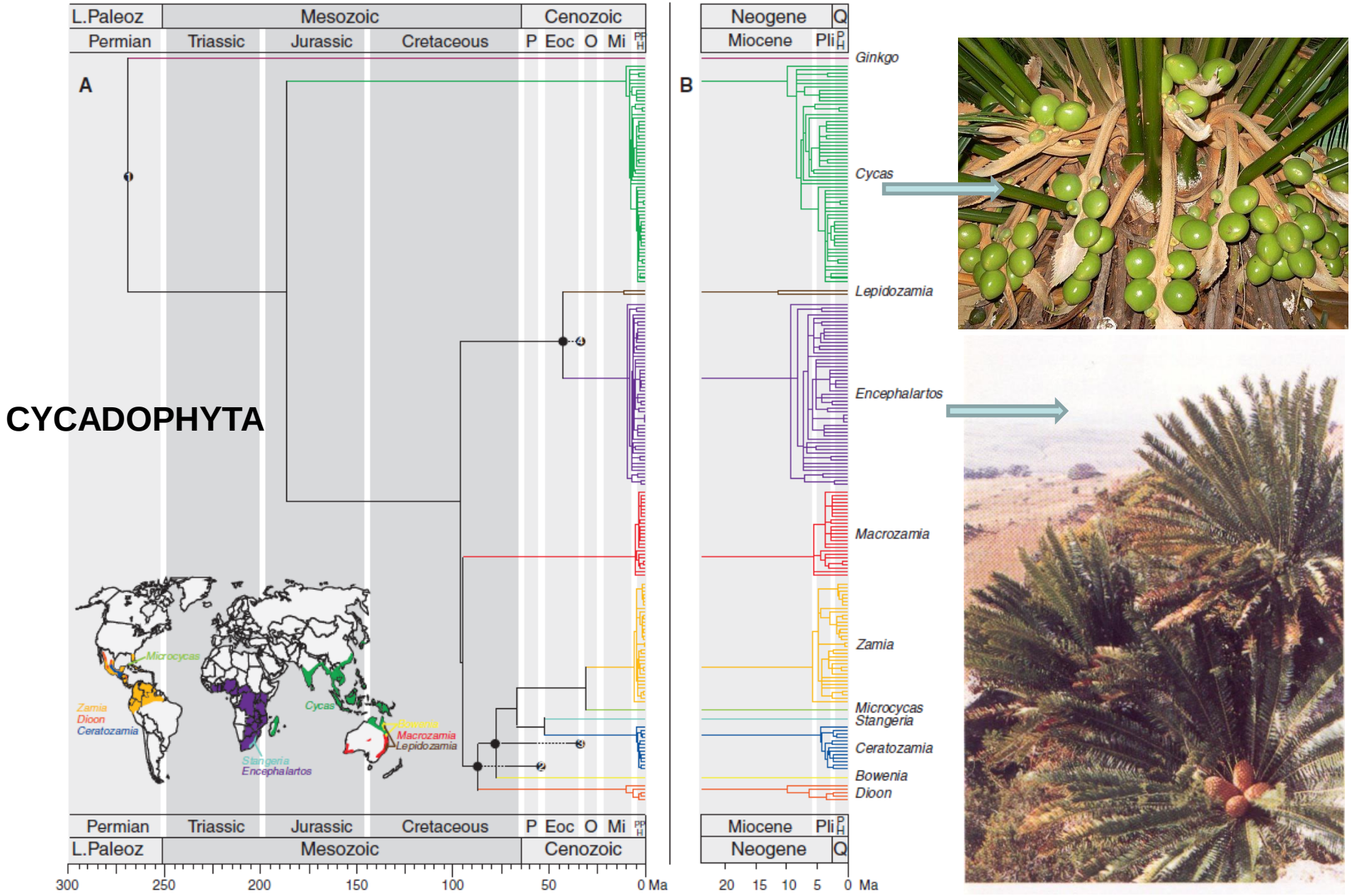

CYCADOPHYTA

Fig. 1. Cycad timetree inferred from *PHYP* data assuming a relaxed molecular clock (*12*), and map showing geographic distribution of genera. (**A**) Timetree and (inset) distribution of genera. Numbered circles mark the ages of fossil constraints, and unnumbered circles mark the inferred ages of the constrained nodes (*9*). Geographic distributions were obtained from (*2*). (**B**) Enlarged view of timetree from (A) focusing on the Miocene–Recent. L. Paleoz, Late Paleozoic; P, Paleocene; Eoc, Eocene; O, Oligocene; Mi, Miocene; PPH, Pleistocene–Pliocene–Holocene; Q, Quaternary; Pli, Pliocene; PH, Pleistocene–Holocene.

Nagalingum *et al.* 2011

Distribution of living Cupressaceae reflects the breakup of Pangea
32 gên., 162 spp.
Mao et al. 2012

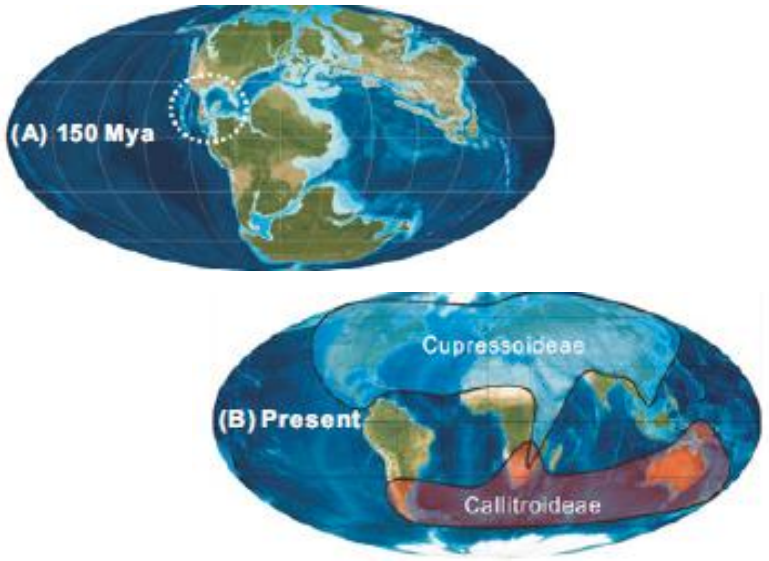

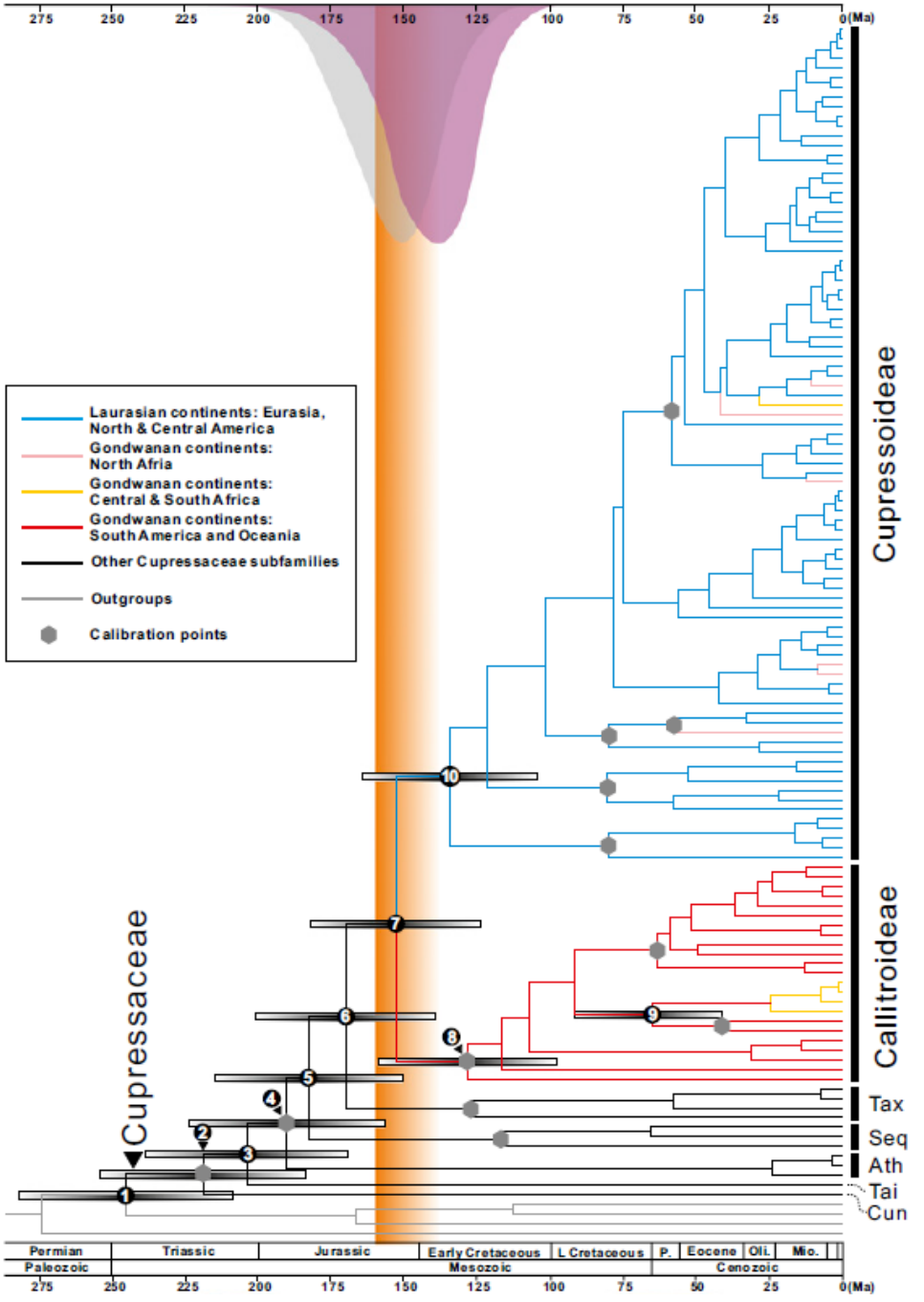

Fig. 1. (*Upper*) Chronogram for 122 Cupressaceae species and 22 outgroups based on an alignment of >7,000 nucleotides of plastid DNA (144-taxon dataset). A geological time scale is shown at the bottom (48). Blue lines represent Cupressoideae restricted to the area of Laurasian continents. Red lines represent Callitroideae restricted to Gondwanan continents. Pink lines represent species occurring in Africa in and north of the Sahara. Yellow lines represent species occurring in Africa south of the Sahara. Gray hexagons represent calibration points. Gray bars represent 95% HPD intervals for nodes 1–10. Gray (run 1) and purple (run 7) normal distributions represent the posterior for the BEAST age estimate of node 7 when uniform or lognormal priors were applied to calibration points. Orange shading indicates the period of decreasing feasibility of floristic exchange between Laurasia and Gondwana. Divergence times of nodes 5, 6, 7, 8, and 10 overlap with the fragmentation of Pangea. (*Lower*) Maps show (*A*) a paleocontinent reconstruction at 150 Ma and (*B*) the current distribution of Callitroideae and Cupressoideae. The stippled circle in *A* emphasizes island chains between North and South America; Ath, Athrotaxidoideae; Cun, Cunninghamioideae; Seq, Sequoioideae; Tai, Taiwanioideae; Tax, Taxodioideae. Reprinted with permission from

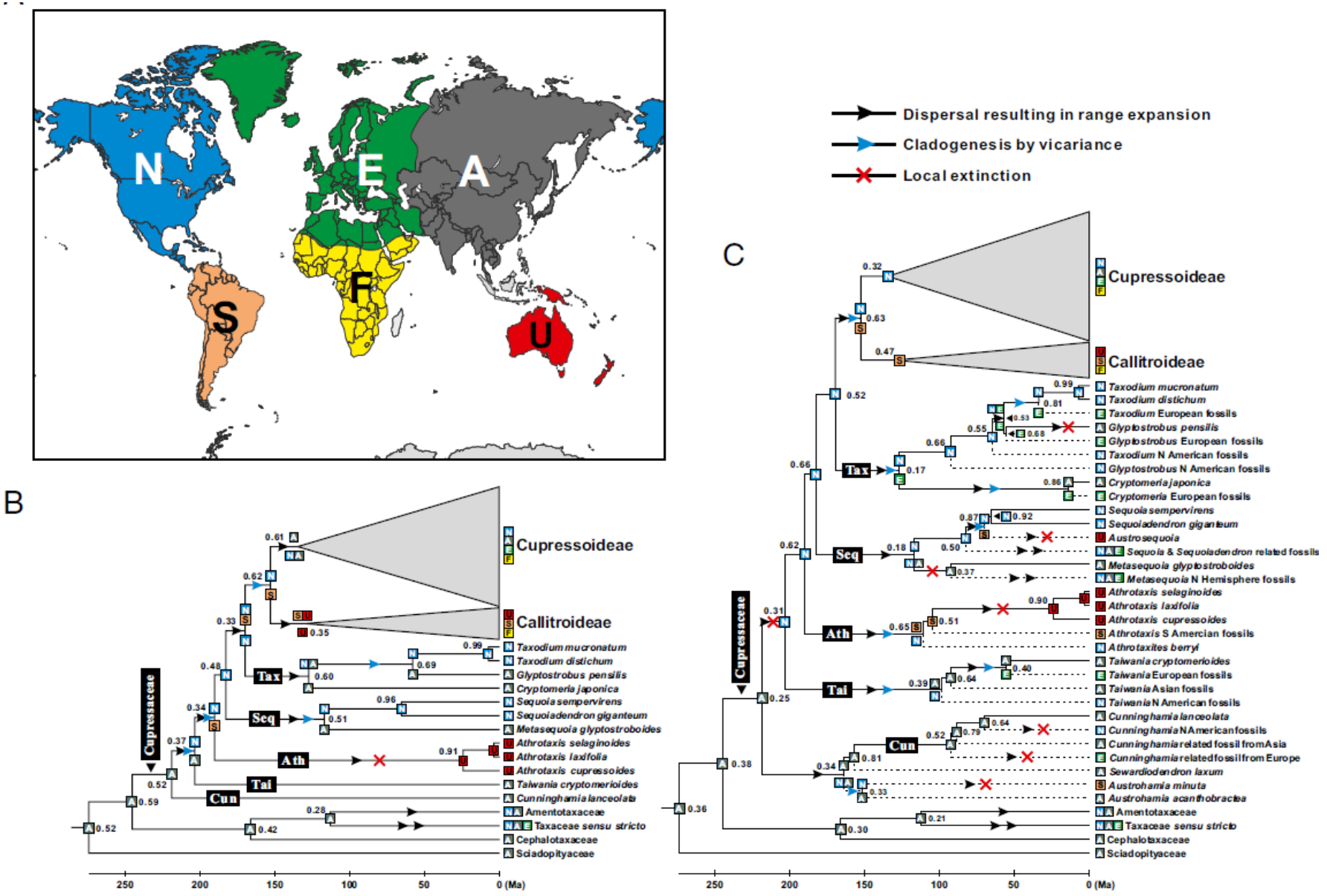

Cupressaceae **Mao et al. 2012**

Ancestral Areas and Diversification Rate Changes.

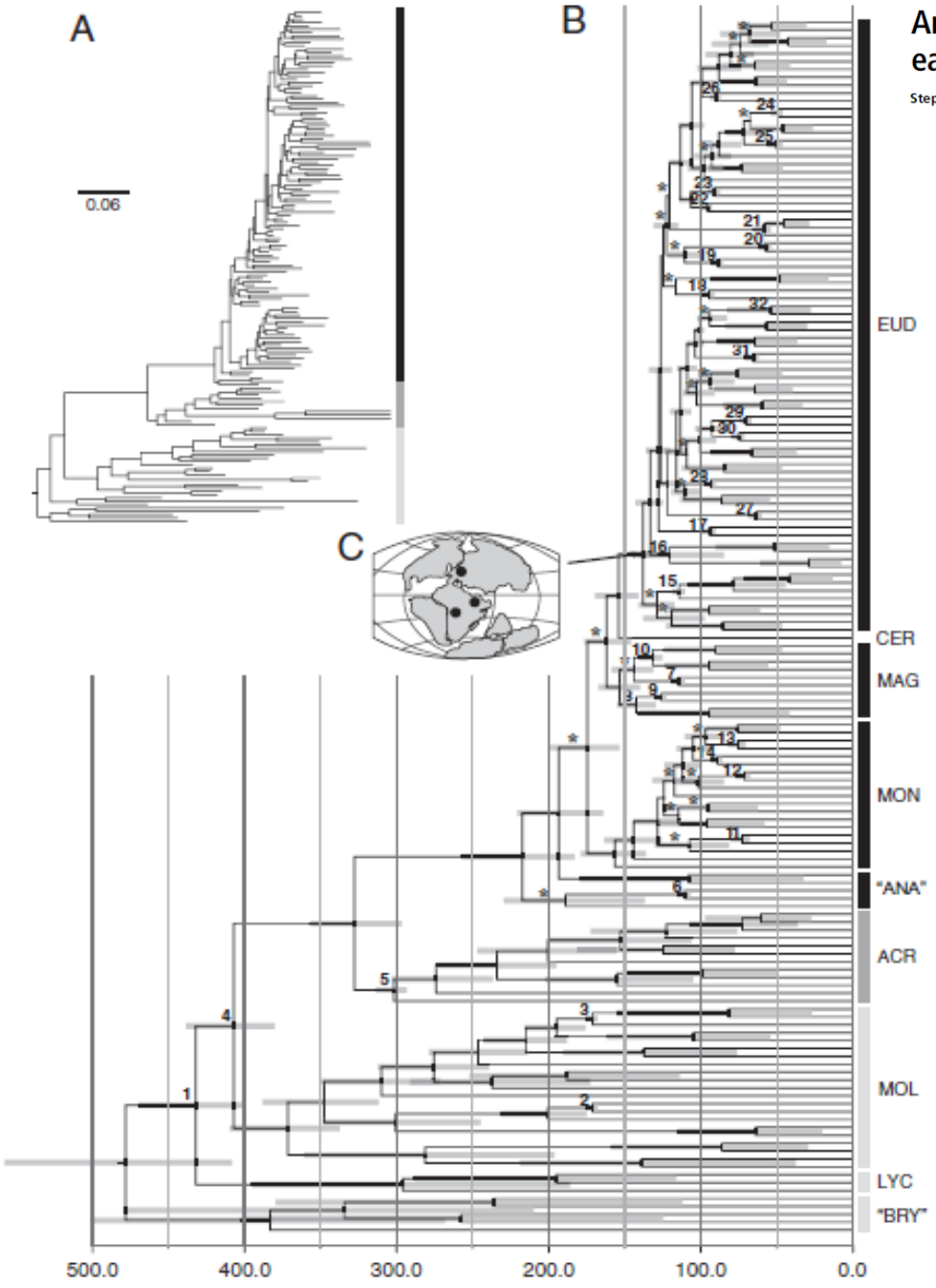

An uncorrelated relaxed-clock analysis suggests an earlier origin for flowering plants

Stephen A. Smith[a,1], Jeremy M. Beaulieu[b], and Michael J. Donoghue[b,1]

Smith et al. 2010

Relaxed-clock

Comprimento dos ramos representa a média das substituições por sítio

Estimativa de idade das Angiospermas: 220 Ma !!!

(Fóssil mais antigo de angiospermas: 136 Ma)

Fig. 1. Phylogenetic tree and divergence time estimates for land plants. (*A*) MrBayes consensus tree from a three-gene (*atp*B, *rbc*L, and 18S) analysis (see Fig S1 for taxon names). Branch lengths represent average substitutions per site. Shaded bars represent *Angiospermae* (black), *Acrogymnospermae* (dark gray), and the rest of the land plants (light gray). (*B*) The maximum clade credibility tree from the divergence time analysis of the same three-gene dataset as in *A*. Studies focused on the root of the land plants (e.g., ref. 81), including outgroups, place the root along the liverwort branch ("bryophytes" paraphyletic). Nodes marked by an asterisk (*) are supported by <0.95 posterior probability. The 95% highest posterior density (HPD) estimates for each well-supported clade are represented by bars. Numbers at nodes correspond to the fossil calibrations in Table S2. (*C*) Map with localities for the first tricolpate pollen records. Clade names follow Cantino et al. (47): ACR, *Acrogymnospermae*; ANA, ANITA grade; BRY, bryophytes; CER, *Ceratophyllum*; EUD, *Eudicotyledonae*; LYC, *Lycopodiophyta*; MAG, *Magnoliidae*; MOL, *Monilophyta*; MON, *Monocotyledonae*.

Some date problems

- Divergence between:
  - Molecular data against fossil date
    - Marsupials and Eutherians (104 vs. >218 Mya)
    - Humans and gorillas (8 vs. 18 Mya)

      (Douzer et al. 2003)
  - Various molecular dates:
    - Rat and mouse
      - Fossil date = 14 Mya
      - Molecular date = 33 Mya, 35 Mya, 41 Mya, 42 Mya, and 23 Mya

Dodson 2003

- 7 Calibration points
  - Together none were congruent with paleontological dates
  - 3 points recovered
    2 dates

Dodson 2003

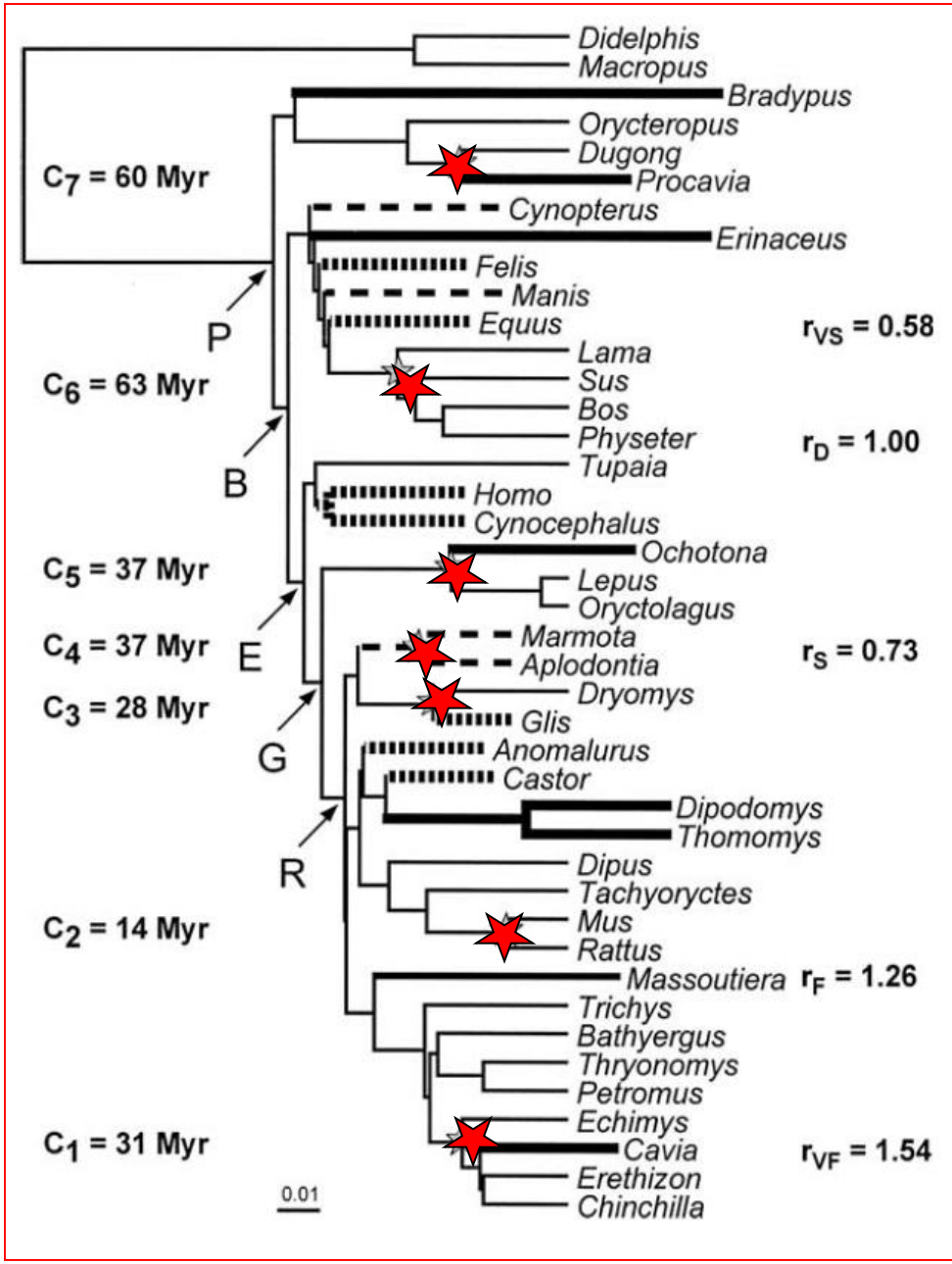

Malvaciphyllum macondicus

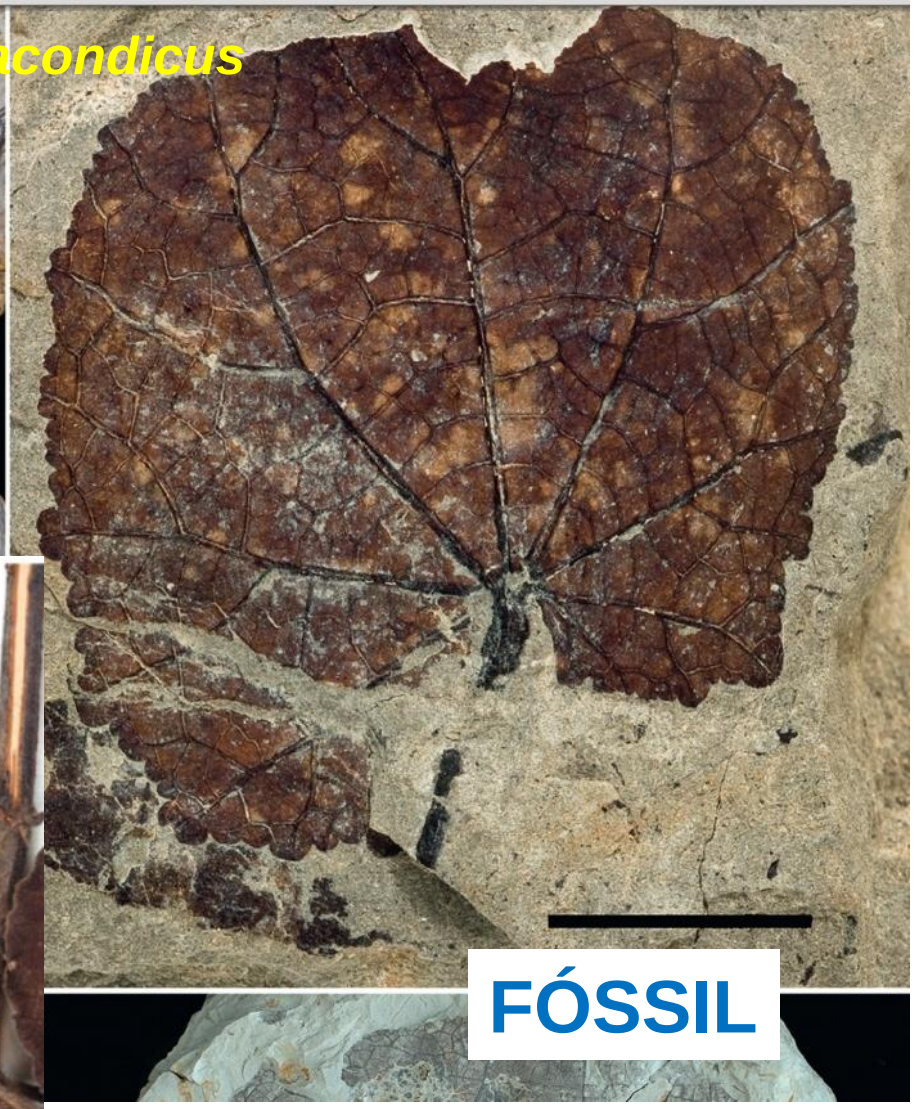

FÓSSIL

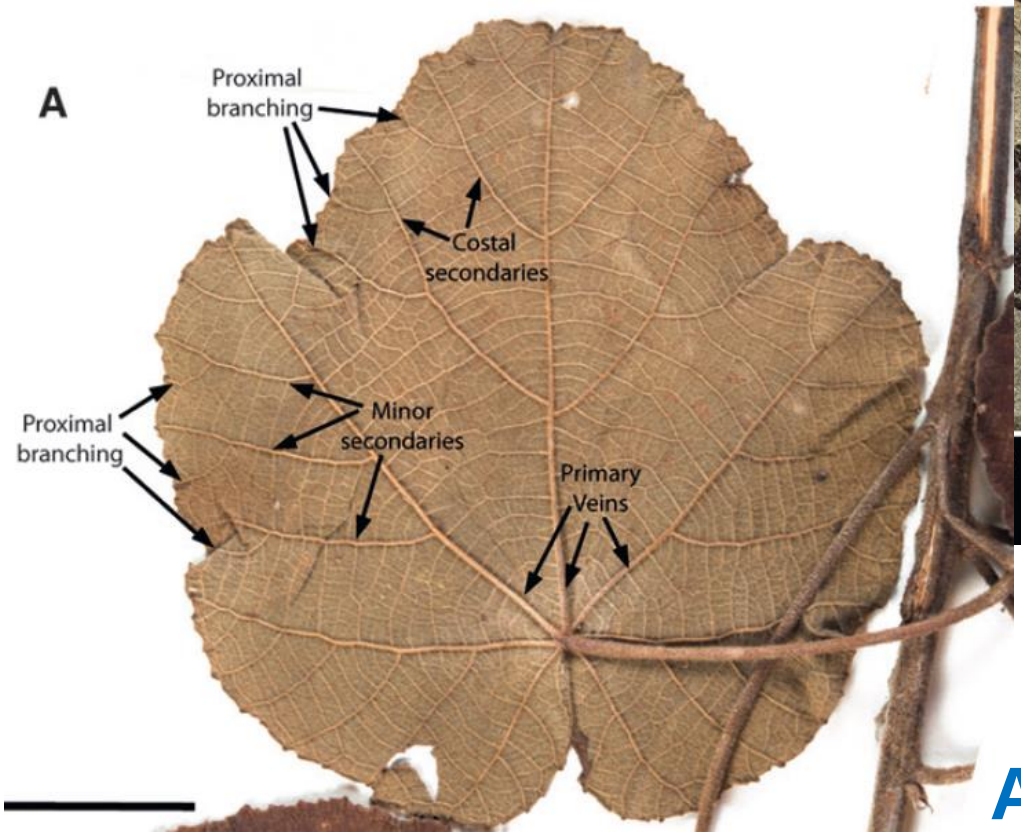

ATUAL

Malvaceae - Colômbia

PALEOCENO médio

Carvalho et al. 2011

PALEOCENE MALVACEAE FROM NORTHERN SOUTH AMERICA AND THEIR BIOGEOGRAPHICAL IMPLICATIONS[1]

MÓNICA R. CARVALHO[2–4,7], FABIANY A. HERRERA[3,5], CARLOS A. JARAMILLO[3], SCOTT L. WING[6], AND RICARDO CALLEJAS[2]

[2]Instituto de Biología, Universidad de Antioquia, Medellín, Colombia; [3]Smithsonian Tropical Research Institute, CTPA, Panama City, Panama; [4]Department of Geosciences, Pennsylvania State University, University Park, Pennsylvania 16802 USA; [5]Department of Biology and Florida Museum of Natural History, University of Florida, Gainesville, Florida 32611 USA; and [6]Department of Paleobiology, Smithsonian Museum of Natural History, Washington D.C. 20013 USA

- *Premise of the study:* The clade Bombacoideae + Malvoideae ('Malvatheca group' sensu Baum et al.) in Malvaceae comprises a mostly tropical lineage with derived taxa that now thrive in higher latitudes. The sparse fossil record, especially for Malvoideae, obscures interpretations of past distributions. We describe fossil leaves of Malvoideae from the middle-late Paleocene Cerrejón Formation in Colombia, which contains evidence for the earliest known neotropical rainforest.
- *Methods:* Fifty-six leaf compressions belonging to Malvaceae were collected from the Cerrejón Formation in northern Colombia. Leaf architectural characters were scored and optimized for 81 genera of Malvaceae. Synapomorphic characters and unique character combinations support natural affinities for the fossil leaves. Fossil pollen from the same formation was also assessed.
- *Key results:* Despite convergence of overall leaf architecture among many Malvaceae, *Malvaciphyllum macondicus* sp. nov. can be assigned to the clade Eumalvoideae because of distal and proximal bifurcations of the costal secondary and agrophic veins, a synapomorphy for this clade.
- *Conclusions:* The leaf compressions, the oldest fossils for Eumalvoideae, indicate a minimum divergence time of 58–60 Ma, older than existing estimates from molecular analyses of living species. The abundance of eumalvoid leaves and of bombacoid pollen in the midlate Paleocene of Colombia suggests that the Malvatheca group (Malvoideae + Bombacoideae) was already a common element in neotropical forests and does not support an Australasian origin for Eumalvoideae.

Palinofósseis *Tubulifloridites* (ASTERACEAE) do Cretáceo na Antártida:

Datados 76-66 m.a. = 20 m.a. mais antigos que os conhecidos até hoje.

Barreda et al. 2015

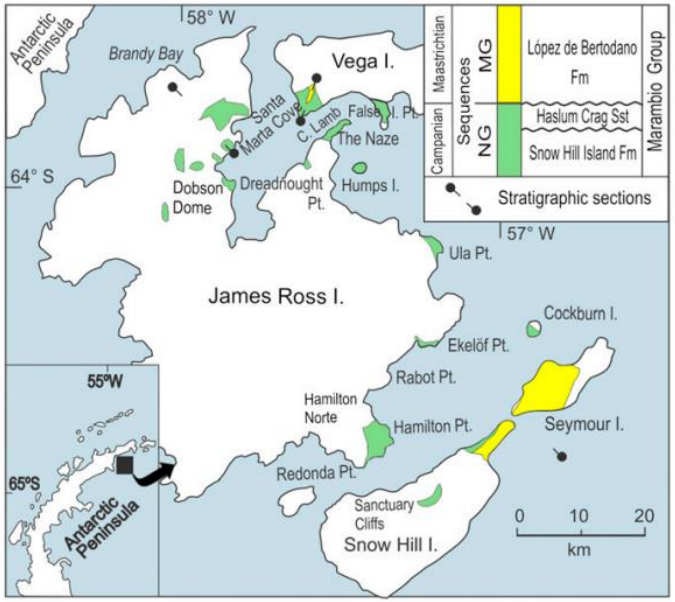

Fig. 1. Map showing distribution of Upper Cretaceous rocks of the Snow Hill Island and López de Bertodano Formations. The studied sections in Brandy Bay–Santa Marta Cove (James Ross Island) and Cape Lamb (Vega Island) are also indicated. Adapted from Olivero (7).

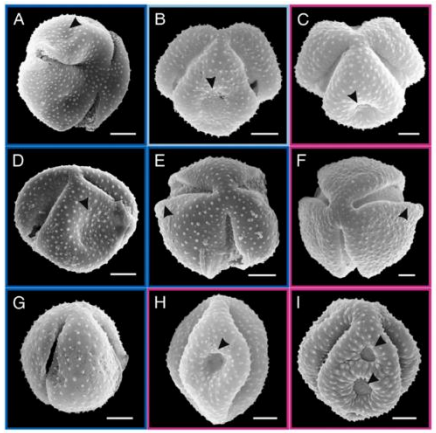

Fig. 4. Fossil and extant representatives of Asteraceae observed by scanning electron microscopy. (*A*, *D*, *E*, *G*) Specimens of *Tubulifloridites lilliei* type A from the Late Cretaceous of Antarctica (blue frames). (*A*) Subpolar view showing details of sculpture and poorly defined depressions (arrowhead); note the microgranulate apertural membrane. (*D*) Subequatorial view showing a poorly defined depression (arrowhead). (*E*) Polar view with small apocolpium and thickened colpi margins. (*G*) Equatorial view showing the microechinate-baculate-verrucate sculpture. (*B*) Specimen of *Quilembaypollis tayuoides* Barreda and Palazzesi from the Miocene of Patagonia (light blue frame) that shares morphological features with both the Cretaceous and extant asteraceous specimens; note the microechinate-baculate sculpture. (*C*, *F*, *H*, *I*) Extant species of *Dasyphyllum* (pink frames) showing variations in the development and number of intercolpal depressions. (*C* and *H*) *Dasyphyllum inerme* (Rusby) Cabrera. (*F*) *Dasyphyllum latifolium* (Gardner) Cabrera. (*I*) *Dasyphyllum leptacanthum* (Gardner) Cabrera. (Scale bars, 5 μm.)

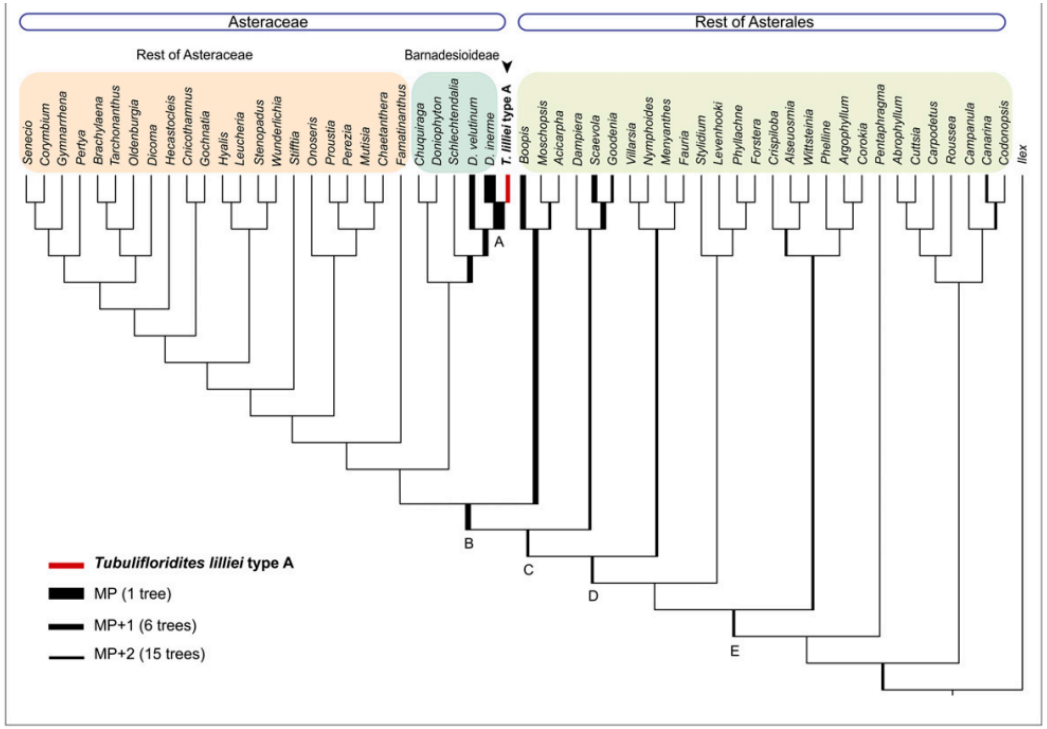

Fig. 2. Phylogenetic analyses of the fossil taxa. Branching positions of the fossil *T. lilliei* type A mapped onto a backbone tree derived from a molecular analysis of Beaulieu et al. (4), with some asteracean taxa added, following a recent comprehensive analyses of Panero et al. (24). Thicker black lines indicate the most parsimonious (MP), one step less parsimonious (MP + 1), and two steps less parsimonious (MP + 2) positions for *T. lilliei* type A. Letters indicate the nodes used to calibrate alternative scenarios, A: Fig. 5; B–E: Fig. S5 and Table S2.

Cronograma das principais linagens de ASTERACEAE

Diversificação mais antiga no Cretáceo Superior (80 m.a.);
maioria das subfamíias teriam divergido durante o Paleógeno.

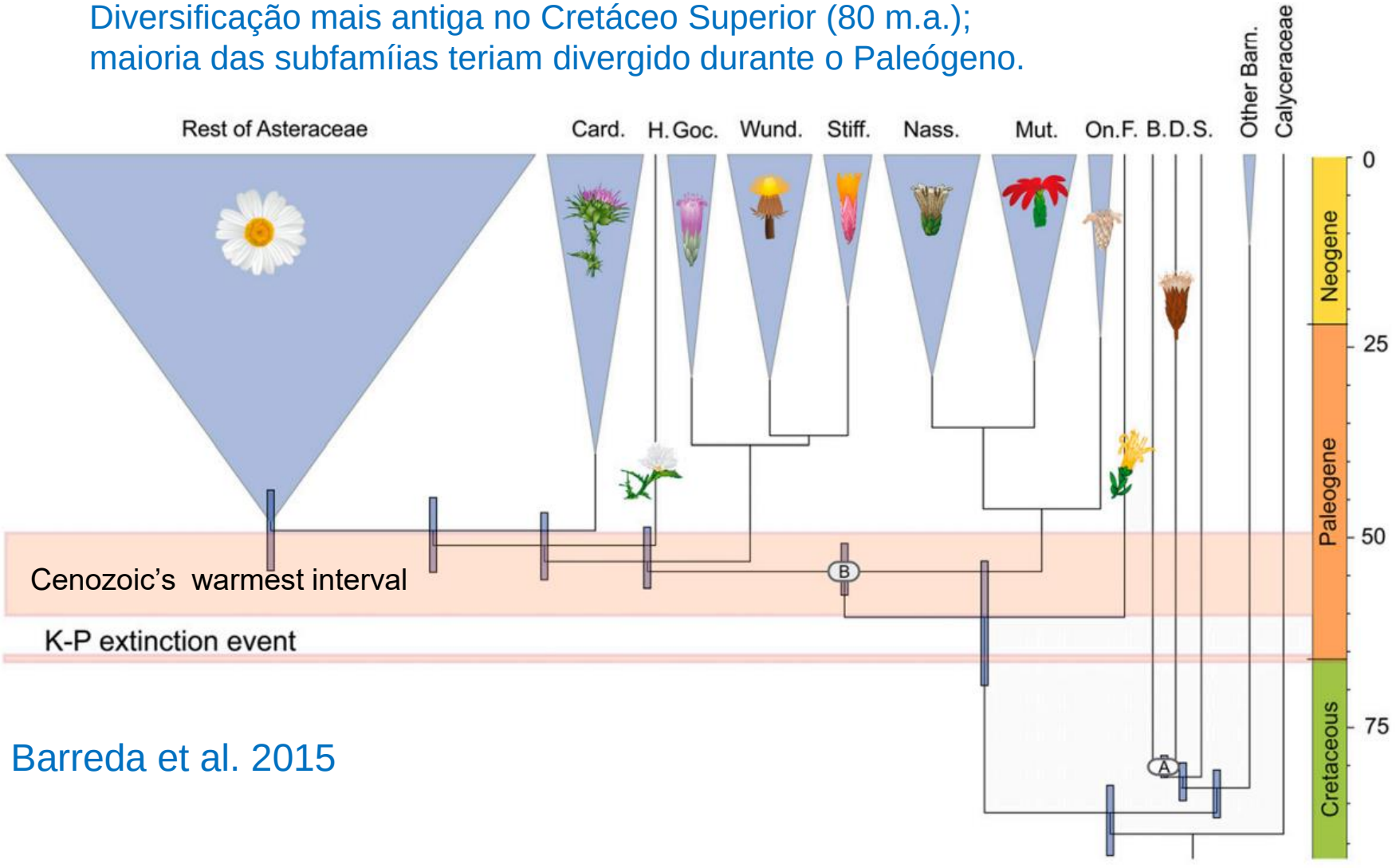

Barreda et al. 2015

Fig. 5. Evolutionary timescale of the diversification of Asteraceae. Chronogram (scale on the right in Mya) estimated using a Bayesian relaxed clock calibrated with a previously described fossil inflorescence from the Eocene ("B") and our newly discovered specimens from the Cretaceous of Antarctica ("A"). We assume that this Cretaceous species (*T. lilliei* type A) represents an extinct branch nested within *Dasyphyllum* (crown representative). Other possible calibration scenarios are illustrated in Fig. S5. Light-blue bars at nodes represent 95% credibility intervals on estimates of divergence times. Orange horizontal lines indicate the timing of the K–P extinction event and the Cenozoic's warmest interval. Most subfamilies of Asteraceae diverged during the Paleogene, but the earliest divergence occurred in the Late Cretaceous. B., *Barnadesia*; Barn., Barnadesioideae (91 species); Card., Carduoideae (2,500+ species); D., *Dasyphyllum*; F., Famatinanthoideae (1 species); Goc., Gochnatioideae (90 species); H., Hecastocleidoideae (1 species); Mut., Mutisieae (254 species); Nass., Nassauvieae (313 species); On., Onoserideae (52 species); S., *Schlechtendalia*; Stiff., Stifftioideae (44 species); Wund., Wunderlichioideae (41 species); rest of Asteraceae (19,600 + species).

Problems

- DNA of even closely related species may evolve at different rates (Welch and Bromham 2005)
  - Mice have consistently faster rates than humans (2:1 synonymous substitutions) (Hermann 2003)
  - Using a constant rate between “Mice and Men” the molecular date is too old
- Cladograms based on morphology data and molecular data are only moderately congruent (Hermann 2003)

Fig. 1. Phylogenies of five angiosperm clades with branch lengths proportional to substitutions per site. Branch colors represent inferred life history states (brown for trees/shrubs; green for herbs). Box plots show substitutions per site per million years for the inferred life history categories; centerline represents the median, hinges mark the first and third quartiles, whiskers extend to the lowest and highest non-outlier. Outliers (not shown) have values >1.5 times beyond the first or third quartiles.

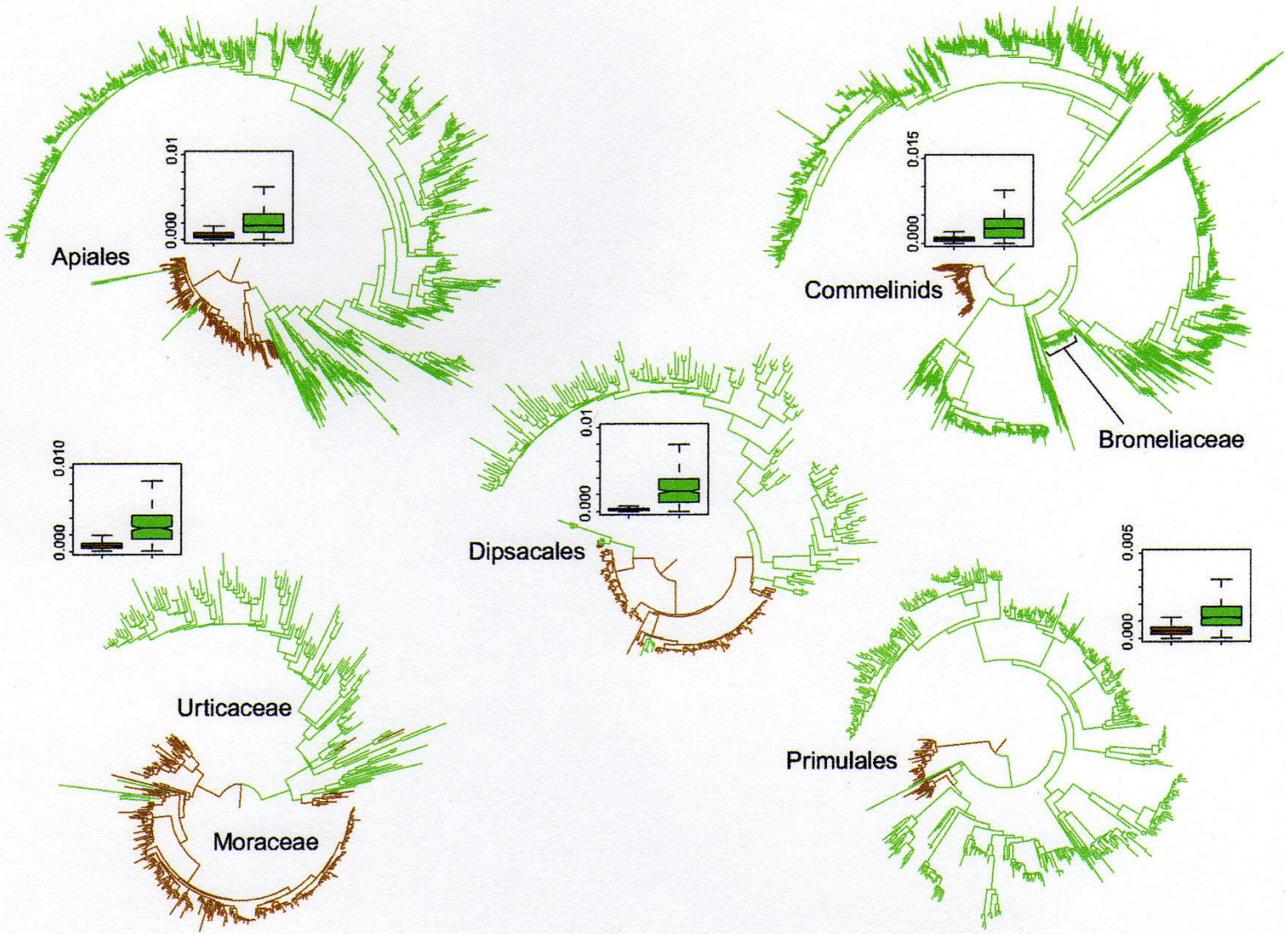

Smith & Donoghue 2008 - Taxas de evolução ligadas a história de vida em plantas

Fig. 2. Dated phylogenies for Apiales and Dipsacales with substitutions per site per million years plotted for 10-million-year intervals through the life of the clade. Branch colors represent inferred life history states (brown for trees/shrubs; green for herbs). Box plots as in Fig. 1. PM, Pittosporaceae and Myodocarpaceae; Dips, Dipsacaceae; M, Morinaceae; L, Linnaceae.

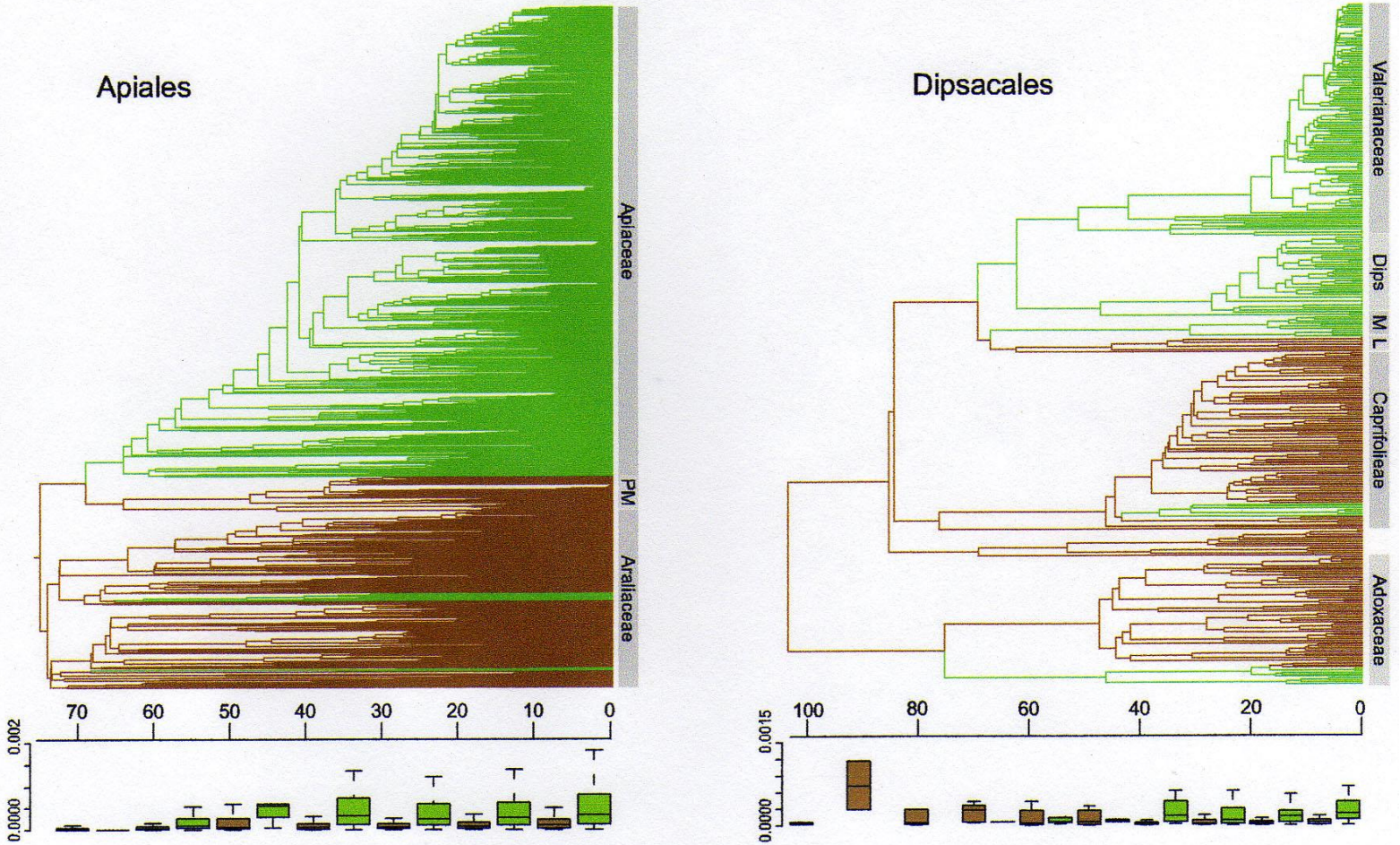

Smith & Donoghue 2008

Smith & Donoghue 2008

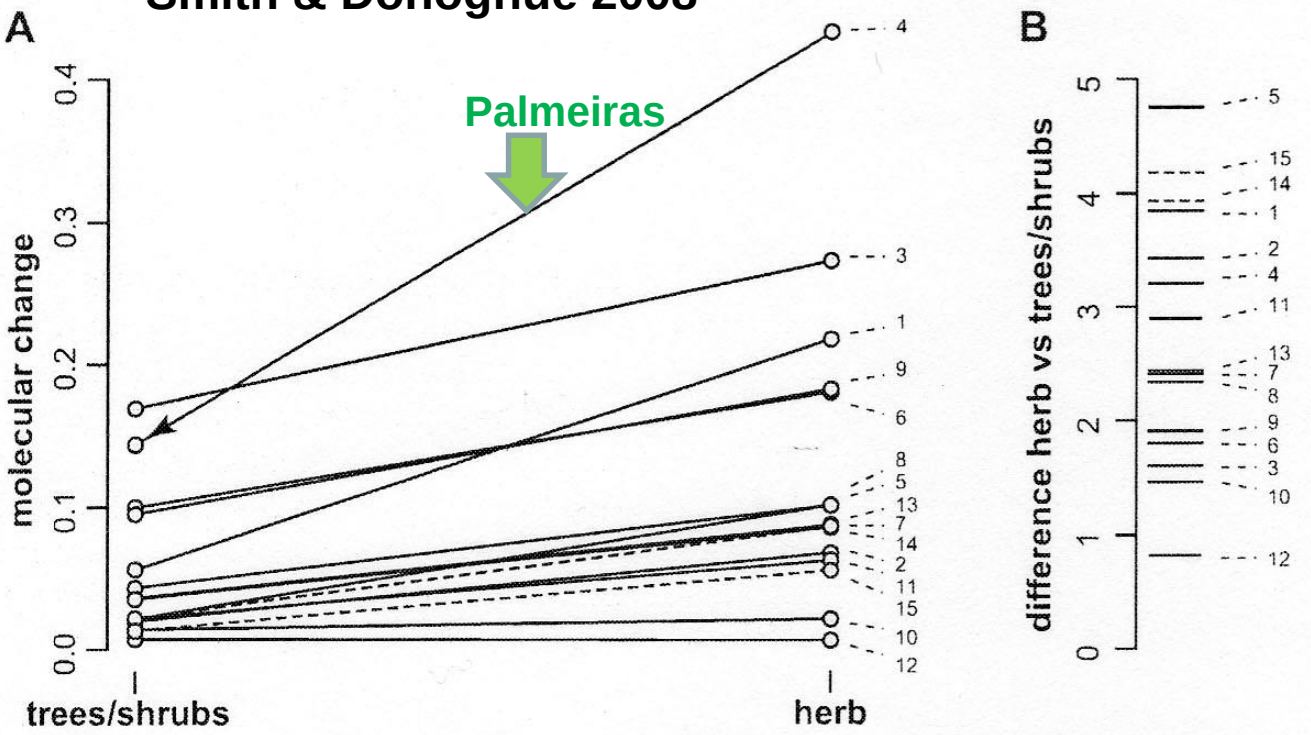

Fig. 3. Branch-length contrasts for trees/shrubs versus herbs. (**A**) Lines are drawn between the accumulated average molecular branch lengths for each tree/shrub clade and its sister herbaceous clade (numbers correspond to those in Table 1). All evolutionary shifts were inferred to be from trees/shrubs to herbs except for the evolution of palms within monocotyledons (arrowhead in contrast 4). Contrasts 1 to 13 were used in an initial sign test ($P = 0.00342$). Alternative contrasts within the Dipsacales (14 and 15) are marked by dotted lines and were substituted for 11 to 13 in one test ($P = 0.00049$); contrasts 11 to 15 were omitted in a third test ($P = 0.00195$). (**B**) Magnitude of change between each tree/shrub clade and its herbaceous sister clades; values above 1 show higher rates of molecular evolution in herbs than in trees/shrubs.

+ ABRUPT DECELERATION OF MOLECULAR EVOLUTION LINKED TO THE ORIGIN OF ARBORESCENCE IN FERNS **Korall et al. 2010**

Received 20 Aug 2012 | Accepted 5 Apr 2013 | Published 21 May 2013

DOI: 10.1038/ncomms2836

Taller plants have lower rates of molecular evolution

Lanfear et al. 2013: 138 famílias de angiospermas

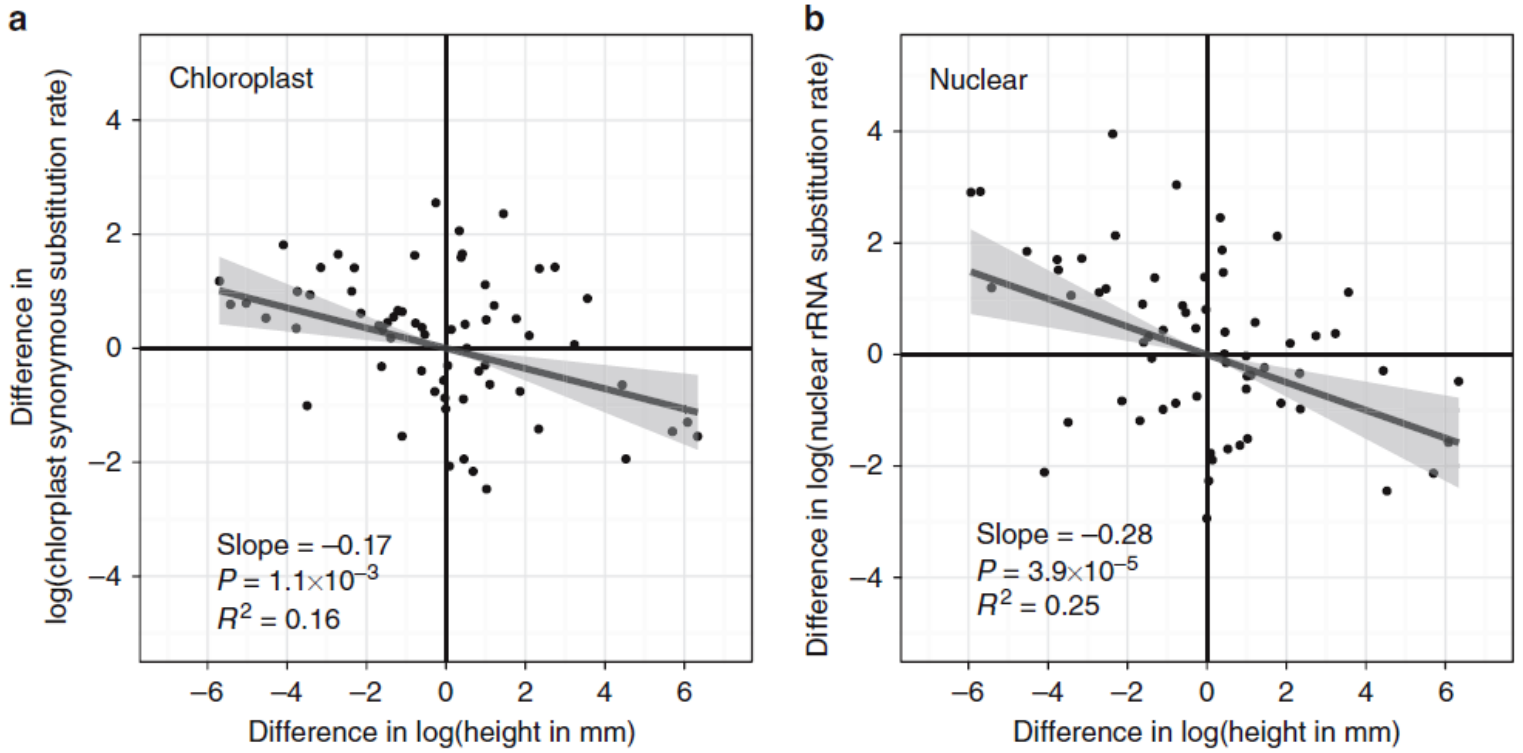

Figure 1 | The relationship between plant height and rates of molecular evolution in angiosperms. Differences in the logarithms of plant height and rates of molecular evolution were measured for sister pairs of angiosperm families. Regressions through zero show a significant negative association between plant height and synonymous substitution rates measured from protein-coding genes in the chloroplast genome (**a**), and between plant height and substitution rates in rRNA genes in the nuclear genome (**b**). In each panel, the best-fit line (dark grey) was estimated using linear regression through the origin, with the 95% confidence intervals around this line shown in light grey (see main text).

Clarke et al. 2011. Establishing a time-scale for plant evolution.

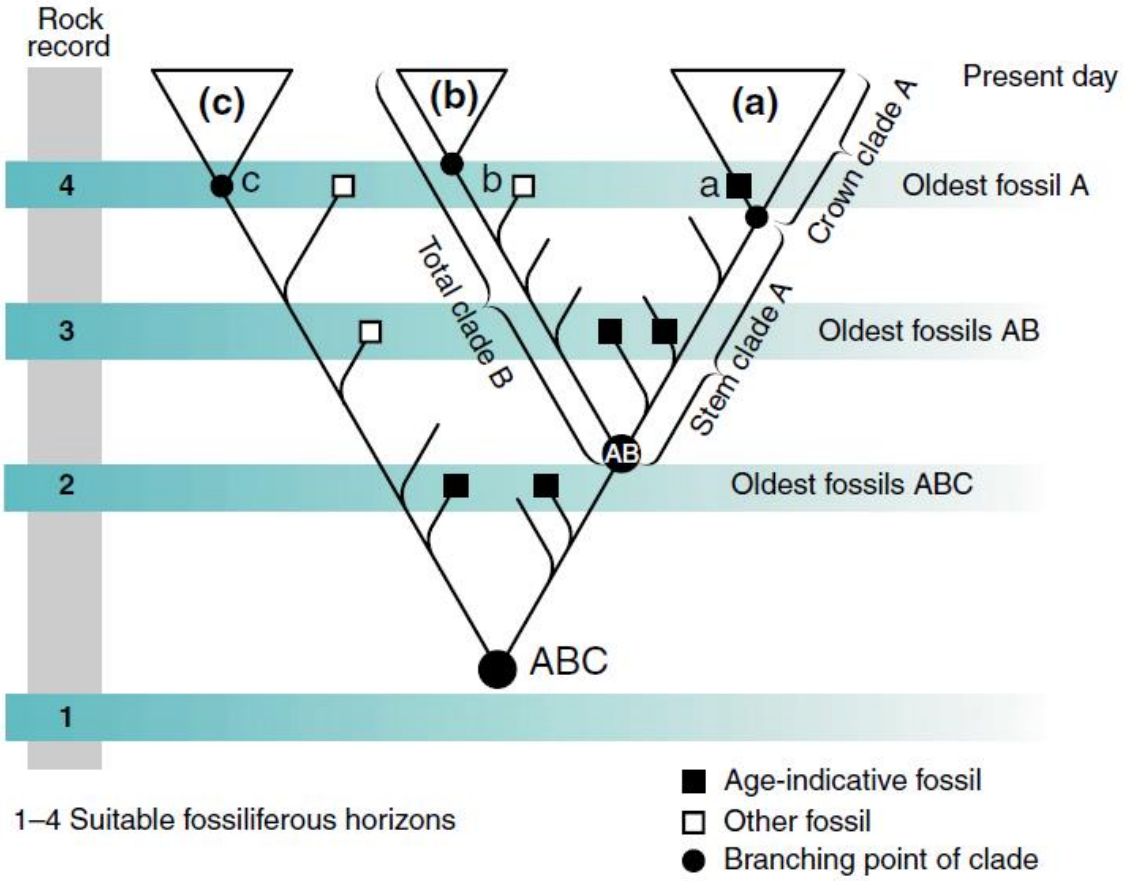

Fig. 1 Definitions of terms used in assigning fossils to clades. The crown clade consists of all living species and their most recent common ancestor, and this is preceded by a stem lineage of purely fossil forms that are closer to their crown clade than to another crown clade. The divergence or splitting point between a species in clade A and a species in clade B is the point AB. This is older than the points of origin of crown clades A and B (indicated as points a and b). Fossils may belong to a crown clade or to a stem lineage, and cladistic evidence should indicate which. The crown clade and the stem clade for a particular lineage are together referred to as the total clade. Therefore, if calibrating the divergence between crown clades a and b, this invariably means finding the oldest reliable fossil belonging to the total clade a and total clade b; the oldest of which will provide the hard minimum constraint for the divergence between the two (point AB). Four fossiliferous horizons are indicated, the source of all relevant fossils. Fossiliferous horizon 1 that contains no fossils assignable to the clade ABC marks a maximum constraint (soft bound) on the age of the clade. Fossiliferous horizon 2 marks a maximum constraint on the age of clade AB. Minimum constraints are indicated by the oldest fossils for ABC, AB and A.

Clarke et al. 2011.

Establishing a time-scale for plant evolution.

Angiospermas:
mínimo 124,4 Ma
máximo 248,4 Ma

Espermatófitas:
mínimo 306,2 Ma
máximo 366,8 Ma

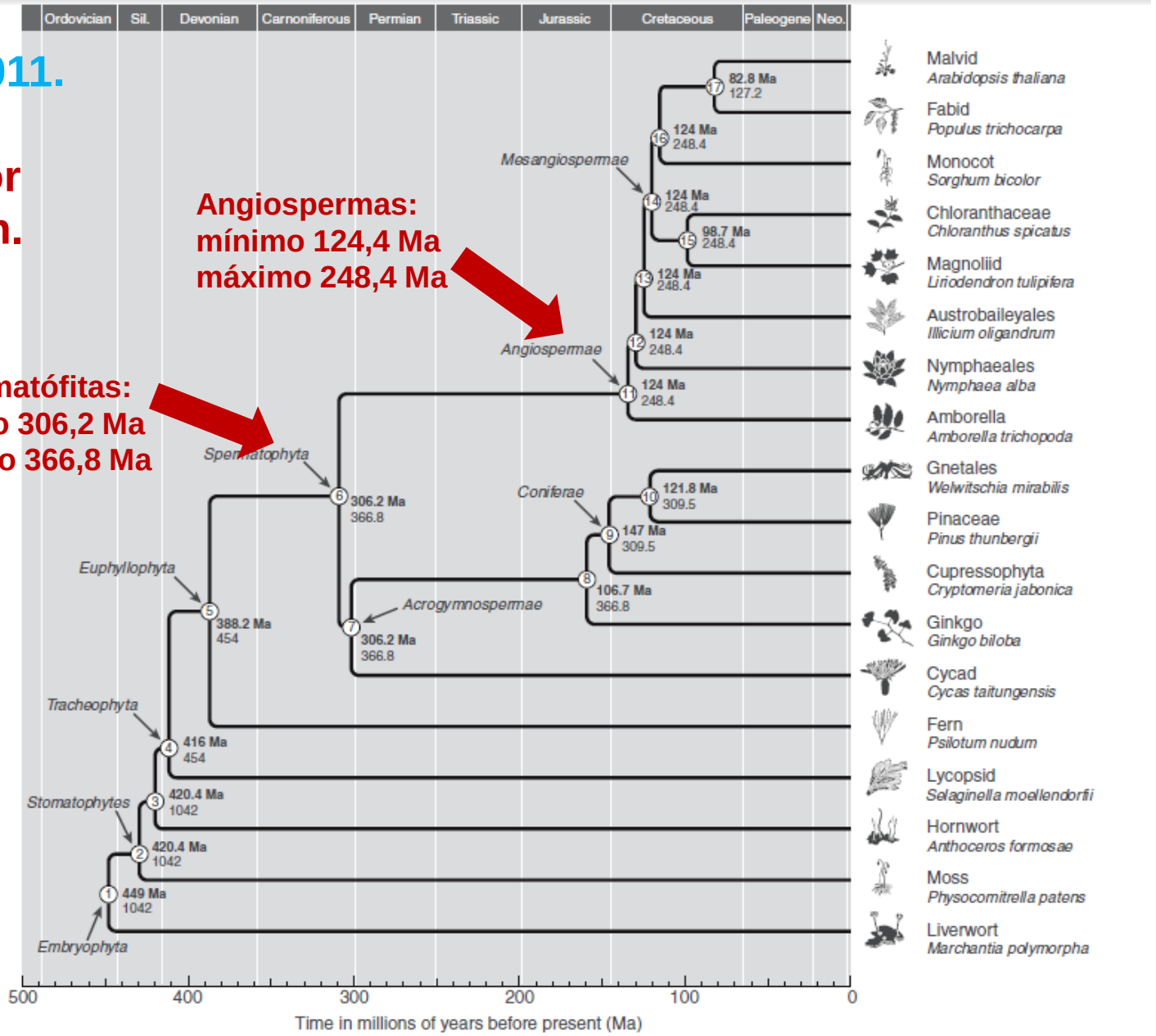

Fig. 2 A representative tree of relationships between model representatives of the major land plant lineages whose plastid or nuclear genomes have been fully sequenced. The topology is based upon a consensus of the most well-supported relationships as reviewed in recent literature (Qiu, 2008; Forest & Chase, 2009; Magallón, 2009; Magallón & Hilu, 2009; Renner, 2009). Calibrations are presented for all 17 nodes, consisting of a hard minimum constraint (bold) and a soft maximum constraint (not bold) for each. Justifications for these minima and maxima . The tree has been scaled to time on the basis of the minimum constraints.

Diversity dynamics: molecular phylogenies need the fossil record

Tiago B. Quental and Charles R. Marshall

Museum of Paleontology and Department of Integrative Biology, University of California at Berkeley, Berkeley, CA 94720, USA

Over the last two decades, new tools in the analysis of molecular phylogenies have enabled study of the diversification dynamics of living clades in the absence of information about extinct lineages. However, computer simulations and the fossil record show that the inability to access extinct lineages severely limits the inferences that can be drawn from molecular phylogenies. It appears that molecular phylogenies can tell us only when there have been changes in diversification rates, but are blind to the true diversity trajectories and rates of origination and extinction that have led to the species that are alive today. We need to embrace the fossil record if we want to fully understand the diversity dynamics of the living biota.

Molecular phylogenies and rates of diversification

Understanding the patterns and processes of diversification has long been of interest to paleontologists as we use the fossil record to document biodiversity change through time [1]. However, interest in diversity dynamics among biologists and the greater public has grown, particularly as we become aware of the impact of humans on the biosphere. Among biologists, the study of biodiversity dynamics was invigorated by the proposal that the rates and processes of diversification could be inferred from molecular phylogenies. This is particularly important given that many taxonomic groups have poor-to-non-existent fossil records [2]. In particular, the pioneering contributions of Nee et al. [3–5] and Harvey et al. [6] provided methods for detecting mass extinction events and for estimating speciation and extinction rates from molecular phylogenies despite the absence of the extinct species (but see [7] and [8]). This work was presaged by Thompson [9], and there were also parallel efforts by Hey determining if a molecular phylogeny is consistent with a constant rate of diversification, or if there has been a decrease in the diversification rate (inferred when molecular phylogenies have significantly negative γ values). There is now a sizeable literature which indicates that many clades have decreasing diversification rates [12,15–17], in fact for about half of the 160 well-sampled phylogenies analyzed [15]. Considerable attention is now focused on exploring the implications of these findings for the evolutionary and ecological mechanisms responsible

Glossary

Boundary-crosser method: used to estimate the diversity at the boundary of adjacent geological time intervals by counting the number of taxa that must have crossed the boundary because they are known before and after it. This method has the desirable property of assuring the co-existence of taxa.
Chronogram: a phylogeny with branch lengths adjusted so that they are proportional to absolute time. Also known as a 'time tree'.
Crown group: a monophyletic clade that contains all extant members of the clade in addition to its last common ancestor and all of its descendants, both living and extinct.
Diversification rate: the rate of origination (speciation, λ) minus the rate of extinction (μ): (λ − μ).
Diversity trajectory: a curve that portrays the number of species through time. It permits one to see if a given clade was diversifying or declining.
Equilibrium diversity: assuming diversity-dependent diversification, the expected number of taxa when the speciation and extinction rates are balanced, i.e. when the net diversification rate is zero.
Frequency ratio (FreqRat): statistical method used to measure the incompleteness of the fossil record by estimating the sampling probabilities per unit time (r) using the frequency of taxa that have stratigraphic ranges of one (f_1), two (f_2) or three (f_3) time intervals: $r = (f_2)^2/(f_1)(f_3)$.
γ statistic: a statistic that describes the center of mass for the nodes in a chronogram compared with the expected center of mass under a pure birth model. Nodes concentrated towards the base of a tree indicate a decrease in diversification rates, yielding negative γ values.
LiMe ratio: the ratio of the initial speciation rate (Lambda initial) and the extinction rate at equilibrium (Mu equilibrium). It assumes the existence of diversity equilibrium and, along with the size of the clade, and where the clade happens to be in its diversity trajectory, it plays a major part in determining the

Quental & Marshall 2010
TREE

Ronquist et al. 2012

Syst. Biol. 61(6):973–999, 2012

DOI:10.1093/sysbio/sys058
Advance Access publication on June 20, 2012

A Total-Evidence Approach to Dating with Fossils, Applied to the Early Radiation of the Hymenoptera

FREDRIK RONQUIST[1,*], SERAINA KLOPFSTEIN[1], LARS VILHELMSEN[2], SUSANNE SCHULMEISTER[3], DEBRA L. MURRAY[4], AND ALEXANDR P. RASNITSYN[5]

[1]*Department of Biodiversity Informatics, Swedish Museum of Natural History, Box 50007, SE-104 05 Stockholm, Sweden;* [2]*Department of Entomology, Natural History Museum of Denmark, Universitetsparken 15, DK-2100 Copenhagen Ø, Denmark;* [3]*Faculty of Biology, Department II, Ludwig-Maximilians-University, Großhaderner Straße 2–4, DE-82152 Martinsried, Germany;* [4]*Department of Biology, Duke University, Box 90338, Durham, NC, 27708, USA; and* [5]*Paleontological Institute, Russian Academy of Sciences, Profsoyuznaya Ulitsa 123, Moscow 117647, Russia*
**Correspondence to be sent to: Department of Biodiversity Informatics, Swedish Museum of Natural History, Box 50007, SE-10405 Stockholm, Sweden; E-mail: fredrik.ronquist@nrm.se.*
Fredrik Ronquist and Seraina Klopfstein contributed equally to this article.

Received 1 September 2011; reviews returned 19 October 2011; accepted 7 June 2012
Associate Editor: Thomas Near

Abstract.—Phylogenies are usually dated by calibrating interior nodes against the fossil record. This relies on indirect methods that, in the worst case, misrepresent the fossil information. Here, we contrast such node dating with an approach that includes fossils along with the extant taxa in a Bayesian total-evidence analysis. As a test case, we focus on the early radiation of the Hymenoptera, mostly documented by poorly preserved impression fossils that are difficult to place phylogenetically. Specifically, we compare node dating using nine calibration points derived from the fossil record with total-evidence dating based on 343 morphological characters scored for 45 fossil (4–20% complete) and 68 extant taxa. In both cases we use molecular data from seven markers (~5 kb) for the extant taxa. Because it is difficult to model speciation, extinction, sampling, and fossil preservation realistically, we develop a simple uniform prior for clock trees with fossils, and we use relaxed clock models to accommodate rate variation across the tree. Despite considerable uncertainty in the placement of most fossils, we find that they contribute significantly to the estimation of divergence times in the total-evidence analysis. In particular, the posterior distributions on divergence times are less sensitive to prior assumptions and tend to be more precise than in node dating. The total-evidence analysis also shows that four of the seven Hymenoptera calibration points used in node dating are likely to be based on erroneous or doubtful assumptions about the fossil placement. With respect to the early radiation of Hymenoptera, our results suggest that the crown group dates back to the Carboniferous, ~309 Ma (95% interval: 291–347 Ma), and diversified into major extant lineages much earlier than previously thought, well before the Triassic. [Bayesian inference; fossil dating; morphological evolution; relaxed clock; statistical phylogenetics.]

Morphological Clocks in Paleontology, and a Mid-Cretaceous Origin of Crown Aves. **Lee et al. 2014**

Morphological dating X molecular dating

"...both approaches entail considerable uncertainties:
for example, nonpreservation of fossils always underestimates the antiquity of lineages, whereas rate heterogeneity, saturation, and calibration uncertainty can strongly bias molecular divergence dating."

Polêmica atual na Biogeografia Histórica

Queiroz 2005 – The resurrection of oceanic dispersal in Biogeography. *TREE* 20: 68-73.

Cowie & Holland 2006 – Dispersal is fundamental to biogeography and the evolution of biodiversity on oceanic islands. *J. Biogeogr.* 33.

McGlone 2005 – Goodbye Gondwana. *J. Biogeogr.* 32.

Christenhusz & Chase 2013. Biogeographical patterns of plants in the Neotropics – dispersal rather than plate tectonics is most explanatory. *Bot. J. Linn. Soc.* 171.

X

Arnaud-Haond et al. 2007 - Vicariance patterns in *Posidonia*.

J. Biogeogr. 34(6). (microssatélites)

Cook & Crisp 2005 – Directional asymmetry of long-distance dispersal and colonization could mislead reconstruction of biogeography. *J. Biogeogr.* 32.

Crisp & Cook 2007 - Congruent molecular signature of vicariance across multiple lineages. *Mol. Phyl. Evol. 43*(5). (23 linhagens de plantas da Austrália)

Mao et al. 2012 – Distribution of living Cupressaceae reflects the breakup of Pangea. *PNAS*.

van den Ende et al. 2017 – The existence and break-up of the Antartic land bridge as indicated by both amphi-Pacific distributions and tectonics. *Gondwana Research 44*
(múltiplas linhagens)

Yoder et al. 2006. Has vicariance or dispersal been the predominant biogeographic force in Madagascar? Only time will tell. *Ann. Rev. Ecol. Evol. Syst. 37.*

Polêmica atual na Biogeografia Histórica

Heads 2008 - Biological disjunction along the West Caledonian fault, New Caledonia: a synthesis of molecular phylogenetics and panbiogeography. *Bot. J. Linn. Soc. 158*. (87 táxons de plantas, mariposas e lagartos - padrões de vicariância)

Datações moleculares desafiando datações geológicas!

Boxclaer et al. 2006

Zaragüeta-Bagils et al. 2004. Temporal paralogy, cladograms, and the quality of the fossil record. Geodiversitas 26: 381–389.

Nelson, G. & Ladiges, P.Y. 2009. Biogeography and the molecular dating game: a futile revival of phenetics? *Bull. Soc. géol. Fr. 180: 39–43:*

"In molecular dating, branch lengths are considered parameters that may be estimated by counting similarities and differences in DNA sequences. Long and short branches imply long and short time spans, which might appear informative additions when imposed on a tree that is otherwise cladistic. Recent attempts to apply molecular dating to southern hemisphere biogeography (*Nothofagus, Adansonia)* seem only another "excursion into futility," as was the fate of phenetic systematics".

LIVRO de M. Heads 2012. Molecular Panbiogeography of the Tropics.

Aprimorando a Biogeografia Histórica

Filogenias continuarão sendo fundamentais para nossa compreensão da biogeografia.

MAS para testes rigorosos das hipóteses biogeográficas, temos que incorporar explicitamente um espectro mais amplo de dados nas análises (e.g. tempo, eventos geológicos/climáticos, ecologia).

Novas ferramentas analíticas têm sido desenvolvidas.

BIOGEOGRAFIA HISTÓRICA

“What biogeography is: a place for process”.

‘Vicariância e dispersão são atributos das distribuições bióticas. A Filogeografia tem grande potencial em ajudar a determinar qual desses processos gerou os padrões observados’.

R. M. McDowall 2004

J. Biogeogr. 31.

Bases da Filogeografia: na próxima aula.